Maternal Cardiac Metabolism during Pregnancy

Maternal Cardiac Metabolism during Pregnancy

A dissertation presented

By

Laura Xiaofei-Rose Liu

to

The Division of Medical Sciences

in partial fulfillment of the requirements

for the degree of

Doctor of Philosophy

in the subject of

Human Biology and Translational Medicine

Harvard University

Cambridge, Massachusetts

May 2015

Dissertation Advisor: Dr. Zoltan Arany Laura Xiaofei-Rose Liu

Maternal cardiac metabolism during pregnancy

Abstract

Pregnancy profoundly alters maternal physiology in response to the demands of the fetus. Cardiac output increases in response to an increase in heart rate and stroke volume. Insulin resistance and fetal preference for glucose switches maternal usage to that of predominantly fat consumption. Previous studies have shown that the heart adopts these adaptions, but much still remains unanswered. We sought to fill this gap by exploring cardiac substrate utilization and metabolic regulation during late pregnancy in mice.

We found that by late gestation, serum triglycerides are elevated and serum glucose is unchanged. Furthermore, real-time bioluminescence imaging of late pregnant mouse hearts showed an increase in fatty acid uptake. But greater supply and uptake may not always equal greater oxidation. Using ^{13}C-tracer analysis of Langendorff perfused ex vivo hearts, we observed ~30-50% less glucose usage in late pregnant mouse hearts. Fatty acid utilization, on the other hand, is increased.

The mechanisms regulating substrate switch in late pregnant mouse hearts have not been extensively studied. We determined that mitochondrial DNA copy number, morphology, expression of oxidative phosphorylation (OXPHOS) proteins, and respiratory capacity remain unaltered in late pregnancy. Furthermore, substrate transporter (GLUT4 and CD36) expression and localization are unchanged. Interestingly, pyruvate dehydrogenase kinase 4 (PDK4) is

induced in late pregnant mouse hearts. PDK4 is a crucial regulatory enzyme that can decrease glycolysis by phosphorylation of pyruvate dehydrogenase (PDH). Consistent with this, we observed an increase in phospho-PDH in late pregnancy. Treatment of neonatal rat ventricular myocytes (NRVMs) with progesterone, a pregnancy hormone, induced PDK4 expression. Mifepristone, an antagonist of the progesterone receptor (PR), mitigated PDK4 induction, suggesting that PR-mediated pathway is responsible for this upregulation. Taken together, these studies indicate that the substrate switch in late pregnant mouse hearts resulting in decreased glucose oxidation and increased fatty acid utilization is likely by inhibition of PDH via PDK4 upregulation. Dysregulation of this switch could have implications for cardiac diseases during pregnancy.

Table of Contents

Acknowledgements

This work would not have been possible without the support, encouragement, and help of so many people.

First, I would like to thank Zolt Arany, my PhD mentor for encouraging and pushing me for the past 5 years. I still remember the first time I saw your poster during orientation week, and I remember asking you about PGC-1α and cancer. From then on, I've learned so much from your mentorship and support, and from exploring many different fields and projects together. Thank you for your time, patience and commitment to making me the scientist I am today.

Thank you also to Tony Rosenzweig, my adopted mentor this past year, who so kindly allowed me to join his lab to finish my graduate studies. I am extremely appreciative of your continuous support and have thoroughly enjoyed our conversations and all your career and research advice.

I am also extremely grateful for members of the Arany lab and Rosenzweig lab, past and present. At some point during my PhD candidacy, my lab became my home, and you were the people I saw all day every day. Thank you for the laughter, the conversations, the scientific collaborations and discussions. In particular, I would like to thank Mun Chun (MC) Chan, my official postdoc mentor – we have come a long way – from you proofreading my PQE, my grant proposal to now my dissertation, and from me eating your delicious blueberry lavender cheesecake to… still eating your delicious blueberry lavender cheesecake (☺) – thank you for all your help and conversations, I've learned so much from you. To Glenn Rowe, senior postdoc of the Arany lab, thank you for your encouragement and for letting me interrupt you whenever I needed help or had questions. To other members of the Arany lab, including Cholsoon Jang (my fellow grad student), Jim Rhee, Aihua Jiang, Srilatha Raghuram, Robin Thom, Shogo Wada, George Huang, Nicole Koulisis, Tiffany DeSouza, Ian Patten, Sophia Bampoh, Adeel Safdar and

Caitlin Farrell, thank you for all the research help, the fun times, the burger making contests, the curry contest, the secret Santas, etc. They are memories I will always cherish.

Thank you also to members of the BIDMC Cardiovascular Institute, including Dr. Saumya Das and lab, especially Bridget Simonson, Vinita Sabramanya, and Kirsty Danielson – I am so grateful for your friendship, the conversations about life, and for reminding me that I should go home earlier; Heather Campbell (for answering my countless questions about budget and ordering); and Henry, Henrietta, and B.T. Glen for keeping me company during the long and late nights in lab.

I especially have to thank the Biological and Biomedical Sciences (BBS) office for their continuous support. Kate Hodgins, Maria Bollinger, and Daniel Gonzalez - thank you so much for allowing me to drop by whenever with questions or concerns. I would also like to thank Dr. David Cardozo at the DMS office for meeting with me several times individually. Dr. Cardozo and the BBS office were so supportive in making sure I made the right decisions with Zolt's move to Penn. I really could not have made it through without your help!

I also have to express much gratitude to my dissertation advisory committee (DAC) members, Dr. Norbert Perrimon, Dr. Laurie Goodyear, and Dr. Joseph Loscalzo. Your feedback and insights at each of my DACs were so helpful. Thank you also for bearing with me as I switched projects, and for meeting up with me and speaking with me individually on projects or career decisions. Thank you also for my defense committee members, Dr. Norbert Perrimon, Dr. Lawrence Young, Dr. C. Ron Kahn, and Dr. Thomas Michel – I really appreciate your taking the time to be on my committee and for your feedback and insights on this thesis.

None of this work would have been possible without assistance from collaborators. I am so grateful for help from the following people: Dr. Ananth Karumanchi and lab, including Sarosh

Rana, Suzanne Burke, and Dong Zhang (for teaching me how to set up timed pregnancies, echos, placental conditioned media incubations and sFlt ELISAs); Dr. Ronglih Liao and lab, including Weiting Chang, Seoun Ngoy, and Sudeshna Fisch (for so kindly allowing me to use your Langendorff apparatus while teaching me to do it at the same time); the Longwood Small Animal Imaging Facility (SAIF), especially Soumya Ullas (for all your help with imaging and the wonderful conversations during); the Penn Diabetes Research Mass Spectrometry Core, especially Wenyun Lu and Josh Rabinowitz (for answering all my emails, questions, and so promptly processing my samples); the CLS animal facility staff, especially Janet Veloz and Andrew Sumski (for so patiently responding to my questions and so kindly placing my mouse orders, even in the midst of all my mistakes); Dr. Laurie Goodyear and lab, especially Michael Hirshman (for answering all my questions about muscle incubations, antibodies, and subcellular fractionations); Dr. Lijun Liu and lab (for your patience and help with cardiomyocyte isolations, Langendorff perfusions, and all the countless career advice, and especially spending time during your conference in Boston in my lab to show me how you hang rat hearts); the Microscope core at BIDMC, including Lay-Hong Ang and Yi Zheng (I think I asked you so many questions and made you walk back and forth numerous times, thank you for your patience!); Dr. Barbara Kahn and lab, especially Odile Peroni (for GLUT4 mice reagents); Dr. Jack Lawler for CD36 reagents; Dr. Adam Wende for PDK4 KO mice samples; Dr. Robert Harris for PDK4 antibody and numerous email exchanges; Dr. Takashi Matsui for so patiently helping me with subcellular fractionation, with countless emails, protocols and images; and Dr. Daniel Kelly for speedily providing PDK4.Luciferase constructs.

I would also like to thank those who responded my email requests for help. There were countless emails that went unanswered, so for those who did take the time to respond, including Dr. Steven Kolwicz, Dr. Gary Lopaschuk, and Dr. Patrick Catalano, thank you so much.

I also have to thank the people who made sure I was not in lab on a Friday or Saturday night. These include my friends from the BBS program, people who I have shared so many wonderful memories of graduate school with, including late night game nights, movie nights, traveling to NYC for Colbert and the Daily Show and exploring Boston and the New England area. To: Palak Amin, Elaine Lim, Rigel Chan, and Ying Kai Chan, thank you for all the countless conversations, the Friday night dinners, and the laughter and fun.

Finally, thank you to my family. To the people who knew me before grad school, stuck with me through the hard times of grad school, and who is every bit as responsible for my successes as I am. Thank you especially to my mom, Qian Dong, who has been there for me at every step of my life and who helped me get through the toughest days in grad school, always with the best outlook, optimism and advice. I still remember being in the car with her at 9-years-old, telling her that I had decided to get a PhD, although I am pretty sure I was completely unaware of what it meant. Thank you also to my stepdad (Xinjian Yan), friends close to my heart (Toni and Mickey Haynes), grandma (Xunchun Zhang), aunts (Hui Dong and Wen Liu), uncles (Lifeng Shan and Rongli Sun), and my aunts watching from the stars and the moon (Bing Dong and Ying Dong). I am so grateful for family like you.

Dedication

To my mother (Qian Dong) and grandmother (Xunchun Zhang)

None of this would have been possible without your

love, encouragement and sacrifices.

Thank you.

Figures and Tables

Chapter 1

Chapter 2

Chapter 3

Appendix

Chapter 1: Introduction

Systemic maternal metabolism during pregnancy

The maternal adaptations that occur during pregnancy are complex, coordinated, and dynamic. Profound systemic metabolic changes occur, all to facilitate the growth and well-being of the fetus and placing the needs of the mother second. During early pregnancy, where growth is relatively slow (and placental formation and development of embryonic and gross fetal anatomical features take precedence), maternal metabolism is characterized as anabolic, in which increases in fat storage and insulin sensitivity promote the hoarding of nutrients. This is all in preparation for late pregnancy, a time when both fetal growth and maternal output are at its highest and a time of the greatest energetic needs, which is accordingly deemed a catabolic state (Figure 1.1). Serum changes in many of the macronutrients throughout gestation are presented in Table 1. Concurrently, the hormonal milieu is also dynamically altered during pregnancy (Figure 1.2). Human chorionic gonadotropin (hCG) is secreted early on and acts to signal the initial adaptations of pregnancy, including maintenance of the early secretion of progesterone, which along with estrogen, prolactin, and cortisol, acts to transform the maternal environment for fetal development. The changes in hormone levels are thus synchronized to maternal metabolic alterations, all working in concert to promote the prosperity of the fetus.

Table 1 Maternal serum concentrations of energy substrates in non-pregnant controls, early, and late pregnancy

	Not pregnant	Early pregnancy (5–12 weeks)	Late pregnancy (>32 weeks)
BMR (kJ/24 h)[7]	5430 ± 660[a]	5540 ± 660	7180 ± 1180
Plasma volume (mL)[114]	2699[b]	2768	3689
Serum values			
Fasting glucose (mmol/L)[115]	4.6[c]	4.2	3.9
Fasting insulin (μU/mL)[115]	5.5[c]	4.5	7.5
Free fatty acids (μEq/L)[116]	n.r.	814	900
Triglycerides (mg/dL)[117,118]	77 ± 34	79 ± 27	245 ± 73
LDL (mg/dL)[117,118]	99 ± 23	90 ± 17	136 ± 33
HDL (mg/dL)[117,118]	69 ± 10	67 ± 12	81 ± 17

n.r., not reported; BMR, basal metabolic rate.
[a]Pre-pregnancy.
[b]6–8 weeks postpartum.
[c]10–12 weeks post-natal.

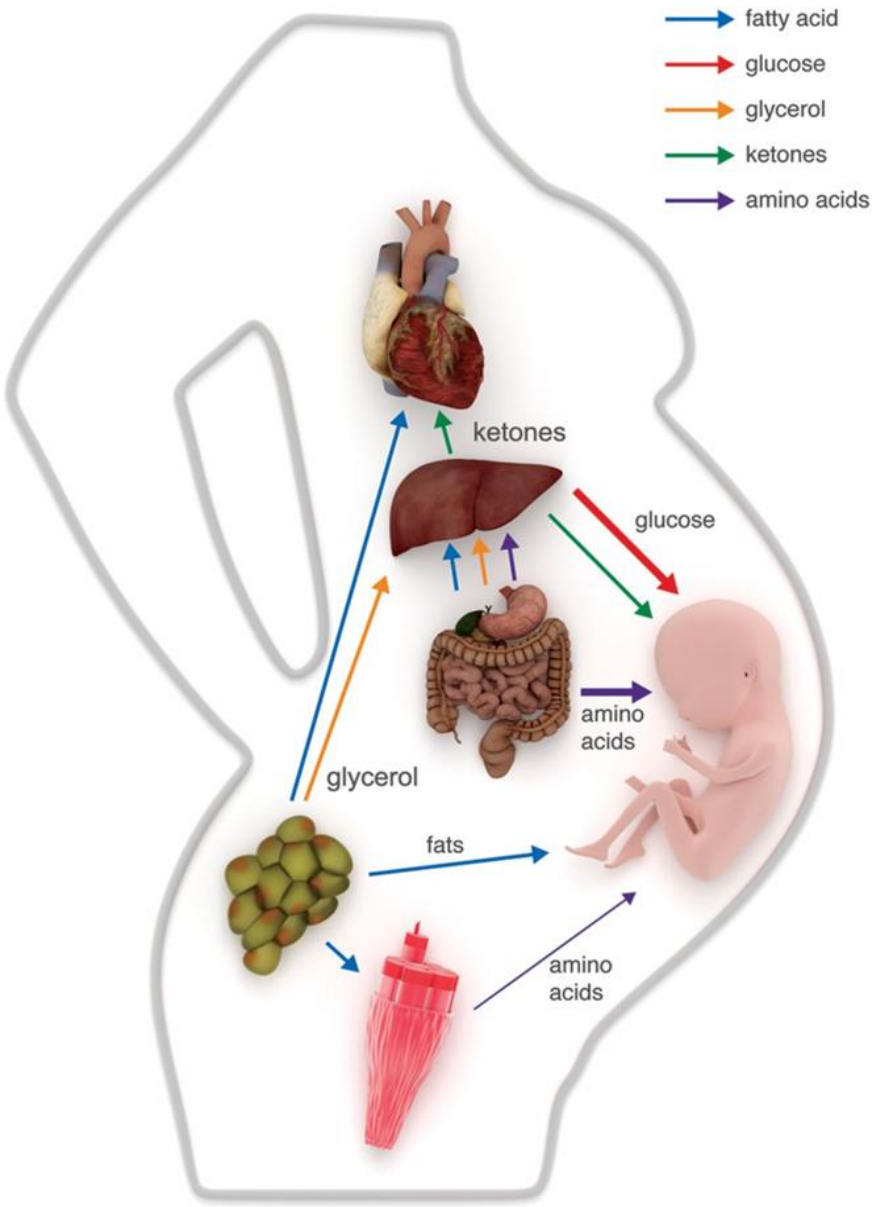

Figure 1.1: Metabolic changes during late pregnancy. Late pregnancy is marked by maternal catabolism that serves to support the dramatic anabolic growth of the foetus. The liver uses glycerol and (less so) amino acids to make glucose for the foetus and consumes fats, generating in the process ketones that are usable by the brain, muscle, and foetus. Adipose tissue releases fatty acids for consumption by both the liver and muscle. The foetus uses amino acids, fats, and roughly half of incoming glucose for anabolic growth, while largely relying on the other half of glucose for energetic needs.

Glucose metabolism

Alterations in glucose metabolism during pregnancy have been well characterized (King, 2000; Lain and Catalano, 2007). The main energetic substrates for the developing fetus are approximately 80% glucose and 20% amino acids, and maternal metabolism acquiesces to those needs by deferring its own glucose usage (Battaglia and Meschia, 1978). Fasting glucose levels begins to decline in the second trimester, and ultimately decreases by 10% by late pregnancy (Lind, 1979). Interestingly, hepatic glucose production increases by 16-30% (via gluconeogenesis and glycogenolysis), and an increase in fasting insulin levels is observed as well

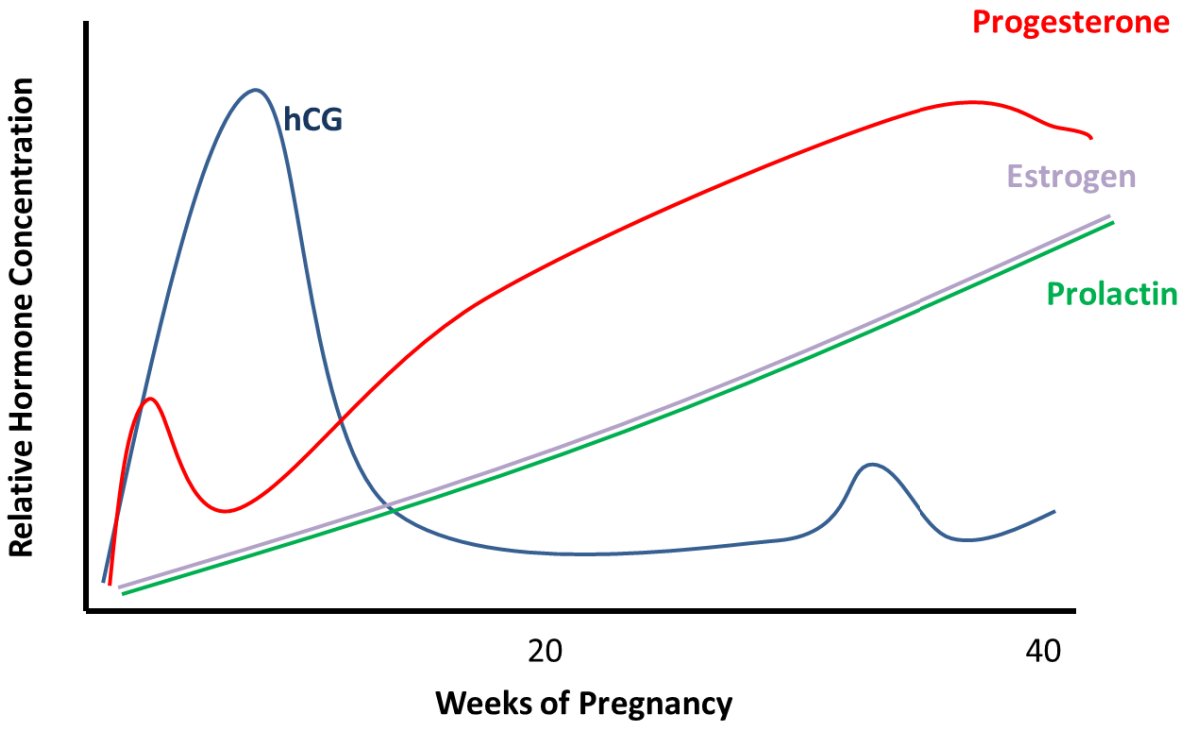

Figure 1.2: Hormonal milieu of pregnancy. Throughout pregnancy, hormones are secreted both early and late, and have been found to be responsible for many of the maternal adaptations of pregnancy. Human chorionic gonadotropin (hCG) is secreted early on and acts to signal the initial adaptations of pregnancy. Progesterone, estrogen, and prolactin all steadily increased throughout pregnancy and peak by around late pregnancy.

(Butte, 2000). Insulin sensitivity is also profoundly affected, as measured by euglycemic-hyperinsulinemic clamps (Buchanan et al., 1990; Catalano et al., 1991; Ryan et al., 1985). In early pregnancy, an approximately 10% decrease in sensitivity is observed, compared to non-pregnant. However, by late pregnancy, various studies have found decreases from 33-78%, a change so drastic that late pregnancy is comparable to a type 2 diabetic state. Furthermore, this may be an underestimate as the fetus utilizes insulin-independent glucose consumption methods. Serum glucagon, on the other hand, is much less affected, and minimal to no changes have been found in late pregnancy.

The mechanisms of insulin resistance in late pregnancy are unknown, although many studies have pointed to hormones as being responsible. Many hormones, including human placental lactogen (HPL), progesterone, prolactin, and cortisol can affect insulin sensitivity (Newbern and Freemark, 2011; Ryan and Enns, 1988; Sutter-Dub, 1979). One placental cytokine, however, has been more strongly correlated to decreased sensitivity than others and was the only predictor among all the hormones to be a strong indicator of insulin responsiveness – tumor necrosis factor-α (TNF-α) (Kirwan et al., 2002). *In vitro* studies have shown that TNF-α affects insulin signaling pathways by increased serine phosphorylation of insulin receptor substrate-1 (IRS-1), therefore preventing interactions with the insulin receptor (Hotamisligil et al., 1996; Rui et al., 2001).

Insulin secretion increases steadily during pregnancy, by approximately 50% in mid-pregnancy, before peaking in the third trimester (Bleicher et al., 1964). This increase is not in response to insulin resistance, as that occurs before the onset of insulin resistance, but is in parallel with the establishment of the placenta and production of hormones during pregnancy; however, it is not clear if hormones contribute to this phenotype. Pancreatic β-cells are also

affected and become hypertrophic and hyperplastic in both animal and human pregnancies (Van Assche et al., 1978). Furthermore, in the limited studies available, there is evidence of greater insulin secretion and synthesis on the cellular level. Lactogenic hormones and activation of the serotonin synthesis pathway in β-cells are responsible for this expansion in order to meet insulin needs during pregnancy (Brelje et al., 1994; Huang et al., 2009; Kim et al., 2010).

Thus, as glucose is the primary substrate source for the fetus, maternal glucose metabolism is altered in many ways, including adapting insulin secretion and sensitivity, so as to facilitate fetal needs.

Lipid Metabolism

Maternal usage of lipids as the primary energy source is the result of the anabolic to catabolic transition that occurs by late pregnancy and facilitates the fetal usage of amino acids and glucose. Maternal adipose stores increases by as much as 3.5 kg on average by late pregnancy, second only to increases in total body weight (Lain and Catalano, 2007). Insulin resistance dictates lipolysis in adipose tissue. Free fatty acids (FFA) and glycerol that are liberated from adipose during pregnancy go to the liver, where they are then re-packaged into VLDLs and released back to the circulation. Thus, a concurrent increase in serum lipids is observed (potentially a result of estrogen effects on the liver), to establish a hyperlipidemic state of 2-4 fold increases in triglycerides, a 25-50% increase of total cholesterol and a 50% increase of LDL (Mshelia et al., 2010). The environment that is created is relatively atherogenic and can increase the risk of endothelial damage during pregnancy. Glycerol is also the primary substrate for gluconeogenesis, allowing amino acids to be saved as a substrate source for the fetus (Zorzano and Herrera, 1986). In addition to the increase in gluconeogenesis in the liver,

ketogenesis is also observed, as another method to decrease maternal glucose usage (Remesy and Demigne, 1986). Ketone bodies can also cross the placental barrier to become a source of energy for the fetus (Herrera, 2002; Seccombe et al., 1977).

The fetus is also capable of taking up fatty acids. Maternal lipoproteins cannot themselves cross the placenta, and so they become a "floating energy deposit" (Ghio et al., 2011). Placental lipoprotein lipases (LPL) can interact with lipoproteins, as can fatty acid binding proteins, to take up the fat (Herrera et al., 2006). The imported lipids are then used for membrane support, triglyceride synthesis, or for the development of adipose tissue. It was previously believed that fetal oxidation of lipids did not exist, due to lack of machinery available during gestation and the presence of malonyl CoA, which can indirectly inhibit β-oxidation. However, recent work has detected both the activity of enzymes involved in fatty acid oxidation and presence of different acylcarnitine species in human fetal tissues (Oey et al., 2006; Rebholz et al., 2011). Perturbations of lipid oxidation also greatly affect fetal growth, leading to smaller fetal sizes or lethality.

Protein metabolism

For both glucose and fat metabolism, adaptations during pregnancy are made in response to existing maternal needs. However, the same is not true for protein metabolism (Kalhan, 2000). Most of the adaptations made are in anticipation of maternal and fetal needs later on as protein metabolism changes early in gestation before fetal growth has drastically increased. What is similar between glucose, fat and protein metabolism is that the end goal is to conserve energy in order to provide for the fetus. There are two ultimate paths for amino acids – they can be either oxidized or stored in tissues. Most amino acids in pregnancy are used for protein synthesis, as the

mother undergoes significant increases in tissue volume. Though there is a net increase in protein storage, there is also an observable decrease in oxidation or catabolism of amino acids that is detected by urea synthesis. Using stable isotope tracers in mice, an approximately 30% decrease in the rate of urea synthesis is observed in the first trimester, and 45% decrease by the third trimester (King, 2000).

Along with glucose, amino acids are another source of substrate for the fetus, accounting for approximately 20% of energetic needs. Thus, maternal metabolism diverts usage of amino acids to facilitate the needs of the fetus. As expected, serum levels of amino acids decrease during pregnancy, and fasting induces hypoaminoacidemia and a reduction in gluconeogenic amino acids (Felig et al., 1972; Schoengold et al., 1978). Furthermore, branched chain amino acid (BCAA) oxidation is also decreased during late pregnancy (Kalhan et al., 1998).

Profound maternal adaptations occur to cater to the needs of the fetus. Early pregnancy is an anabolic environment, while late pregnancy is catabolic, all to satisfy fetal demands. Glucose, lipid, and amino acid levels change to prioritize fetal consumption of glucose (Figure 1.1). Much of the molecular mechanisms responsible for these alterations are unknown and not well studied, though the hormonal milieu has been independently found to be associated with many of these metabolic changes.

Normal cardiac metabolism

Every second of every day, the heart is dutifully working, pumping blood and nutrients out to supply energy to the rest of the body. Any breach to this fidelity and catastrophic disaster

Figure 1.3: Normal cardiac metabolism. Under normal physiological conditions, cardiomyocytes use approximately 70% fatty acid as substrate sources and 30% glucose as substrate sources. Glucose enters the cell via glucose transporters, such as GLUT4, and then undergo glycolysis to form pyruvate that is then converted to acetyl CoA. Pyruvate can also be converted to lactate that can exit the cell, but lactate can also be taken up by cardiomyocytes to form pyruvate. Similarly, fatty acids enter the cell through their respective transporters, such as CD36, and ultimately is transported to the mitochondria to undergo β-oxidation to form acetyl CoA. Acetyl CoA then enters the TCA cycle, which creates and donates reducing equivalents in the form of NADH and $FADH_2$ to the ETC. Electron transfer through the ETC leads to creation of a proton gradient that ultimately leads to the production of ATP by ATP synthase. Due to the high energy demands of the heart, regulation of these pathways can occur at many locations to ensure that constant supply of substrates is always met. Different points of regulation are marked with numbers 1-5: (1) transporter localization; (2) phosphofructokinase-1 (PFK-1); (3) pyruvate dehydrogenase (PDH); (4) lipoprotein lipase (LPL); and (5) malonyl CoA concentrations.

Figure 1.3 (continued)

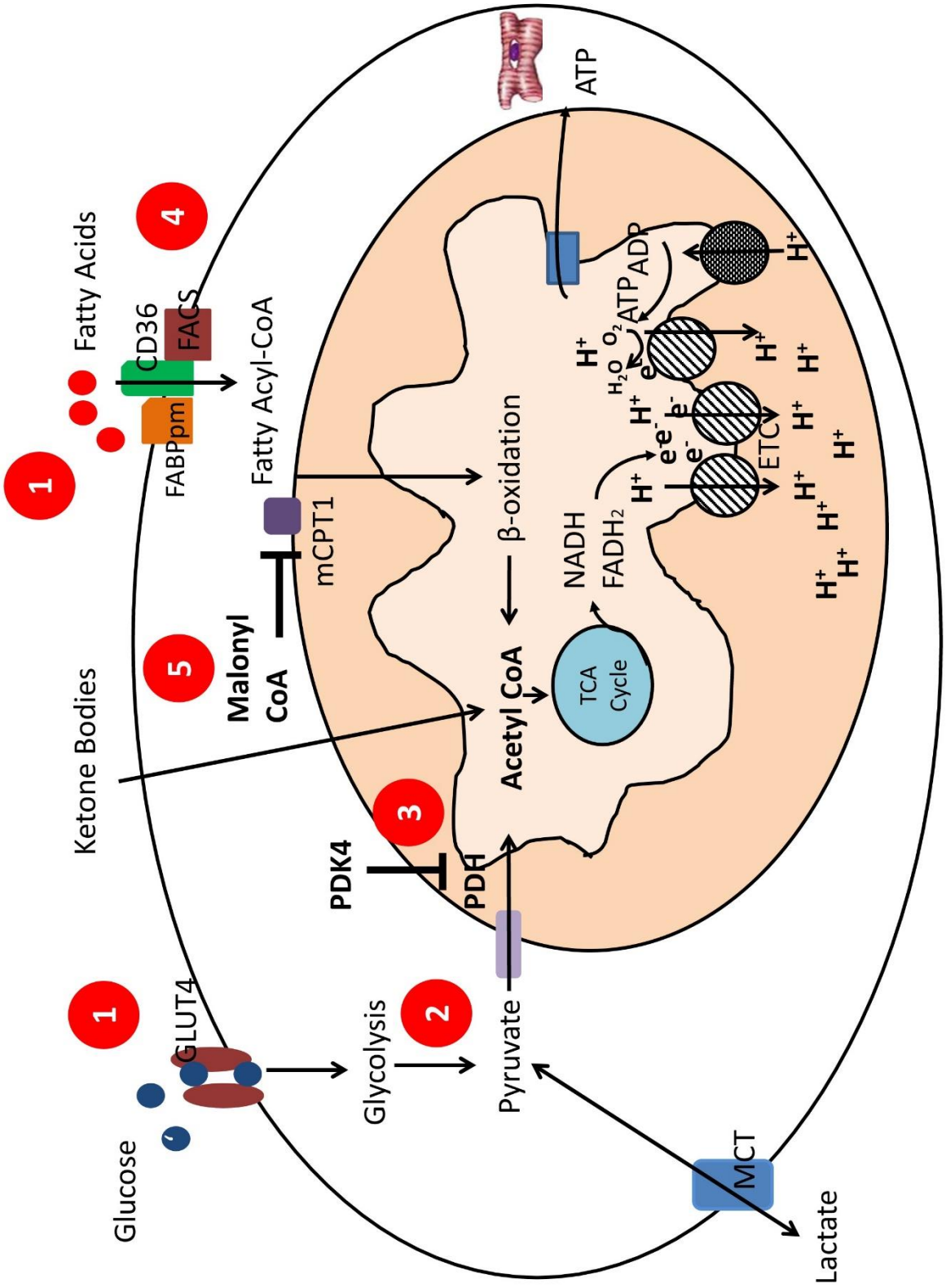

could occur. Thus, it is vitally important that the myocardium fully satisfies its demands. The heart has extremely high energetic needs, the highest amongst all the organs. This is especially critical given its low energy reserves and complete ATP turnover every 10 seconds. Tight metabolic regulation is therefore also necessary to ensure that depletion of energy resources never occurs. There are many facets of regulation, including gene transcriptional control, post-translational modifications, allosteric alterations to critical enzymes, the relative concentrations of substrates to products, level of hormones present in the plasma, and transporter localization in the cell (Kolwicz et al., 2013; Lopaschuk et al., 2010; Stanley et al., 2005).

Thankfully, the heart is "omnivorous", and is able to utilize many different substrates as energy sources. This means that under conditions of stress or disease, when glucose or fat may become limited, the heart is able to continue its high energy output by using other substrates, such as ketone bodies during starvation, amino acids during ischemia, and lactate during exercise (Drake et al., 2012; Gertz et al., 1988; Gold and Yaffe, 1978; Mazer et al., 1990; Stanley, 1991). However, in times of nutrient abundance, the myocardium metabolizes predominantly fatty acids, approximately 60-90%, and satisfies the remaining 10-40% from glucose (Bing et al., 1954). Furthermore, approximately 95% of the ATPs generated are by oxidative phosphorylation in the mitochondria, highlighting the importance of this organelle to sustaining energy needs. The ATPs generated are then used mainly for contractility and to power calcium ATPases and ion pumps.

To fully understand how the heart preferentially utilizes its substrate sources, it is useful to review basic metabolism (Figure 1.3). Glycolysis and fatty acid β-oxidation all converge on a single mitochondrial substrate, acetyl CoA that then enters the tricarboxylic acid (TCA) cycle. However, their beginnings are very different. The source substrates for glycolysis are exogenous

glucose, which can enter the cell via specialized glucose transporters (GLUTs), of which GLUT4 and GLUT1 are the predominant myocardial GLUTs, or stored glycogen, which can be broken down to glucose-6-phosphate to enter glycolysis (Bell et al., 1990). As the glycogen storage pool in the heart is very small and has a rapid turnover, the primary cardiac glycolytic substrate is exogenous glucose (Goodwin et al., 1995; Henning et al., 1996). The net result of glycolysis, which occurs in the cytosol, is two molecules of ATP, pyruvate and NADH. It has been shown that most glycolytic enzymes reside near the sarcolemmal membrane and the sarcoplasmic reticulum (SR), and that the ATP generated from glycolysis is preferentially used for ion channels at these locations (Xu and Becker, 1998; Xu et al., 1995). The end metabolite of glycolysis is pyruvate, which then has three fates: (1) to be converted to lactate and subsequently secreted from the cell; (2) to enter the mitochondria via pyruvate carriers and be decarboxylated to acetyl CoA; or (3) to be carboxylated to TCA intermediates oxaloacetate or malate, a process known as anaplerosis, which accounts for ~5% of flux through the TCA cycle (Brin and Olson, 1952; Smyth, 1940; Spydevold et al., 1976). The purpose of anaplerotic reactions is to replenish and maintain the pool of intermediates available in the TCA in the face of cataplerotic exit.

Fatty acids, on the other hand, arrive at acetyl CoA through a different pathway (Su and Abumrad, 2009). First, as extremely hydrophobic entities, they are unable to travel alone – thus, they enter either bound to albumin or more commonly, in lipoproteins. Lipoprotein lipases (LPL) on the surfaces of endothelial cells can hydrolyze triglycerides to extract fatty acids, which can then enter the cardiomyocyte (Pulinilkunnil and Rodrigues, 2006). There are four factors on the membrane to facilitate uptake, including a fatty acid translocase (FAT), called CD36, the plasma membrane fatty acid binding protein ($FABP_{PM}$), fatty acid transport proteins 1/6 (FATP1/6), and fatty acyl-CoA synthase (FACS) (Ellis et al., 2011; Gimeno et al., 2003; Goldberg et al., 2009;

Paul et al., 2014; Schaap et al., 1999; Sorrentino et al., 1988). The presence of FACS on the membrane allows rapid esterification of the incoming fatty acid. Once inside the cell, the fatty acid has two fates: storage as triglycerides, which occurs to approximately 20% of the incoming fatty acids, or continuation on the path towards β-oxidation. To do the latter, the fatty acid must enter the mitochondria, where β-oxidation takes place. This occurs via a carnitine-based transporter system that includes various enzymes and carriers, including carnitine palmitoyltransferase I (CPT-I), a heavily regulated enzyme located on the outer mitochondrial membrane, and CPT-II, located on the inner mitochondrial membrane (Bremer, 1983). The end product is the presence of long chain acyl CoAs in the mitochondria, where they can then undergo β-oxidation to create acetyl CoAs, NADH, and $FADH_2$.

Acetyl CoA formed from both glycolysis and fatty acid oxidation enters the TCA cycle, where it produces reducing equivalents in the form of NADH and $FADH_2$ that act to deliver electrons to the electron transport chain (ETC) located on the inner mitochondrial membrane (Stanley et al., 2005). The donation of electrons to the ETC couples the reduction of oxygen into water to generate a proton gradient that ultimately powers the ATP synthase to form ATP from ADP. This ATP is then used to power the cardiomyocyte for many different processes. Thus, the complete oxidation of glucose through aerobic metabolism generates >30 molecules of ATP, compared with the two molecules that form from glycolysis alone.

Regulation of cardiac metabolism

In order to ensure constant substrate supply to the heart, regardless of stress or external environment, many regulatory points exist in these metabolic pathways (Figure 1.3). First, the levels of substrate availability greatly determine usage – for example, fatty acid concentrations

can range from 0.2-0.8 mM throughout the course of a day (Dole, 1956). Furthermore, during conditions of ischemia, early starvation, or diabetes, levels can increase to greater than 1.0 mM (Gold and Yaffe, 1978; Roy et al., 2013; Yi et al., 2006). Elevated concentrations of fatty acids can compete with glucose for substrate uptake, through the "Randle cycle" or the "glucose-fatty acid cycle," in which elevated fatty acid oxidation rates can decrease glycolysis. Conversely, decreases in plasma fatty acid concentrations will activate oxidation of pyruvate. Secondly, the transporters that are responsible for uptake of substrates are also regulated by their localization. CD36 and GLUT4 are normally located in intracellular vesicles and upon stimulation with insulin or contraction, can travel to plasma membranes, to allow uptake of their corresponding substrates (Bonen et al., 2000; Boucher et al., 2014; Gimeno et al., 2003; Luiken et al., 2002a; Slot et al., 1991). Many signaling pathways regulate transporter localization. The PI3K/Akt pathway, for example, has been well studied to trigger GLUT4 vesicle translocation upon activation by insulin signaling (Matsui et al., 2001; Walsh, 2006). The AMP-activated protein kinase (AMPK) pathway is another that is critically involved in sensing nutrient status and responding accordingly (Zaha and Young, 2012). Known as the "cellular fuel gauge," it is a pivotal defense against cellular stresses. For example, upon detecting high ratios of AMP/ATP, ADP/ATP, or Cr/PCr, AMPK will then phosphorylate downstream targets, including the GTPases that control GLUT4 and CD36 vesicle fusion in order to promote plasma membrane localization of transporters (Chavez et al., 2008; Thong et al., 2007). In addition, AMPK can inhibit endocytosis of GLUT4 or CD36-containing vesicles (Yang and Holman, 2005).

Another regulatory point is through pivotal enzymes in metabolic pathways to control flux. For example, phosphofructokinase-1 (PFK-1), a glycolytic enzyme involved in the first irreversible step of glycolysis to make fructose-1,6-bisphosphate (F-1,6-BP), is activated by ADP

and AMP, but inhibited by ATP, citrate, and its end product, F-1,6-BP (Mor et al., 2011). Hormones, such as insulin, glucagon, and epinephrine, are also known to regulate its activity, as well as post-translational modifications, such as phosphorylation by AMPK (Marsin et al., 2000). Pyruvate dehydrogenase (PDH), another critical enzyme, catalyzes the conversion of pyruvate to acetyl CoA (Kobayashi and Neely, 1983a, b). This enzyme is instrumental in regulating the entry of carbons into the TCA cycle from glycolysis, and is itself regulated by a family of kinases and phosphatases (Jeoung and Harris, 2010; Zhang et al., 2014). The pyruvate dehydrogenase kinase (PDK) family, of which PDK2 and PDK4 are most prominently expressed in the heart, can phosphorylate and inactivate PDH to block pyruvate contribution to the TCA cycle (Holness and Sugden, 2003). It is a key step in shifting the contribution of carbons from glycolysis to that of fatty acid oxidation. PDK4 is known to be regulated by many processes. States of starvation, diabetes, and hypoxia, in which FFA are in abundant, activate PDK4 to inhibit pyruvate conversion to acetyl CoA (Razeghi et al., 2001; Wu et al., 1998). Conversely, states in which there are decreases in the acetyl CoA:free CoA or NADH:NAD+ ratios inhibit PDK4 to activate PDH (Lee et al., 2004).

Enzymes in the fatty acid oxidation pathway also are subject to regulation as well. For example, the activity of LPL determines the fat uptake status of the heart (Augustus et al., 2004). In nutrient states in which there are greater fatty acid oxidation, such as diabetes or starvation, elevated activity and levels of cardiac LPL is observed on the endothelial lumen (Kersten, 2014; Kotlar and Borensztajn, 1977; Sugden et al., 1993). AMPK can also increase the amount of LPL present on the endothelium (An et al., 2005). CPT-I, which is involved in the formation of long chain acylcarnitines, is another critical point of control. Malonyl CoA binds to and strongly inhibits CPT-I, acting as a negative regulator of fatty acid oxidation (Foster, 2012; McGarry et

al., 1977). Malonyl CoA has an extremely rapid turnover time, with a half-life of approximately 1.25 minutes. Thus, when levels of malonyl CoA decrease, rates of fatty acid oxidation increase. Carboxylation of cytosolic acetyl CoA by the enzyme acetyl CoA carboxylase (ACC) forms malonyl CoA, and decarboxylation of malonyl CoA by malonyl CoA decarboxylase (MCD) creates more acetyl CoAs. Mouse models with genetic ablation of ACC increase oxidation of fatty acids, as expected due to decreased malonyl CoA levels (Kolwicz et al., 2012). AMPK can phosphorylate and inhibit ACC, preventing malonyl CoA formation to augment fatty acid oxidation (Park et al., 2002).

Nitric oxide (NO) has also been shown to have direct effects on cardiac metabolism. In addition to its known role as a vasodilator, many studies have found that NO can directly alter substrate usage. Infusion of dogs with L-NAME, an inhibitor of NO, for 10 days increased glucose oxidation, while decreasing fatty acid oxidation (Recchia et al., 1999; Recchia et al., 2002). In addition, hearts from eNOS-deficient mice increase glucose uptake (Tada et al., 2000). Consistent with all this, dogs treated with a NO donor, nitroglycerin, had blocked AMPK-induced GLUT4 translocalization during ischemic insult.

Another vital point of regulation is transcriptional regulation of metabolic genes (Leone and Kelly, 2011). The family of nuclear receptor transcription factors collectively known as the peroxisome proliferator-activated receptors (PPARs) has been well characterized in terms of their contribution to cardiac flux control. The three members of the PPAR family are PPARα, PPARβ/δ, and PPARγ, of which PPARα is best known to upregulate fatty acid oxidation genes in the heart. When PPARα is upregulated, genes involved in all facets of fatty acid uptake and oxidation are concurrently induced, including CD36, FATP1, FABP, FACS, MCD, CPT-I, and PDK4. Mice with deletion of PPARα show decreased expression of fatty acid genes and

decreased fatty acid oxidation (Gilde et al., 2003). Conversely, overexpression of PPARα shows an increase in fat uptake, oxidation, and cardiac lipotoxicity (Barger et al., 2000). The PPARs are also known to be activated by another well-characterized family of transcriptional coactivators, the PGC-1 (PPARγ coactivator 1) family, of which PGC-1α is the best studied member (Rowe et al., 2010). PGC-1α can activate mitochondrial biogenesis, fatty acid oxidation and oxidative phosphorylation by co-activating with multiple transcription factors, including ERRs and PPARs (Patten and Arany, 2012; Russell et al., 2004). Though mice with cardiac-specific deletion of PGC-1α have normal mitochondrial content, they still have decreased oxidative phosphorylation and contractile function (Arany et al., 2005). Furthermore, they also develop heart disease during pregnancy, similar to a clinical condition known as peripartum cardiomyopathy (PPCM).

Changes in substrate utilization occur during neonatal development and in certain disease states. For example, embryonic and fetal cardiac development are both characterized by a dependence on glycolysis and lactate production (Lopaschuk and Jaswal, 2010). There is very little detectable fat usage. It is not until 7 days after birth that a shift occurs in substrate preference, more closely matching what is observed in adult hearts (Taegtmeyer et al., 2010). PPARα, PGC-1α, and AMPK expression levels parallel the increase in fat consumption. During diseased states, another substrate change, known as “fetal shift,” is a hallmark of heart failure. Human positron emission tomography (PET) studies of heart failure patients have shown a decreased utilization in fatty acids and an increase in glucose (Davila-Roman et al., 2002; Yazaki et al., 1999). Much work has gone into understanding how this shift occurs and whether it is a beneficial or maladaptive response.

Myocardial and hemodynamics alterations in pregnancy

Maternal systemic metabolism undergoes major shifts in order to facilitate the growing needs of the fetus. This is reflected in the adaptations that occur in cardiac metabolism, both in response to fetal demands and also increased demands for cardiac work (Melchiorre et al., 2012). Though there have been many studies devoted to characterizing the hemodynamic changes that occur throughout pregnancy, many discrepancies have been observed, owing to varying methods of data collection and analysis (Bamfo et al., 2007; Turan et al., 2008; Zentner et al., 2009). For example, the small sample size of many studies have led to conclusions that may be more indicative of individual profiles rather than the collective majority. Furthermore, different measurement tools/methods or inconsistent use of controls, such as non-pregnant, early pregnancy or post-partum stages, have also contributed to contradicting conclusions (Hinderliter et al., 1992; Masaki et al., 1989; Volman et al., 2007). Thus, it is important to understand the exact experimental parameters of each experiment before making conclusions.

Even though there is variability in hemodynamic measurements during pregnancy, some parameters are consistent and reproducible. An increase in preload is seen, owing to the rise in blood volume, which contributes to the "physiological anemia" of pregnancy. There is also a concomitant decrease in afterload, in accordance with decreases in systemic vascular resistance (SVR) and mean arterial pressure (MAP) starting in the fifth week of pregnancy and peaking at the beginning of the third trimester (Capeless and Clapp, 1989; Gilson et al., 1997; Savu et al., 2012). The hormonal environment has been hypothesized to be responsible for the alterations in preload and afterload. For example, vasodilators, such as NO and prostaglandins, have been shown to decrease peripheral resistance (Anderson et al., 1976; Haynes et al., 1993; Shaamash et al., 2000).

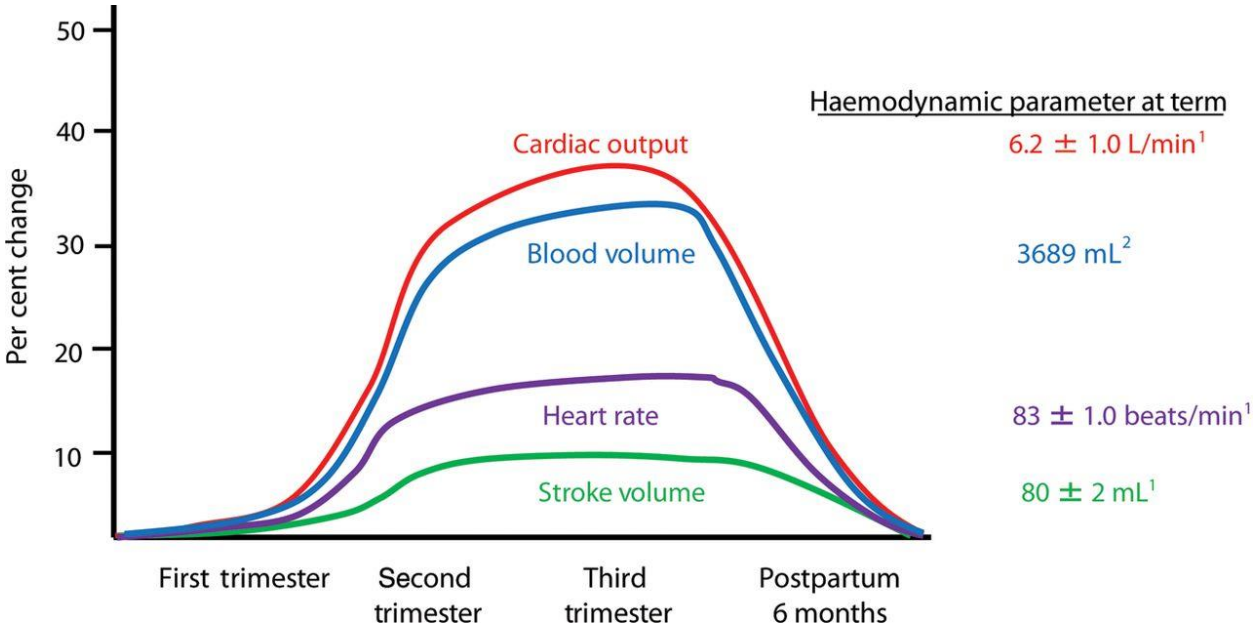

Figure 1.4: Hemodynamics changes during pregnancy. Cardiac output, heart rate, stroke volume, and blood volume all increase between 5 and 8 weeks of gestation, peak by mid-pregnancy, and is sustained until the end of pregnancy. These parameters are reversed by 6 months postpartum. 1, Clark *et al*., 1989; 2, Hytten and Paintin, 1963.

Other cardiac parameters, such as cardiac output, have been extremely well characterized and found to be consistent among different studies (Figure 1.4). Beginning as early as the fifth week of pregnancy, cardiac output starts to increase, rising to as much as 50% above baseline at its peak around mid to late pregnancy (Capeless and Clapp, 1989; Gilson et al., 1997; Hunter and Robson, 1992; Mabie et al., 1994; Mone et al., 1996; van Oppen et al., 1996). By two weeks postpartum, this effect is reversed. Cardiac output measurements are secondary to heart rate and stroke volume, which increase by approximately 15-30% and 15-25% at their peak, and also return to normal by 10-14 days postpartum. Systolic blood pressure, on the other hand, has been shown to stay constant throughout most of pregnancy while diastolic blood pressure decreases initially, is stable or slightly decreases throughout the second trimester, and finally increases near

the end of pregnancy (Atkins et al., 1981; Delachaux et al., 2006; Desai et al., 2004; Mabie et al., 1994; Mone et al., 1996; Volman et al., 2007; Zentner et al., 2009).

The discrepancies in hemodynamics studies surround systolic and diastolic cardiac function. Diastolic function is less studied, and different studies have come to divergent conclusions. Some have shown no alterations in diastolic function, while others have reported decreases by late pregnancy (Bamfo et al., 2007; Kametas et al., 2001; Mesa et al., 1999; Valensise et al., 2000; Zentner et al., 2009). Systolic function, as indicated by ejection fraction and fractional shortening, is better studied. However, increases, decreases, and no change have all been observed (Desai et al., 2004; Pandey et al., 2010; Valensise et al., 2000). Thus, these cardiac parameters are currently incompletely defined.

Structural and morphological changes also occur during pregnancy (Chung and Leinwand, 2014). By late gestation, enlargements in all four chambers of the heart are observed. Furthermore, wall thickness and mass also increase, as well as the size of all the valves. Eccentric cardiac hypertrophy has also been noted, due to the prolonged cardiac volume overload (Estensen et al., 2013). Individual cardiomyocyte size also increases with significant elongation observed in cardiomyocytes isolated from pregnant mouse hearts. The Akt/PI3K pathway, which is known to play a role in other cardiac hypertrophy models, is upregulated in mid-pregnancy and is sustained to the end of pregnancy (Chung et al., 2012b). Progesterone treatment of neonatal cardiomyocytes increases cell size, suggesting that hormones could be responsible for these adaptations. Blockage of MEK1 abrogated this effect, indicating that the cardiac hypertrophy of pregnancy is mediated through Akt and MEK1 pathways. One study found that the potassium channel Kv4.3 is downregulated during pregnancy, resulting in longer QT intervals and the tyrosine kinase c-Src is upregulated, contributing to cardiac hypertrophy of late

pregnancy (Eghbali et al., 2005). Ovariectomized mice treated with estrogen reproduced the pregnancy effects of Kv4.3 and c-Src, which was reversed by a receptor antagonist.

The molecular mechanisms underlying cardiac remodeling during pregnancy have also been studied (Chung et al., 2012b). The classical markers of pathological hypertrophy, such as the ratio of α-myosin heavy chain (MHC):β-MHC, skeletal α-actin, and atrial natriuretic factor (ANF), are unchanged during pregnancy. Furthermore, no cardiac fibrosis is detected in the pregnant heart as seen in the diseased heart.

Cardiac metabolism changes during pregnancy

The metabolic adaptations of the heart during pregnancy are not well characterized. However, a similar theme of forgoing energy sources to suit the needs of the fetus is present. The first experiments to study cardiac metabolism during pregnancy involved [^{3}H]-2-deoxyglucose tracer injections in rats to determine glucose utilization. The studies found decreases of 46% around mid-pregnancy (day 15), ultimately lowering to 74% by late pregnancy (day 20) (Sugden et al., 1992). Conversely, the same group also observed an increase in fatty acids and ketone bodies in late pregnant serum, but did not detect differences in cardiac PDH activity (Sugden and Holness, 1993a, e). More recently, studies found an increase in cardiac NO synthesis and eNOS expression in late pregnant dog hearts (Williams et al., 2008; Williams et al., 2007). This is accompanied by a decrease in glucose uptake and a corresponding increase in fatty acid uptake. Treatment with L-NAME reversed the effects seen, leading the group to conclude that NO plays a role in the substrate switch of late pregnancy. However, the precise mechanism is not known.

Mechanisms explaining this substrate switch are not fully understood. As mentioned previously, in one study, PDH activity is unchanged. Mitochondrial morphology remains normal

during pregnancy, as observed with confocal microscopy (Bassien-Capsa et al., 2006). The drastic decrease in glucose utilization does not match the small decrease in serum glucose levels. Furthermore, two studies in rats found no change in GLUT4 or PDK4 expression in late pregnancy (Nieuwenhuizen et al., 1998; Rimbaud et al., 2009).

The hormonal state of pregnancy could regulate the substrate switch that is observed. Most studies on the effects of estrogen on metabolism are in the context of hormone replacement therapy, but evidence of estrogen increasing fatty acid uptake is observed with PET (Herrero et al., 2005). In addition, estrogen also can increase both eNOS and NO levels. Furthermore, male mice with PPARα deletion have massive cardiac lipotoxicity that ultimately resulted in early mortality (Djouadi et al., 1998). However, estrogen supplementation in these mice rescued the phenotype, suggesting the importance of estrogen in regulating fatty acid utilization.

Thus, much work still needs to be accomplished in characterizing the metabolic changes in response to pregnancy.

Cardiac diseases during pregnancy

How do insufficient maternal metabolic adaptations during pregnancy lead to disease? In particular, can complications arise from deviant cardiac metabolism? Pregnancy is considered a stress test to the body, both exacerbating known problems and unmasking unknown complications. Gestational diabetes is characterized by the intolerance of glucose during pregnancy, which can be a result of the lack of β-cell changes in response to the insulin resistance environment of pregnancy. Preeclampsia, a disease that manifests in late pregnancy, is characterized by high blood pressure and proteins in the urine (Powe et al., 2011). In recognizing the effects of aberrant pregnancy alterations on the heart, the American Heart Association (AHA)

recently added diseases of pregnancy, such as preeclampsia, gestational diabetes, and pregnancy induced hypertension, as risk factors for cardiovascular disease (CVD) (Intapad and Alexander, 2013a, c). A woman who has had preeclampsia has double the risk of CVD approximately 5-15 years post-delivery. Could these derangements of pregnancy affect cardiac metabolic responses that manifest as CVD post pregnancy? The cardiac metabolic effects from these diseases have not been well studied.

The stress on cardiac function during pregnancy is also capable of revealing latent cardiac vulnerabilities. Women who have had a myocardial infarction during pregnancy have worse long term prognosis than those who have not (Kealey, 2010; Roth and Elkayam, 1996). In addition, pregnant mouse hearts undergoing ischemia/reperfusion injury show increased infarct sizes compared to non-pregnant controls (Li et al., 2012). The underlying mechanisms are unexplored, but the increased reliance on fatty acids during pregnancy could result in an inability of the heart to adapt when necessary to other insults.

A pregnancy-associated disease that directly affects cardiac capacity is peripartum cardiomyopathy (PPCM), a rare (affecting 1:300-1:3000 of live births) but deadly condition that occurs during late gestation or immediately postpartum (Bello et al., 2013). It is diagnosed by systolic heart failure in otherwise healthy women. Recent studies have pointed towards vascular insufficiency as the cause for PPCM, perhaps with a metabolic deficiency undertone. In mouse studies, cardiac deletion of the transcription factor STAT3 leads to PPCM (Halkein et al., 2013; Hilfiker-Kleiner et al., 2007). Prolactin, a hormone secreted in late pregnancy, is abnormally cleaved to a 16 kDa anti-angiogenic fragment by unregulated reactive oxygen species (ROS) response. Clinical trials with an inhibitor of prolactin secretion, bromocriptine, has showed promising but limited results. Another study corroborating vascular deficits of PPCM was in

mice with cardiac deletions in PGC-1α (Patten et al., 2012). As previously described, PGC-1α is a transcriptional co-activator known to regulate mitochondrial biogenesis, fatty acid oxidation, and the angiogenetic response. Female mice without PGC-1α become even more vulnerable to the anti-angiogenic environment of late pregnancy, and develop PPCM. Cardiac function was fully rescued with injections of bromocriptine and VEGF, suggesting that both models share a similar vascular dropout pathway.

How aberrant cardiac metabolic adaptations can contribute to PPCM has not been explored. The vascular deficiency state of PPCM (as seen in both STAT3 and PGC-1α knockout models) suggests that there is also an inadequate supply of nutrients and fuel to the cardiac tissues. In addition, PGC-1α is known to regulate PPARα, an important regulator of fat utilization, and depletion of PPARα could be detrimental to cardiac function. However, how this mechanism can be extrapolated to human PPCM is unknown.

Conclusion

Intense metabolic alterations occur during pregnancy, all in response to fetal demands for glucose. Systemic insulin resistance defines maternal metabolism. The heart also adopts this switch, although the regulatory mechanism for this have not been thoroughly explored. Understanding what contributes to metabolic flux control can have significant implications in pregnancy-associated cardiac diseases, including PPCM. We thus propose to examine in this thesis the maternal cardiac metabolic adaptations that occur during pregnancy in mice.

All figures, tables and portions of the text were adapted from:

Liu, L.X., Arany, Z. (2014). Maternal cardiac metabolism during pregnancy. Cardiovasc Res. 101(4): 545-553.

References

An, D., Pulinilkunnil, T., Qi, D., Ghosh, S., Abrahani, A., and Rodrigues, B. (2005). The metabolic "switch" AMPK regulates cardiac heparin-releasable lipoprotein lipase. Am J Physiol Endocrinol Metab *288*, E246-253.

Anderson, R.J., Berl, T., McDonald, K.M., and Schrier, R.W. (1976). Prostaglandins: effects on blood pressure, renal blood flow, sodium and water excretion. Kidney Int *10*, 205-215.

Arany, Z., He, H., Lin, J., Hoyer, K., Handschin, C., Toka, O., Ahmad, F., Matsui, T., Chin, S., Wu, P.H., et al. (2005). Transcriptional coactivator PGC-1 alpha controls the energy state and contractile function of cardiac muscle. Cell Metab *1*, 259-271.

Atkins, A.F., Watt, J.M., Milan, P., Davies, P., and Crawford, J.S. (1981). A longitudinal study of cardiovascular dynamic changes throughout pregnancy. Eur J Obstet Gynecol Reprod Biol *12*, 215-224.

Augustus, A., Yagyu, H., Haemmerle, G., Bensadoun, A., Vikramadithyan, R.K., Park, S.Y., Kim, J.K., Zechner, R., and Goldberg, I.J. (2004). Cardiac-specific knock-out of lipoprotein lipase alters plasma lipoprotein triglyceride metabolism and cardiac gene expression. J Biol Chem *279*, 25050-25057.

Bamfo, J.E., Kametas, N.A., Nicolaides, K.H., and Chambers, J.B. (2007). Maternal left ventricular diastolic and systolic long-axis function during normal pregnancy. Eur J Echocardiogr *8*, 360-368.

Barger, P.M., Brandt, J.M., Leone, T.C., Weinheimer, C.J., and Kelly, D.P. (2000). Deactivation of peroxisome proliferator-activated receptor-alpha during cardiac hypertrophic growth. J Clin Invest *105*, 1723-1730.

Bassien-Capsa, V., Fouron, J.C., Comte, B., and Chorvatova, A. (2006). Structural, functional and metabolic remodeling of rat left ventricular myocytes in normal and in sodium-supplemented pregnancy. Cardiovasc Res *69*, 423-431.

Battaglia, F.C., and Meschia, G. (1978). Principal substrates of fetal metabolism. Physiol Rev *58*, 499-527.

Bell, G.I., Kayano, T., Buse, J.B., Burant, C.F., Takeda, J., Lin, D., Fukumoto, H., and Seino, S. (1990). Molecular biology of mammalian glucose transporters. Diabetes Care *13*, 198-208.

Bello, N., Rendon, I.S., and Arany, Z. (2013). The relationship between pre-eclampsia and peripartum cardiomyopathy: a systematic review and meta-analysis. J Am Coll Cardiol *62*, 1715-1723.

Bing, R.J., Siegel, A., Ungar, I., and Gilbert, M. (1954). Metabolism of the human heart. II. Studies on fat, ketone and amino acid metabolism. Am J Med *16*, 504-515.

Bleicher, S.J., O'Sullivan, J.B., and Freinkel, N. (1964). Carbohydrate Metabolism in Pregnancy. V. The Interrelations of Glucose, Insulin and Free Fatty Acids in Late Pregnancy and Post Partum. N Engl J Med *271*, 866-872.

Bonen, A., Luiken, J.J., Arumugam, Y., Glatz, J.F., and Tandon, N.N. (2000). Acute regulation of fatty acid uptake involves the cellular redistribution of fatty acid translocase. J Biol Chem *275*, 14501-14508.

Boucher, J., Kleinridders, A., and Kahn, C.R. (2014). Insulin receptor signaling in normal and insulin-resistant states. Cold Spring Harb Perspect Biol *6*.

Brelje, T.C., Parsons, J.A., and Sorenson, R.L. (1994). Regulation of islet beta-cell proliferation by prolactin in rat islets. Diabetes *43*, 263-273.

Bremer, J. (1983). Carnitine--metabolism and functions. Physiol Rev *63*, 1420-1480.

Brin, M., and Olson, R.E. (1952). Metabolism of cardiac muscle. VI. Competition between L(+)-Lactate uniformly labeled with C14 and C14-carbonyl-labeled pyruvate. J Biol Chem *199*, 475-483.

Buchanan, T.A., Metzger, B.E., Freinkel, N., and Bergman, R.N. (1990). Insulin sensitivity and B-cell responsiveness to glucose during late pregnancy in lean and moderately obese women with normal glucose tolerance or mild gestational diabetes. Am J Obstet Gynecol *162*, 1008-1014.

Butte, N.F. (2000). Carbohydrate and lipid metabolism in pregnancy: normal compared with gestational diabetes mellitus. Am J Clin Nutr *71*, 1256S-1261S.

Capeless, E.L., and Clapp, J.F. (1989). Cardiovascular changes in early phase of pregnancy. Am J Obstet Gynecol *161*, 1449-1453.

Catalano, P.M., Tyzbir, E.D., Roman, N.M., Amini, S.B., and Sims, E.A. (1991). Longitudinal changes in insulin release and insulin resistance in nonobese pregnant women. Am J Obstet Gynecol *165*, 1667-1672.

Chavez, J.A., Roach, W.G., Keller, S.R., Lane, W.S., and Lienhard, G.E. (2008). Inhibition of GLUT4 translocation by Tbc1d1, a Rab GTPase-activating protein abundant in skeletal muscle, is partially relieved by AMP-activated protein kinase activation. J Biol Chem *283*, 9187-9195.

Chung, E., and Leinwand, L.A. (2014). Pregnancy as a cardiac stress model. Cardiovasc Res *101*, 561-570.

Chung, E., Yeung, F., and Leinwand, L.A. (2012). Akt and MAPK signaling mediate pregnancy-induced cardiac adaptation. J Appl Physiol (1985) *112*, 1564-1575.

Clark, S.L., Cotton, D.B., Lee, W., Bishop, C., Hill, T., Southwick, J., Pivarnik, J., Spillman, T., DeVore, G.R., Phelan, J., et al. (1989). Central hemodynamic assessment of normal term pregnancy. Am J Obstet Gynecol *161*, 1439-1442.

Davila-Roman, V.G., Vedala, G., Herrero, P., de las Fuentes, L., Rogers, J.G., Kelly, D.P., and Gropler, R.J. (2002). Altered myocardial fatty acid and glucose metabolism in idiopathic dilated cardiomyopathy. J Am Coll Cardiol *40*, 271-277.

Delachaux, A., Waeber, B., Liaudet, L., Hohlfeld, P., and Feihl, F. (2006). Profound impact of uncomplicated pregnancy on diastolic, but not systolic pulse contour of aortic pressure. J Hypertens *24*, 1641-1648.

Desai, D.K., Moodley, J., and Naidoo, D.P. (2004). Echocardiographic assessment of cardiovascular hemodynamics in normal pregnancy. Obstet Gynecol *104*, 20-29.

Djouadi, F., Weinheimer, C.J., Saffitz, J.E., Pitchford, C., Bastin, J., Gonzalez, F.J., and Kelly, D.P. (1998). A gender-related defect in lipid metabolism and glucose homeostasis in peroxisome proliferator- activated receptor alpha- deficient mice. J Clin Invest *102*, 1083-1091.

Dole, V.P. (1956). A relation between non-esterified fatty acids in plasma and the metabolism of glucose. J Clin Invest *35*, 150-154.

Drake, K.J., Sidorov, V.Y., McGuinness, O.P., Wasserman, D.H., and Wikswo, J.P. (2012). Amino acids as metabolic substrates during cardiac ischemia. Exp Biol Med (Maywood) *237*, 1369-1378.

Eghbali, M., Deva, R., Alioua, A., Minosyan, T.Y., Ruan, H., Wang, Y., Toro, L., and Stefani, E. (2005). Molecular and functional signature of heart hypertrophy during pregnancy. Circ Res *96*, 1208-1216.

Ellis, J.M., Mentock, S.M., Depetrillo, M.A., Koves, T.R., Sen, S., Watkins, S.M., Muoio, D.M., Cline, G.W., Taegtmeyer, H., Shulman, G.I., et al. (2011). Mouse cardiac acyl coenzyme a synthetase 1 deficiency impairs Fatty Acid oxidation and induces cardiac hypertrophy. Mol Cell Biol *31*, 1252-1262.

Estensen, M.E., Beitnes, J.O., Grindheim, G., Aaberge, L., Smiseth, O.A., Henriksen, T., and Aakhus, S. (2013). Altered maternal left ventricular contractility and function during normal pregnancy. Ultrasound Obstet Gynecol *41*, 659-666.

Felig, P., Kim, Y.J., Lynch, V., and Hendler, R. (1972). Amino acid metabolism during starvation in human pregnancy. J Clin Invest *51*, 1195-1202.

Foster, D.W. (2012). Malonyl-CoA: the regulator of fatty acid synthesis and oxidation. J Clin Invest *122*, 1958-1959.

Gertz, E.W., Wisneski, J.A., Stanley, W.C., and Neese, R.A. (1988). Myocardial substrate utilization during exercise in humans. Dual carbon-labeled carbohydrate isotope experiments. J Clin Invest *82*, 2017-2025.

Ghio, A., Bertolotto, A., Resi, V., Volpe, L., and Di Cianni, G. (2011). Triglyceride metabolism in pregnancy. Adv Clin Chem *55*, 133-153.

Gilde, A.J., van der Lee, K.A., Willemsen, P.H., Chinetti, G., van der Leij, F.R., van der Vusse, G.J., Staels, B., and van Bilsen, M. (2003). Peroxisome proliferator-activated receptor (PPAR) alpha and PPARbeta/delta, but not PPARgamma, modulate the expression of genes involved in cardiac lipid metabolism. Circ Res *92*, 518-524.

Gilson, G.J., Samaan, S., Crawford, M.H., Qualls, C.R., and Curet, L.B. (1997). Changes in hemodynamics, ventricular remodeling, and ventricular contractility during normal pregnancy: a longitudinal study. Obstet Gynecol *89*, 957-962.

Gimeno, R.E., Ortegon, A.M., Patel, S., Punreddy, S., Ge, P., Sun, Y., Lodish, H.F., and Stahl, A. (2003). Characterization of a heart-specific fatty acid transport protein. J Biol Chem *278*, 16039-16044.

Gold, A.J., and Yaffe, S.R. (1978). Effects of prolonged starvation on cardiac energy metabolism in the rat. J Nutr *108*, 410-416.

Goldberg, I.J., Eckel, R.H., and Abumrad, N.A. (2009). Regulation of fatty acid uptake into tissues: lipoprotein lipase- and CD36-mediated pathways. J Lipid Res *50 Suppl*, S86-90.

Goodwin, G.W., Arteaga, J.R., and Taegtmeyer, H. (1995). Glycogen turnover in the isolated working rat heart. J Biol Chem *270*, 9234-9240.

Halkein, J., Tabruyn, S.P., Ricke-Hoch, M., Haghikia, A., Nguyen, N.Q., Scherr, M., Castermans, K., Malvaux, L., Lambert, V., Thiry, M., et al. (2013). MicroRNA-146a is a therapeutic target and biomarker for peripartum cardiomyopathy. J Clin Invest *123*, 2143-2154.

Haynes, W.G., Noon, J.P., Walker, B.R., and Webb, D.J. (1993). Inhibition of nitric oxide synthesis increases blood pressure in healthy humans. J Hypertens *11*, 1375-1380.

Henning, S.L., Wambolt, R.B., Schonekess, B.O., Lopaschuk, G.D., and Allard, M.F. (1996). Contribution of glycogen to aerobic myocardial glucose utilization. Circulation *93*, 1549-1555.

Herrera, E. (2002). Lipid metabolism in pregnancy and its consequences in the fetus and newborn. Endocrine *19*, 43-55.

Herrera, E., Amusquivar, E., Lopez-Soldado, I., and Ortega, H. (2006). Maternal lipid metabolism and placental lipid transfer. Horm Res *65 Suppl 3*, 59-64.

Herrero, P., Soto, P.F., Dence, C.S., Kisrieva-Ware, Z., Delano, D.A., Peterson, L.R., and Gropler, R.J. (2005). Impact of hormone replacement on myocardial fatty acid metabolism: potential role of estrogen. J Nucl Cardiol *12*, 574-581.

Hilfiker-Kleiner, D., Kaminski, K., Podewski, E., Bonda, T., Schaefer, A., Sliwa, K., Forster, O., Quint, A., Landmesser, U., Doerries, C., et al. (2007). A cathepsin D-cleaved 16 kDa form of prolactin mediates postpartum cardiomyopathy. Cell *128*, 589-600.

Hinderliter, A.L., Light, K.C., and Willis, P.W.t. (1992). Racial differences in left ventricular structure in healthy young adults. Am J Cardiol *69*, 1196-1199.

Holness, M.J., and Sugden, M.C. (2003). Regulation of pyruvate dehydrogenase complex activity by reversible phosphorylation. Biochem Soc Trans *31*, 1143-1151.

Hotamisligil, G.S., Peraldi, P., Budavari, A., Ellis, R., White, M.F., and Spiegelman, B.M. (1996). IRS-1-mediated inhibition of insulin receptor tyrosine kinase activity in TNF-alpha- and obesity-induced insulin resistance. Science *271*, 665-668.

Huang, C., Snider, F., and Cross, J.C. (2009). Prolactin receptor is required for normal glucose homeostasis and modulation of beta-cell mass during pregnancy. Endocrinology *150*, 1618-1626.

Hunter, S., and Robson, S.C. (1992). Adaptation of the maternal heart in pregnancy. Br Heart J *68*, 540-543.

Hytten, F.E., and Paintin, D.B. (1963). Increase in plasma volume during normal pregnancy. J Obstet Gynaecol Br Emp *70*, 402-407.

Intapad, S., and Alexander, B.T. (2013a). Future cardiovascular risk: Interpreting the importance of increased blood pressure during pregnancy. Circulation *127*, 668-669.

Intapad, S., and Alexander, B.T. (2013b). Pregnancy Complications and Later Development of Hypertension. Curr Cardiovasc Risk Rep *7*, 183-189.

Jeoung, N.H., and Harris, R.A. (2010). Role of pyruvate dehydrogenase kinase 4 in regulation of blood glucose levels. Korean Diabetes J *34*, 274-283.

Kalhan, S.C. (2000). Protein metabolism in pregnancy. Am J Clin Nutr *71*, 1249S-1255S.

Kalhan, S.C., Rossi, K.Q., Gruca, L.L., Super, D.M., and Savin, S.M. (1998). Relation between transamination of branched-chain amino acids and urea synthesis: evidence from human pregnancy. Am J Physiol *275*, E423-431.

Kametas, N.A., McAuliffe, F., Hancock, J., Chambers, J., and Nicolaides, K.H. (2001). Maternal left ventricular mass and diastolic function during pregnancy. Ultrasound Obstet Gynecol *18*, 460-466.

Kealey, A. (2010). Coronary artery disease and myocardial infarction in pregnancy: a review of epidemiology, diagnosis, and medical and surgical management. Can J Cardiol *26*, 185-189.

Kersten, S. (2014). Physiological regulation of lipoprotein lipase. Biochim Biophys Acta *1841*, 919-933.

Kim, H., Toyofuku, Y., Lynn, F.C., Chak, E., Uchida, T., Mizukami, H., Fujitani, Y., Kawamori, R., Miyatsuka, T., Kosaka, Y., et al. (2010). Serotonin regulates pancreatic beta cell mass during pregnancy. Nat Med *16*, 804-808.

King, J.C. (2000). Physiology of pregnancy and nutrient metabolism. Am J Clin Nutr *71*, 1218S-1225S.

Kirwan, J.P., Hauguel-De Mouzon, S., Lepercq, J., Challier, J.C., Huston-Presley, L., Friedman, J.E., Kalhan, S.C., and Catalano, P.M. (2002). TNF-alpha is a predictor of insulin resistance in human pregnancy. Diabetes *51*, 2207-2213.

Kobayashi, K., and Neely, J.R. (1983a). Effects of increased cardiac work on pyruvate dehydrogenase activity in hearts from diabetic animals. J Mol Cell Cardiol *15*, 347-357.

Kobayashi, K., and Neely, J.R. (1983b). Mechanism of pyruvate dehydrogenase activation by increased cardiac work. J Mol Cell Cardiol *15*, 369-382.

Kolwicz, S.C., Jr., Olson, D.P., Marney, L.C., Garcia-Menendez, L., Synovec, R.E., and Tian, R. (2012). Cardiac-specific deletion of acetyl CoA carboxylase 2 prevents metabolic remodeling during pressure-overload hypertrophy. Circ Res *111*, 728-738.

Kolwicz, S.C., Jr., Purohit, S., and Tian, R. (2013). Cardiac metabolism and its interactions with contraction, growth, and survival of cardiomyocytes. Circ Res *113*, 603-616.

Kotlar, T.J., and Borensztajn, J. (1977). Oscillatory changes in muscle lipoprotein lipase activity of fed and starved rats. Am J Physiol *233*, E316-319.

Lain, K.Y., and Catalano, P.M. (2007). Metabolic changes in pregnancy. Clin Obstet Gynecol *50*, 938-948.

Lee, F.N., Zhang, L., Zheng, D., Choi, W.S., and Youn, J.H. (2004). Insulin suppresses PDK-4 expression in skeletal muscle independently of plasma FFA. Am J Physiol Endocrinol Metab *287*, E69-74.

Leone, T.C., and Kelly, D.P. (2011). Transcriptional control of cardiac fuel metabolism and mitochondrial function. Cold Spring Harb Symp Quant Biol *76*, 175-182.

Li, J., Umar, S., Iorga, A., Youn, J.Y., Wang, Y., Regitz-Zagrosek, V., Cai, H., and Eghbali, M. (2012). Cardiac vulnerability to ischemia/reperfusion injury drastically increases in late pregnancy. Basic Res Cardiol *107*, 271.

Lind, T. (1979). Metabolic changes in pregnancy relevant to diabetes mellitus. Postgrad Med J *55*, 353-357.

Lopaschuk, G.D., and Jaswal, J.S. (2010). Energy metabolic phenotype of the cardiomyocyte during development, differentiation, and postnatal maturation. J Cardiovasc Pharmacol *56*, 130-140.

Lopaschuk, G.D., Ussher, J.R., Folmes, C.D., Jaswal, J.S., and Stanley, W.C. (2010). Myocardial fatty acid metabolism in health and disease. Physiol Rev *90*, 207-258.

Luiken, J.J., Dyck, D.J., Han, X.X., Tandon, N.N., Arumugam, Y., Glatz, J.F., and Bonen, A. (2002). Insulin induces the translocation of the fatty acid transporter FAT/CD36 to the plasma membrane. Am J Physiol Endocrinol Metab *282*, E491-495.

Mabie, W.C., DiSessa, T.G., Crocker, L.G., Sibai, B.M., and Arheart, K.L. (1994). A longitudinal study of cardiac output in normal human pregnancy. Am J Obstet Gynecol *170*, 849-856.

Marsin, A.S., Bertrand, L., Rider, M.H., Deprez, J., Beauloye, C., Vincent, M.F., Van den Berghe, G., Carling, D., and Hue, L. (2000). Phosphorylation and activation of heart PFK-2 by AMPK has a role in the stimulation of glycolysis during ischaemia. Curr Biol *10*, 1247-1255.

Masaki, D.I., Greenspoon, J.S., and Ouzounian, J.G. (1989). Measurement of cardiac output in pregnancy by thoracic electrical bioimpedance and thermodilution. A preliminary report. Am J Obstet Gynecol *161*, 680-684.

Matsui, T., Tao, J., del Monte, F., Lee, K.H., Li, L., Picard, M., Force, T.L., Franke, T.F., Hajjar, R.J., and Rosenzweig, A. (2001). Akt activation preserves cardiac function and prevents injury after transient cardiac ischemia in vivo. Circulation *104*, 330-335.

Mazer, C.D., Stanley, W.C., Hickey, R.F., Neese, R.A., Cason, B.A., Demas, K.A., Wisneski, J.A., and Gertz, E.W. (1990). Myocardial metabolism during hypoxia: maintained lactate oxidation during increased glycolysis. Metabolism *39*, 913-918.

McGarry, J.D., Mannaerts, G.P., and Foster, D.W. (1977). A possible role for malonyl-CoA in the regulation of hepatic fatty acid oxidation and ketogenesis. J Clin Invest *60*, 265-270.

Melchiorre, K., Sharma, R., and Thilaganathan, B. (2012). Cardiac structure and function in normal pregnancy. Curr Opin Obstet Gynecol *24*, 413-421.

Mesa, A., Jessurun, C., Hernandez, A., Adam, K., Brown, D., Vaughn, W.K., and Wilansky, S. (1999). Left ventricular diastolic function in normal human pregnancy. Circulation *99*, 511-517.

Mone, S.M., Sanders, S.P., and Colan, S.D. (1996). Control mechanisms for physiological hypertrophy of pregnancy. Circulation *94*, 667-672.

Mor, I., Cheung, E.C., and Vousden, K.H. (2011). Control of glycolysis through regulation of PFK1: old friends and recent additions. Cold Spring Harb Symp Quant Biol *76*, 211-216.

Mshelia, D.S., Kullima, A., Gali, R.M., Kawuwa, M.B., Mamza, Y.P., Habu, S.A., and Dangaji, U. (2010). The use of plasma lipid and lipoprotein ratios in interpreting the hyperlipidaemia of pregnancy. J Obstet Gynaecol *30*, 804-808.

Newbern, D., and Freemark, M. (2011). Placental hormones and the control of maternal metabolism and fetal growth. Curr Opin Endocrinol Diabetes Obes *18*, 409-416.

Nieuwenhuizen, A.G., Schuiling, G.A., Bonen, A., Paans, A.M., Vaalburg, W., and Koiter, T.R. (1998). Glucose consumption by various tissues in pregnant rats: effects of a 6-day euglycaemic hyperinsulinaemic clamp. Acta Physiol Scand *164*, 325-334.

Oey, N.A., Ruiter, J.P., Attie-Bitach, T., Ijlst, L., Wanders, R.J., and Wijburg, F.A. (2006). Fatty acid oxidation in the human fetus: implications for fetal and adult disease. J Inherit Metab Dis *29*, 71-75.

Pandey, A.K., Banerjee, A.K., Das, A., Bhawani, G., Kumar, A., Majumadar, B., and Bhattacharya, A.K. (2010). Evaluation of maternal myocardial performance during normal pregnancy and post partum. Indian Heart J *62*, 64-67.

Park, S.H., Gammon, S.R., Knippers, J.D., Paulsen, S.R., Rubink, D.S., and Winder, W.W. (2002). Phosphorylation-activity relationships of AMPK and acetyl-CoA carboxylase in muscle. J Appl Physiol (1985) *92*, 2475-2482.

Patten, I.S., and Arany, Z. (2012). PGC-1 coactivators in the cardiovascular system. Trends Endocrinol Metab *23*, 90-97.

Patten, I.S., Rana, S., Shahul, S., Rowe, G.C., Jang, C., Liu, L., Hacker, M.R., Rhee, J.S., Mitchell, J., Mahmood, F., et al. (2012). Cardiac angiogenic imbalance leads to peripartum cardiomyopathy. Nature *485*, 333-338.

Paul, D.S., Grevengoed, T.J., Pascual, F., Ellis, J.M., Willis, M.S., and Coleman, R.A. (2014). Deficiency of cardiac Acyl-CoA synthetase-1 induces diastolic dysfunction, but pathologic hypertrophy is reversed by rapamycin. Biochim Biophys Acta *1841*, 880-887.

Powe, C.E., Levine, R.J., and Karumanchi, S.A. (2011). Preeclampsia, a disease of the maternal endothelium: the role of antiangiogenic factors and implications for later cardiovascular disease. Circulation *123*, 2856-2869.

Pulinilkunnil, T., and Rodrigues, B. (2006). Cardiac lipoprotein lipase: metabolic basis for diabetic heart disease. Cardiovasc Res *69*, 329-340.

Razeghi, P., Young, M.E., Abbasi, S., and Taegtmeyer, H. (2001). Hypoxia in vivo decreases peroxisome proliferator-activated receptor alpha-regulated gene expression in rat heart. Biochem Biophys Res Commun *287*, 5-10.

Rebholz, S.L., Burke, K.T., Yang, Q., Tso, P., and Woollett, L.A. (2011). Dietary fat impacts fetal growth and metabolism: uptake of chylomicron remnant core lipids by the placenta. Am J Physiol Endocrinol Metab *301*, E416-425.

Recchia, F.A., McConnell, P.I., Loke, K.E., Xu, X., Ochoa, M., and Hintze, T.H. (1999). Nitric oxide controls cardiac substrate utilization in the conscious dog. Cardiovasc Res *44*, 325-332.

Recchia, F.A., Osorio, J.C., Chandler, M.P., Xu, X., Panchal, A.R., Lopaschuk, G.D., Hintze, T.H., and Stanley, W.C. (2002). Reduced synthesis of NO causes marked alterations in myocardial substrate metabolism in conscious dogs. Am J Physiol Endocrinol Metab *282*, E197-206.

Remesy, C., and Demigne, C. (1986). Adaptation of hepatic gluconeogenesis and ketogenesis to altered supply of substrates during late pregnancy in the rat. J Dev Physiol *8*, 195-205.

Rimbaud, S., Sanchez, H., Garnier, A., Fortin, D., Bigard, X., Veksler, V., and Ventura-Clapier, R. (2009). Stimulus specific changes of energy metabolism in hypertrophied heart. J Mol Cell Cardiol *46*, 952-959.

Roth, A., and Elkayam, U. (1996). Acute myocardial infarction associated with pregnancy. Ann Intern Med *125*, 751-762.

Rowe, G.C., Jiang, A., and Arany, Z. (2010). PGC-1 coactivators in cardiac development and disease. Circ Res *107*, 825-838.

Roy, V.K., Kumar, A., Joshi, P., Arora, J., and Ahanger, A.M. (2013). Plasma free Fatty Acid concentrations as a marker for acute myocardial infarction. J Clin Diagn Res *7*, 2432-2434.

Rui, L., Aguirre, V., Kim, J.K., Shulman, G.I., Lee, A., Corbould, A., Dunaif, A., and White, M.F. (2001). Insulin/IGF-1 and TNF-alpha stimulate phosphorylation of IRS-1 at inhibitory Ser307 via distinct pathways. J Clin Invest *107*, 181-189.

Russell, L.K., Mansfield, C.M., Lehman, J.J., Kovacs, A., Courtois, M., Saffitz, J.E., Medeiros, D.M., Valencik, M.L., McDonald, J.A., and Kelly, D.P. (2004). Cardiac-specific induction of the transcriptional coactivator peroxisome proliferator-activated receptor gamma coactivator-1alpha promotes mitochondrial biogenesis and reversible cardiomyopathy in a developmental stage-dependent manner. Circ Res *94*, 525-533.

Ryan, E.A., and Enns, L. (1988). Role of gestational hormones in the induction of insulin resistance. J Clin Endocrinol Metab *67*, 341-347.

Ryan, E.A., O'Sullivan, M.J., and Skyler, J.S. (1985). Insulin action during pregnancy. Studies with the euglycemic clamp technique. Diabetes *34*, 380-389.

Savu, O., Jurcut, R., Giusca, S., van Mieghem, T., Gussi, I., Popescu, B.A., Ginghina, C., Rademakers, F., Deprest, J., and Voigt, J.U. (2012). Morphological and functional adaptation of the maternal heart during pregnancy. Circ Cardiovasc Imaging *5*, 289-297.

Schaap, F.G., Binas, B., Danneberg, H., van der Vusse, G.J., and Glatz, J.F. (1999). Impaired long-chain fatty acid utilization by cardiac myocytes isolated from mice lacking the heart-type fatty acid binding protein gene. Circ Res *85*, 329-337.

Schoengold, D.M., deFiore, R.H., and Parlett, R.C. (1978). Free amino acids in plasma throughout pregnancy. Am J Obstet Gynecol *131*, 490-499.

Seccombe, D.W., Harding, P.G., and Possmayer, F. (1977). Fetal utilization of maternally derived ketone bodies for lipogenesis in the rat. Biochim Biophys Acta *488*, 402-416.

Shaamash, A.H., Elsnosy, E.D., Makhlouf, A.M., Zakhari, M.M., Ibrahim, O.A., and HM, E.L.-d. (2000). Maternal and fetal serum nitric oxide (NO) concentrations in normal pregnancy, pre-eclampsia and eclampsia. Int J Gynaecol Obstet *68*, 207-214.

Slot, J.W., Geuze, H.J., Gigengack, S., James, D.E., and Lienhard, G.E. (1991). Translocation of the glucose transporter GLUT4 in cardiac myocytes of the rat. Proc Natl Acad Sci U S A *88*, 7815-7819.

Smyth, D.H. (1940). The oxidation of pyruvate by heart muscle. Biochem J *34*, 1046-1056.

Sorrentino, D., Stump, D., Potter, B.J., Robinson, R.B., White, R., Kiang, C.L., and Berk, P.D. (1988). Oleate uptake by cardiac myocytes is carrier mediated and involves a 40-kD plasma membrane fatty acid binding protein similar to that in liver, adipose tissue, and gut. J Clin Invest *82*, 928-935.

Spydevold, S., Davis, E.J., and Bremer, J. (1976). Replenishment and depletion of citric acid cycle intermediates in skeletal muscle. Indication of pyruvate carboxylation. Eur J Biochem *71*, 155-165.

Stanley, W.C. (1991). Myocardial lactate metabolism during exercise. Med Sci Sports Exerc *23*, 920-924.

Stanley, W.C., Recchia, F.A., and Lopaschuk, G.D. (2005). Myocardial substrate metabolism in the normal and failing heart. Physiol Rev *85*, 1093-1129.

Su, X., and Abumrad, N.A. (2009). Cellular fatty acid uptake: a pathway under construction. Trends Endocrinol Metab *20*, 72-77.

Sugden, M.C., Changani, K.K., Bentley, J., and Holness, M.J. (1992). Cardiac glucose metabolism during pregnancy. Biochem Soc Trans *20*, 195S.

Sugden, M.C., and Holness, M.J. (1993a). Cardiac carbohydrate and lipid utilization during late pregnancy. Biochem Soc Trans *21 (Pt 3)*, 312S.

Sugden, M.C., and Holness, M.J. (1993b). Control of muscle pyruvate oxidation during late pregnancy. FEBS Lett *321*, 121-126.

Sugden, M.C., Holness, M.J., and Howard, R.M. (1993). Changes in lipoprotein lipase activities in adipose tissue, heart and skeletal muscle during continuous or interrupted feeding. Biochem J *292 (Pt 1)*, 113-119.

Sutter-Dub, M.T. (1979). Effects of pregnancy and progesterone and/or oestradiol on the insulin secretion and pancreatic insulin content in the perfused rat pancreas. Diabete Metab *5*, 47-56.

Taegtmeyer, H., Sen, S., and Vela, D. (2010). Return to the fetal gene program: a suggested metabolic link to gene expression in the heart. Ann N Y Acad Sci *1188*, 191-198.

Tada, H., Thompson, C.I., Recchia, F.A., Loke, K.E., Ochoa, M., Smith, C.J., Shesely, E.G., Kaley, G., and Hintze, T.H. (2000). Myocardial glucose uptake is regulated by nitric oxide via endothelial nitric oxide synthase in Langendorff mouse heart. Circ Res *86*, 270-274.

Thong, F.S., Bilan, P.J., and Klip, A. (2007). The Rab GTPase-activating protein AS160 integrates Akt, protein kinase C, and AMP-activated protein kinase signals regulating GLUT4 traffic. Diabetes *56*, 414-423.

Turan, O.M., De Paco, C., Kametas, N., Khaw, A., and Nicolaides, K.H. (2008). Effect of parity on maternal cardiac function during the first trimester of pregnancy. Ultrasound Obstet Gynecol *32*, 849-854.

Valensise, H., Novelli, G.P., Vasapollo, B., Borzi, M., Arduini, D., Galante, A., and Romanini, C. (2000). Maternal cardiac systolic and diastolic function: relationship with uteroplacental resistances. A Doppler and echocardiographic longitudinal study. Ultrasound Obstet Gynecol *15*, 487-497.

Van Assche, F.A., Aerts, L., and De Prins, F. (1978). A morphological study of the endocrine pancreas in human pregnancy. Br J Obstet Gynaecol *85*, 818-820.

van Oppen, A.C., Stigter, R.H., and Bruinse, H.W. (1996). Cardiac output in normal pregnancy: a critical review. Obstet Gynecol *87*, 310-318.

Volman, M.N., Rep, A., Kadzinska, I., Berkhof, J., van Geijn, H.P., Heethaar, R.M., and de Vries, J.I. (2007). Haemodynamic changes in the second half of pregnancy: a longitudinal, noninvasive study with thoracic electrical bioimpedance. BJOG *114*, 576-581.

Walsh, K. (2006). Akt signaling and growth of the heart. Circulation *113*, 2032-2034.

Williams, J.G., Ojaimi, C., Qanud, K., Zhang, S., Xu, X., Recchia, F.A., and Hintze, T.H. (2008). Coronary nitric oxide production controls cardiac substrate metabolism during pregnancy in the dog. Am J Physiol Heart Circ Physiol *294*, H2516-2523.

Williams, J.G., Rincon-Skinner, T., Sun, D., Wang, Z., Zhang, S., Zhang, X., and Hintze, T.H. (2007). Role of nitric oxide in the coupling of myocardial oxygen consumption and coronary vascular dynamics during pregnancy in the dog. Am J Physiol Heart Circ Physiol *293*, H2479-2486.

Wu, P., Sato, J., Zhao, Y., Jaskiewicz, J., Popov, K.M., and Harris, R.A. (1998). Starvation and diabetes increase the amount of pyruvate dehydrogenase kinase isoenzyme 4 in rat heart. Biochem J *329 (Pt 1)*, 197-201.

Xu, K.Y., and Becker, L.C. (1998). Ultrastructural localization of glycolytic enzymes on sarcoplasmic reticulum vesticles. J Histochem Cytochem *46*, 419-427.

Xu, K.Y., Zweier, J.L., and Becker, L.C. (1995). Functional coupling between glycolysis and sarcoplasmic reticulum Ca2+ transport. Circ Res *77*, 88-97.

Yang, J., and Holman, G.D. (2005). Insulin and contraction stimulate exocytosis, but increased AMP-activated protein kinase activity resulting from oxidative metabolism stress slows endocytosis of GLUT4 in cardiomyocytes. J Biol Chem *280*, 4070-4078.

Yazaki, Y., Isobe, M., Takahashi, W., Kitabayashi, H., Nishiyama, O., Sekiguchi, M., and Takemura, T. (1999). Assessment of myocardial fatty acid metabolic abnormalities in patients with idiopathic dilated cardiomyopathy using 123I BMIPP SPECT: correlation with clinicopathological findings and clinical course. Heart *81*, 153-159.

Yi, L.Z., He, J., Liang, Y.Z., Yuan, D.L., and Chau, F.T. (2006). Plasma fatty acid metabolic profiling and biomarkers of type 2 diabetes mellitus based on GC/MS and PLS-LDA. FEBS Lett *580*, 6837-6845.

Zaha, V.G., and Young, L.H. (2012). AMP-activated protein kinase regulation and biological actions in the heart. Circ Res *111*, 800-814.

Zentner, D., du Plessis, M., Brennecke, S., Wong, J., Grigg, L., and Harrap, S.B. (2009). Deterioration in cardiac systolic and diastolic function late in normal human pregnancy. Clin Sci (Lond) *116*, 599-606.

Zhang, S., Hulver, M.W., McMillan, R.P., Cline, M.A., and Gilbert, E.R. (2014). The pivotal role of pyruvate dehydrogenase kinases in metabolic flexibility. Nutr Metab (Lond) *11*, 10.

Zorzano, A., and Herrera, E. (1986). Comparative utilization of glycerol and alanine as liver gluconeogenic substrates in the fed late pregnant rat. Int J Biochem *18*, 583-587.

Chapter 2:

Intrinsic cardiac adaptations of late pregnancy leads to substrate switch

Attributions: Laura Liu performed all experiments for this section unless otherwise stated. Soumya Ullas (Longwood Small Animal Imaging Facility) conducted the bioluminescence imaging experiments. Seoun Ngoy, Ronglih Liao, and Weiting Chang advised with Langendorff perfusions. Wenyun Lu (Penn Metabolomics Core) performed mass spectrometry experiments.

Abstract

During pregnancy, the maternal myocardium makes adaptations to facilitate fetal needs for glucose. Little is known about the exact metabolic nature of the heart in pregnancy. We propose to characterize the cardiac energetic state of late pregnancy. Serum triglyceride profiles increase in mid- and late pregnancy, but no change in serum glucose levels is observed. Furthermore, import of fat into late pregnant mouse hearts was elevated compared to non-pregnant. Using metabolic tracer studies, we found that late pregnant mouse hearts are metabolically defined by a ~50% decrease in glucose usage, and accompanied by a ~20% increase in fatty acid utilization. These data indicate occurrence of intrinsic cardiac adaptations that result in a substrate switch in late pregnancy.

Introduction

Hormones, cytokines, chemokines, and metabolites are continuously secreted into the blood in response to a dynamic physiological milieu. Integration of these signals leads to complex responses. Understanding these responses can provide mechanistic details vital to how we view these many processes, and impact how we develop therapeutics to different diseased states.

There is a dramatic change in metabolic demand and use during pregnancy - increasing maternal insulin resistance throughout gestation, and switching preference away from glucose to allow fetal consumption (King, 2000). It is known that the heart adopts similar adaptations during pregnancy, but much still remains unanswered. The exact metabolic state of the heart in pregnancy in mice remains to be fully characterized (Liu and Arany, 2014). Furthermore, how this metabolism changes during diseased states such as gestational diabetes, preeclampsia, or

peripartum cardiomyopathy (PPCM) has never been studied. Gestational diabetes and preeclampsia are both known to increase risk for cardiovascular disease (CVD) 10-15 years post-delivery (Intapad and Alexander, 2013a). The metabolic cardiac insults that occur during pregnancy are not known. In addition, previous work has pointed to PPCM being a vasculo-metabolic disease, and whether metabolic dysfunction precedes disease phenotype is unknown (Hilfiker-Kleiner et al., 2007; Patten et al., 2012). Examination into this could potentially provide a new therapeutic perspective to treating these diseases. Therefore, characterization of metabolic changes in the heart is the first step in understanding what happens in normal, and eventually, abnormal pregnancy.

^{13}C metabolic flux analysis

There are many ways to paint a picture of the metabolic profile of a cell or tissue under various conditions (Metallo and Vander Heiden, 2013). For example, measurements of the rates of metabolite influx or efflux, intracellular concentrations of intermediates, kinetics of each metabolic pathway, or downstream signaling targets all illuminate the state of the cell. Each study conducted in isolation could lead to incomplete conclusions. Cellular uptake assays or conditioned media detection assays do not provide information about the usage of a metabolite per se, but rather a broad overview of the entrance and exit. Proteomics and metabolomics can determine the abundance of proteins and metabolites in different pathways, but yield stationary images of the energetic state of the cell. There is no information gleaned about kinetics of different pathways or the direction of metabolite flow. For example, a decreased abundance of a metabolite could signal a decrease in synthesis or increase in consumption – two very different endpoints. More recently, the use of stable-isotope tracers, such as ^{13}C or ^{15}N, has gained traction

due to the advance of mass spectrometry (MS) and nuclear magnetic resonance (NMR). The power of these tracers lies in their ability to give time-dependent flux information. Thus, integrating metabolomics with different tracer studies could paint a more complete metabolic imagery.

The work flow of flux analysis is relatively simple, although key principles must be satisfied (Zamboni and Sauer, 2009). First, a type of tracer must be chosen. Currently, stable isotope tracers have greatly facilitated experimental design. The advantages of stable isotope tracers over previously popular radioisotopes (most commonly used were ^{14}C and ^{3}H) has led to more robust flux analysis (Coggan, 1999). Radioisotope measurements are made in response to the radioactive decay of an unstable nucleus and can be very sensitive. However, in addition to the costs and safety of handling radioactive materials, quantification of activity is observed in the byproducts produced from reactions, such as $^{3}H_2O$ or $^{14}CO_2$, which does not allow recycling back to the parent compound. The metabolic rates determined by radioactively labeled substrates are absolute rates. Stable isotopes, on the other hand, as the name suggests, do not decay and are typically one or two mass numbers heavier than the most abundant stable isotope, which makes them a suitable target for detection by mass spectrometry though relative metabolic rates are determined.

Choosing the type of stable isotope tracer to use is a key component of ^{13}C tracer analysis. Beginning with ^{13}C-glucose, ^{13}C-pyruvate, ^{13}C-lactate, or ^{13}C-fatty acids can enlighten rates through different pathways. For example, studies using ^{13}C-lactate, ^{13}C-pyruvate, and ^{13}C-glucose in ex vivo perfused mouse hearts determined a constant influx and efflux of exogenous lactate and pyruvate, though preference is for the uptake of pyruvate over lactate (Khairallah et al., 2004). Furthermore, exogenous lactate contributes more to the pyruvate pool, approximately

42%, than any other carbohydrate. In addition to selection of the metabolite tracer, the number of heavy isotopes can also provide valuable information (Metallo and Vander Heiden, 2013). For example, the pentose phosphate pathway (PPP) is often studied with 1,2-^{13}C2-glucose, that is heavy isotope labeling of the first and second carbons of glucose. If flux through PPP is observed, then loss of the first labeled carbon would be seen in the metabolites of glycolysis, whereas if flux does not occur through PPP, both carbon would be labeled in the glycolytic intermediates (Brekke et al., 2014).

Applications of stable isotope labeling can be employed in many models, including whole animals, ex vivo perfused organs, or in cell culture (Vaillant et al., 2014; Yi et al., 2006). After incubation or perfusion with the labeled substrate (in which conditions should mimic physiology in concentration and availability of multiple energy sources), samples are quickly frozen to ensure that no metabolic alterations can occur post treatment. Then, metabolites from the source tissue or cell are isolated and introduced to the detection system, with either MS or NMR as previously mentioned (Des Rosiers et al., 2004; Fan and Lane, 2011). There is more widespread use of MS, due to the fact that it is cheaper, more sensitive (can detect in the pmol to nmol range in contrast to NMR which can detect μmol to mmol range), and more expansive in metabolite detection. Furthermore, MS offers the additional benefit of being able to determine all the mass isotopomers of each metabolite, including the unlabeled component. NMR, on the other hand, measures the positional isotopomer. The power of NMR is in its ability to make dynamic, real-time measurements, while MS is based on single, terminal time point. Ideally, a combination of NMR or MS methods can provide a clearer picture, but practically speaking, MS has many advantages that we utilize in our experiments as well, so we will focus here mostly on MS methods of metabolite detection.

After extraction of metabolites, the samples are injected into the mass spectrometer, where it is ionized into fragments that are then sorted based on their mass to charge (m/z) ratio. That ratio is recorded as a spectrum. It is important that the crude measurement is corrected for natural abundance, which for ^{13}C is 1.11% and 0.365% for ^{15}N (Buescher et al., 2015). The relative distribution of the mass isotopomers can then denoted as mn (or m+n), where n is the number of ^{13}C in the isotopomer. For example, in the case of glucose, its labeling will begin with m+0, for the unlabeled ^{12}C species, and up to m+6, for six labeled carbons. The mass isotopomer representation is of the fractional abundance of each of species of isotopomer over all species:

$$\text{Fractional Abundance of each isotopomer} = \frac{m(0,1\ldots n)}{m0+m1+\cdots+mn}$$

Figure 2.1 shows the mass isotopomer distribution for a given TCA metabolites, with either uniformly labeled glucose or fatty acid. The potential isotopomer species for the intermediates from the first and second turn of the TCA cycle are shown, such that the second turn combines with a fully labeled acetyl CoA, although depending on the perfusion environment, could be just as if not more likely for an unlabeled acetyl CoA to combine with the m+2 oxaloacetate.

While this strategy for studying metabolic flux yields a more vivid image than previous techniques, there are still limitations (Buescher et al., 2015). First, compartmentalization within cells can be confounding, as there are no ways to differentiate between subcellular localization. Metabolites are also known to traverse subcellular spaces, but current flux analyses characterize whole cell fluxes. Second, the technique is only as useful as the design. Thus, if only ^{13}C-glucose

was used, the results will paint an incomplete picture, and so it is important to use multiple labeled sources, and also concurrently provide both physiological concentrations and varieties of metabolites. For example, our studies use both ^{13}C-glucose and ^{13}C-fat to characterize the metabolic state of late pregnant mouse hearts. This provides a more completely, though not wholly sufficient, profile of substrate utilization.

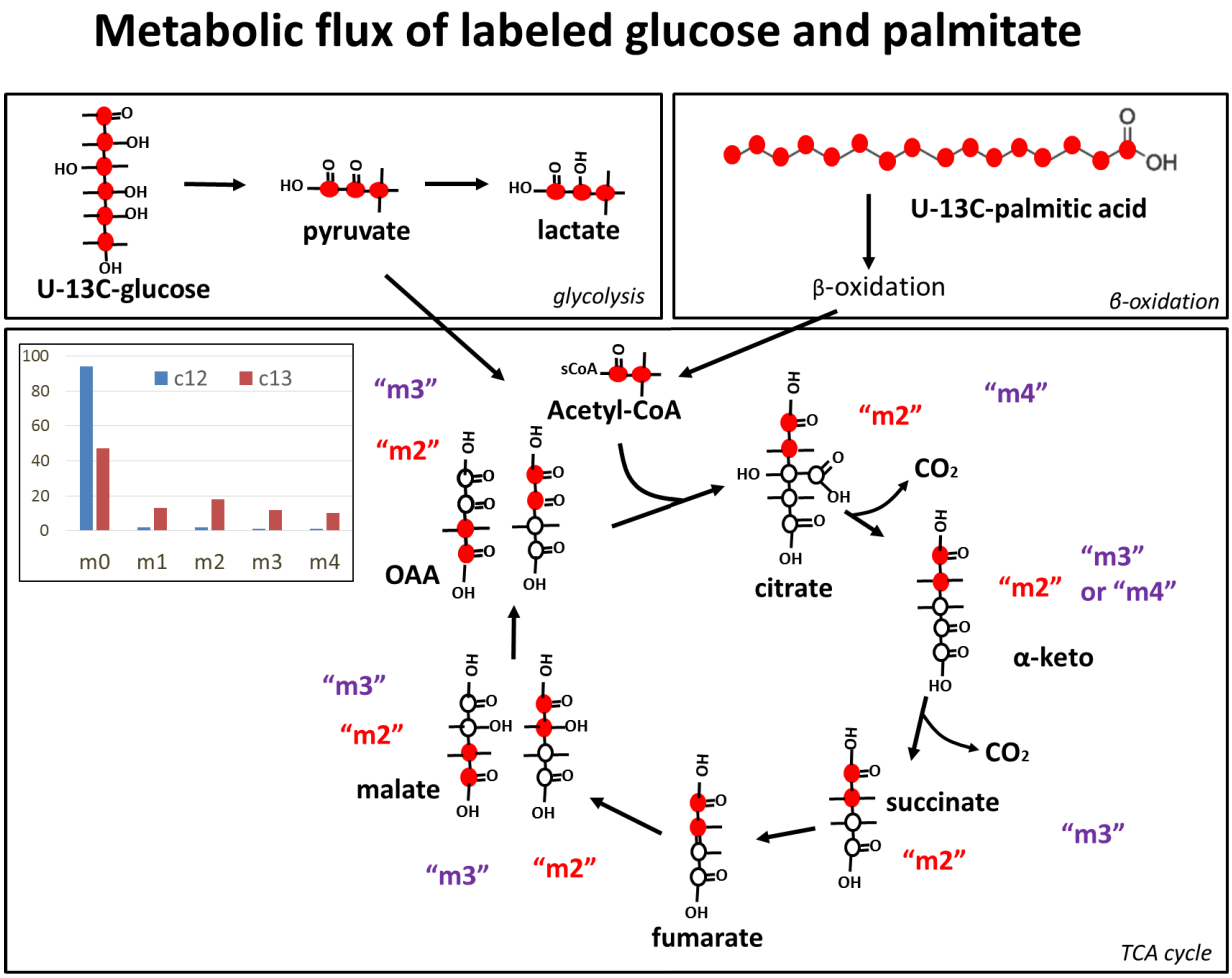

Figure 2.1: ^{13}C-metabolic flux analysis. Perfusion with U-^{13}C-glucose or U-^{13}C-palmitic acid yields m2 labeled acetyl CoA that then enters the TCA. Each cycle through the TCA produces different mass isotopomer species for each intermediate. After the first cycle (red), all TCA intermediates are m2 isotopomers, but after the second cycle (purple), depending on the location of the labeling, other isotopomer species are formed. Furthermore, if the second cycle incorporation is with an unlabeled acetyl CoA, different combinations of mass isotopomer would be observed (not shown here). Ultimately, a plot of the different mass isotopomer species for each metabolite can be plotted.

Langendorff perfusion studies

There are many ways to characterize metabolism in late pregnant hearts, either via isolated cardiomyocytes, in the whole mouse, or ex vivo. Isolated adult cardiomyocytes do not survive long and are extremely sensitive to external conditions, and so can be physiologically irrelevant. Interpretations from whole animal studies are complicated by contamination by other organs and secreted factors. Ex vivo Langendorff perfusions are perhaps one of the most popular and simplest ways to study the heart without confounding elements.

Developed by Oskar Langendorff in 1895, the principle behind this technique is relatively simple (Bell et al., 2011; Liao et al., 2012). Cannulation of the aorta provides retrograde perfusion to the heart. This closes the aortic valves and perfuses the coronary blood vessels. The perfusate travels from the coronary sinus to the right ventricle from the right atrium, before being drained through the pulmonary artery. Since then, others have added to this simple model to allow cardiac functional parameters to be measured, such as the addition of a water-filled balloon connected to a pressure transducer that is then inflated inside the heart to determine left ventricular function. The heart is also paced to around 400 beats per minute. Thus, the Langendorff setup can be designed to create as close to the physiological environment of the heart in the whole body system as possible.

Langendorff perfusion studies are at the core of many cardiac function and metabolism studies. For example, perfusing ^{13}C-substrates into an ex vivo heart allows the investigator to have precise control over surrounding conditions. Oxygenating the solution with 95% oxygen, 5% carbon dioxide can sustain cardiac function for hours in this model. Other applications, such as in ischemia/reperfusion during heart failure, have also readily used the Langendorff model to

answer mechanistic questions. How this model, along with metabolic flux analysis advancements, have contributed our understanding of cardiac metabolism is reviewed below.

Cardiac metabolism and ^{13}C flux analysis

Langendorff perfusion of ^{13}C-substrates, followed by NMR or MS detection, on normal and diseases hearts have elucidated much about how the heart utilizes substrates and how pathological conditions affect energy usage (Des Rosiers and Chatham, 2005). For example, detection of anaplerotic TCA intermediates (m3 isotopomers of oxaloacetate, fumarate or malate and absence of these species in succinate and α-ketoglutarate) has shown that anaplerosis contributes to approximately 10% of the flux through the TCA cycle (Des Rosiers et al., 2011; Nuutinen et al., 1981; Vincent et al., 2004; Vincent et al., 2003). In addition, it is possible to determine the source of anaplerosis as either pyruvate, glutamate, or propionyl CoA from β-oxidation, with different ^{13}C substrates (Lauzier et al., 2013). Contributions of anaplerosis to heart failure has also been explored. One group found an increase in the formation of malate from pyruvate (by malic enzyme) in pressure-overload hypertrophied hearts (Pound et al., 2009). This cytosolic malate then enters the mitochondria as an anaplerotic substrate via the 2-oxoglutarate-malate carrier. Interestingly, this was also linked to decreased triglyceride synthesis, which was the result of a depletion of NADPH by malic enzyme.

As an "omnivore," the heart can use many different substrates. When it chooses to use one over another has been widely investigated with tracer studies. Fatty acids and glucose are the predominant substrates, but it was unclear how the heart uses other carbohydrates under normal conditions. ^{13}C-pyruvate and ^{13}C-lactate perfusion of the ex vivo heart, as mentioned above has demonstrated clearly that both are important contributors of carbon into the TCA (Khairallah et

al., 2004). In addition, using different forms of labeled fatty acids has elucidated much about fatty acid oxidation. For example, one study used ^{13}C-oleate, ^{13}C-docosanoate, and ^{13}C-palmitate and discovered that peroxisomal β-oxidation plays a role in mitochondrial β-oxidation by the formation of malonyl CoA derived from peroxisomal acetyl CoA (Reszko et al., 2004).

With genetically altered rodent models and metabolic flux analysis, much can be gleaned about cardiac changes during heart failure. For example, ^{13}C-NMR of PPARα-null mouse hearts demonstrated a switch to glucose utilization at baseline, though these mice exhibit normal cardiac function (Gelinas et al., 2008; Luptak et al., 2005). At high work stimulating situations, however, these hearts have no energy reserves or ability to process substrates and show depressed cardiac function. Interestingly, this was rescued by breeding to a transgenic line that overexpresses GLUT1, which can provide sources of glucose and glycogen. Mice with cardiac specific ACC deletion (ACC -/-) have, at baseline, a 60% increase in fatty acid oxidation, as predicted due to decreased malonyl CoA levels (Kolwicz et al., 2012). These mice also have normal cardiac output. After 8 weeks of transverse aortic constriction (TAC), ACC -/- mice are comparable to sham control mice, and have normal cardiac function and metabolism. This suggests that increased fatty acid oxidation can be protective against pressure overload hypertrophy.

These studies illustrate the power of ^{13}C-tracer studies in Langendorff perfused mouse hearts in elucidating the metabolic phenotypes of normal and diseased conditions. We use these methods to characterize the metabolic state of mouse hearts in late pregnancy.

Results

Cardiac morphometrics and serum metabolites in pregnancy

After 18 days of pregnancy (late pregnancy, LP) in wild-type, C57/bl6 mice, ratios of the heart weight to tibia length increased approximately 13% in the late pregnant mouse (Figure 2.2), which confirms the results of previous studies. The heart weight to body weight ratio decreased to over 30%, as expected due to increases in body weight during pregnancy (Figure 2.2A). Concurrently, a significant increase in total cardiac RNA was observed, while a trend towards increased total cardiac DNA is also present (Figure 2.3).

The extracellular environment of mid (day 12) and late pregnancy (day 18) was characterized in non-fasted mice, and of late pregnancy was characterized in non-fasted rats. Serum triglycerides in mice increases by mid pregnancy and is sustained through the rest of pregnancy (Figure 2.4A). No change in serum glucose is observed in mice (Figure 2.4C) at any time points. Interestingly, free fatty acids in the blood is decreased by approximately 50% in late pregnancy, but no change is detected in mid pregnancy (Figure 2.4E). There are much more

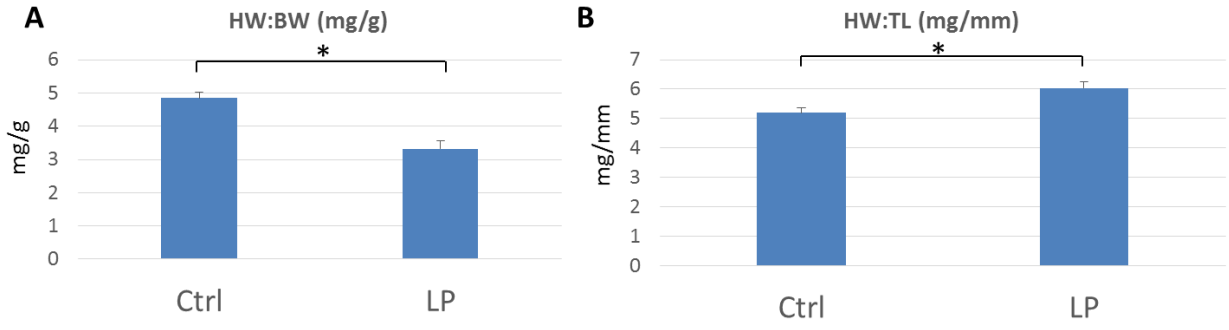

Figure 2.2: Cardiac hypertrophy occurs in late pregnancy. Timed pregnancy was carried out in C57/Bl6 mice at 3 months of age until day 18 of pregnancy (LP), and morphometric measurements were taken. Heart weight:body weight (HW:BW, A) and height weight:tibia length (HW:TL, B) measurements were made for mice in late pregnancy (n=5) compared to non-pregnant controls (n=5). (*p-value < 0.05)

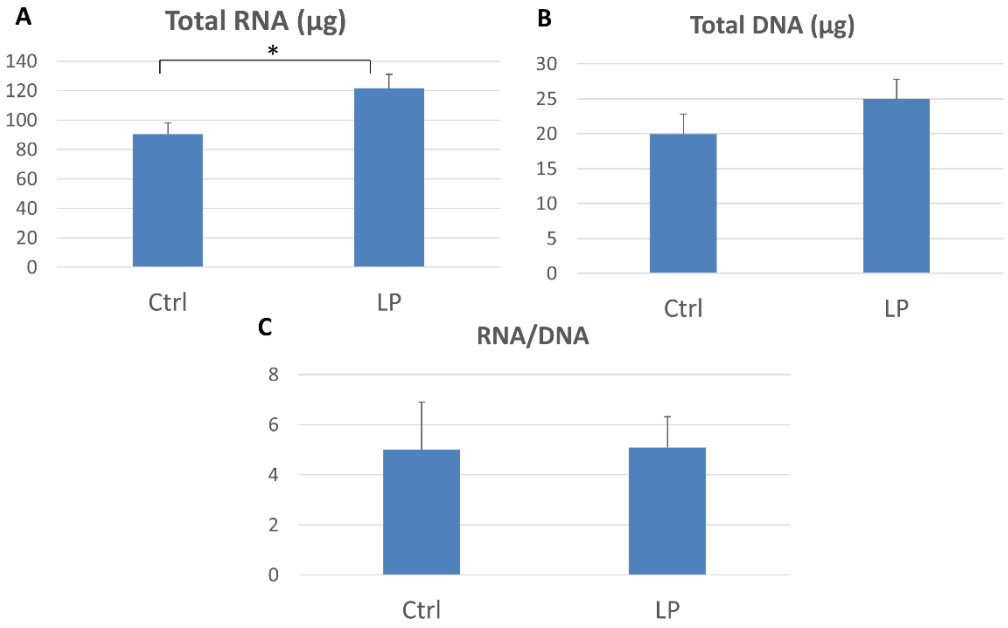

Figure 2.3: Total RNA is increased in late pregnancy. Timed pregnancy was carried out in C57/Bl6 mice at 3 months of age until day 18 of pregnancy (LP). (A) RNA and (B) DNA were isolated from late pregnant mice (n=5) from 20 mg of heart tissue and non-pregnant controls (n=5). Total RNA and DNA were calculated from the total heart weight of each mouse. The RNA to DNA ratio was also calculated (D). (*p-value < 0.05)

dramatic inductions in late pregnant rats. Serum triglycerides increase almost 7-fold, followed by an almost 40% reduction in glucose usage (Figure 2.4B and D). We did not evaluate the free fatty acid levels in rat pregnancies.

Fatty acid uptake in late pregnancy

After assessing the physiological milieu of late pregnancy in mice, we characterized the fat uptake status. Does more triglycerides in the serum mean there is greater fat import? Previous studies in dogs and rats found an increase in fat uptake and utilization in late pregnancy, but mouse hearts have not been characterized. *In vivo* bioluminescence imaging was conducted with

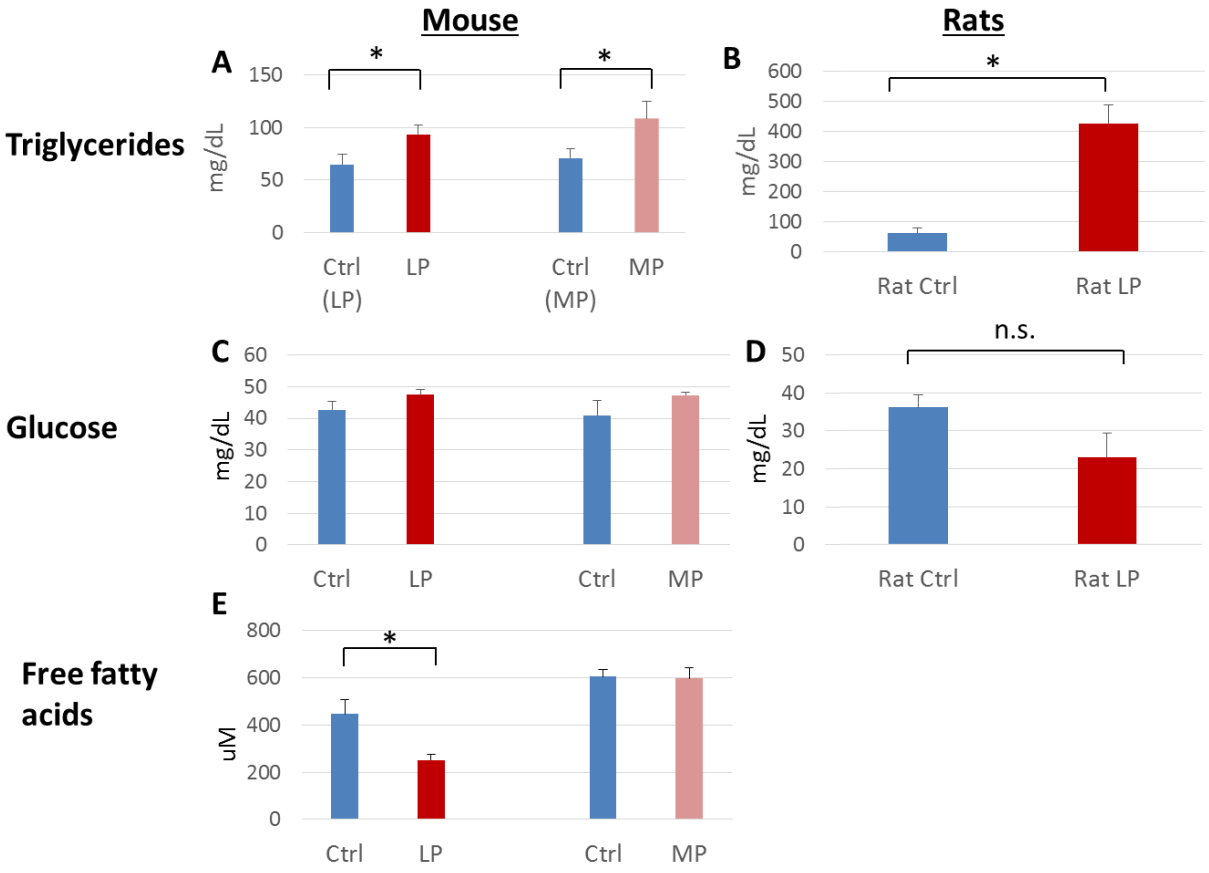

Figure 2.4: Serum metabolite profile in pregnant mice and rats. Serum was collected from non-fasted mice and rats at day 12 (MP) and day 18 (LP) of pregnancy, and assayed for triglycerides (A and B), glucose (C and D), and free fatty acids (E). (*p-value < 0.05)

a transgenic mouse that ubiquitously expresses luciferase (Luc) under the β-actin promoter. Anesthetized mice were injected with a probe (FFA-SS-Luc) that links a 16 carbon, nonesterified free fatty acid to luciferin. Upon entering the cell, luciferin is liberated from the free fatty acid and can then be detected by bioluminescence (Figure 2.5A). Day 18 pregnant Luc mice were injected with the FFA-SS-Luc and compared to non-pregnant controls (the same probe concentrations were injected in both conditions). There is a 20% increase in fat uptake in late pregnant mouse hearts (Figure 2.5E). Hearts were quickly excised from Luc mice and bioluminescence imaging was conducted on isolated tissue. A similar increase in fatty acid uptake was observed in excised hearts from late pregnant mice (data not shown). Overall, an increase in dynamics and saturation of fatty acids in late pregnant mouse hearts is observed.

Metabolic flux analysis in late pregnancy

To determine if the increase in fatty acid uptake parallels utilization, ^{13}C metabolic tracer analyses were carried out. In Langendorff perfused systems, the heart is able to work close to physiological conditions, and intrinsic properties of the heart are assessed without confounding variables. Furthermore, ventricular pressure can be continuously measured with a fluid-filled balloon inserted into the left ventricle. The heart is also paced at 420 beats per minute to ensure continuous beating. We began with optimization studies. Wild-type C57/bl6 mouse hearts were perfused with a non-circulating modified Krebs-Henseleit Buffer (mKHB, Table 2.1).

Table 2.1: Langendorff perfusion buffer components
118 mM NaCl
4.8 mM KCl
2.5 mM $CaCl_2$
1.2 mM KH_2PO_4
1.2 mM $MgSO_4$
25 mM $NaHCO_3$
0.1 mM EDTA
50 µM L-carnitine
5 mM Glucose
0.4 mM Palmitic acid
1.5 mM Lactate
0.2 mM Pyruvate
0.5 mM Glutamine

Figure 2.5: Increased fatty acid uptake in late pregnant mouse hearts. Mice with whole body luciferase expression were set up to day 18 of pregnancy. (A) A FFA-luciferin probe was intravenously injected in non-pregnant and late pregnant mice. Once inside the cell, glutathione (GSH) cleaves the probe to liberate luciferin, which can then be converted to oxyluciferin and a photon of light by luciferase. Quantification of photon flux in bioluminescence imaging can then be conducted to assess fatty acid uptake. (B) HW:TL ratios are shown for the quantified mouse sets. (C) Bioluminescence images were taken at various time points up to 7.51 minutes, with late pregnant (right) and control (left) mice. The region of interest (ROI) is circled in red and corresponds to the location of the heart. (D) Dynamics of uptake for the representative set in (B) are plotted over time, and overall total flux at the time of saturation around 6-7 minutes was plotted for 7 late pregnant mouse sets (E). (Ctrl (n=7), LP (n=6), *p-value < 0.05)

Figure 2.5 (continued)

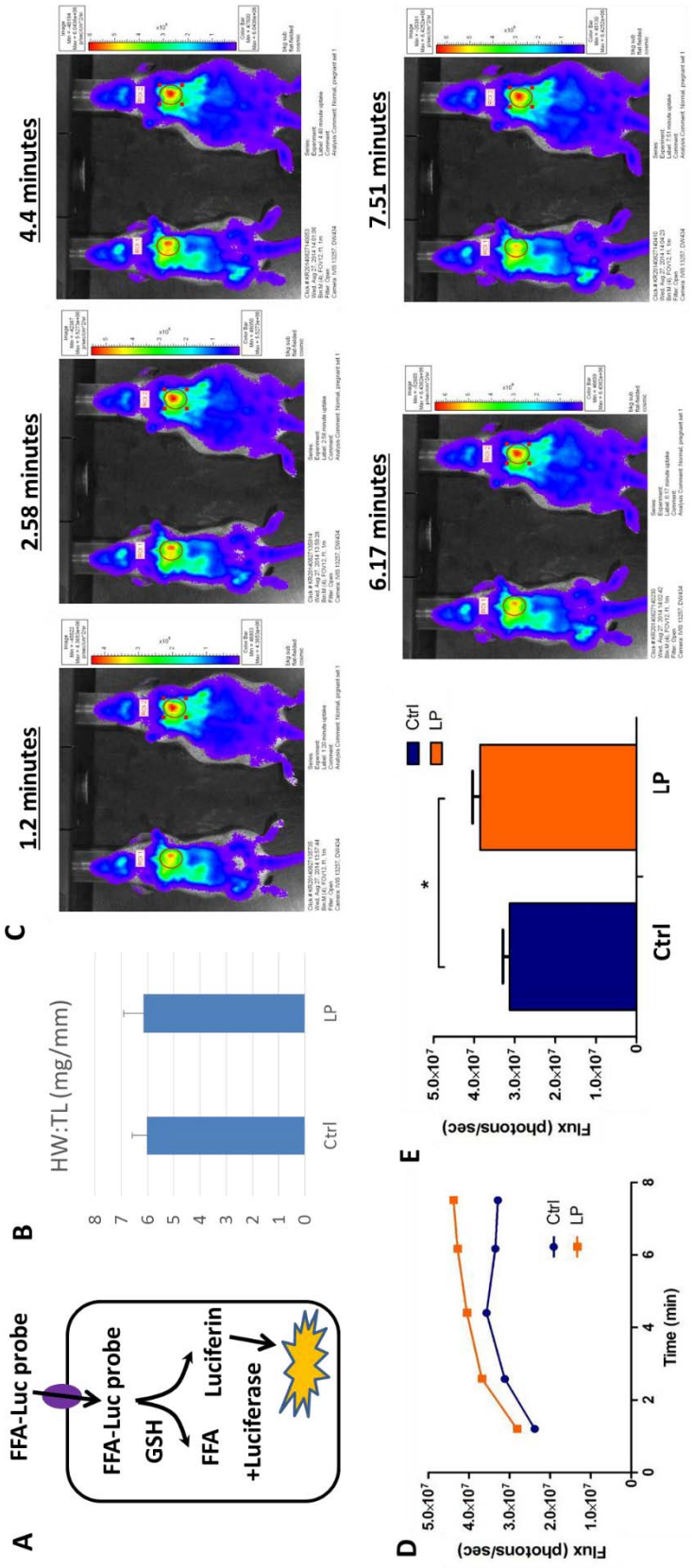

Contents of this buffer were chosen from previously published papers (Khairallah et al., 2004). In short, components of the buffer were selected so as to be as close to physiological conditions as possible. Hearts were equilibrated first for 20 minutes with unlabeled buffer. Then, the perfusate was switched to either no labeled substrates, ^{13}C-glucose, ^{13}C-palmitic acid, or ^{13}C-glutamine mKHB for 25 minutes (all ^{13}C-substrates were uniformly labeled). We found that glutamine was not a utilized substrate for heart tissue, as there was very little incorporation of ^{13}C with labeled glutamine perfusion (data not shown), so the results presented here will include only hearts perfused with ^{13}C-glucose and ^{13}C-palmitic acid. We detected incorporation of ^{13}C in the intermediates of glycolysis and TCA after perfusion with ^{13}C-glucose and ^{13}C-palmitic acid (Figure 2.6A). The greater abundance of labeled TCA metabolites from ^{13}C-palmitic acid compared to ^{13}C-glucose is due to the presence of physiological levels of unlabeled pyruvate and lactate, which dilutes out labeling with ^{13}C-glucose. Furthermore, perfusion with ^{13}C-glucose for 45 minutes yielded increased labeled isotopomer species for TCA intermediates (Figure 2.6B). We concluded that 25 minutes of perfusion with labeled substrates is sufficient to detect labeled downstream intermediates.

Next, late pregnant mouse hearts were perfused for 25 minutes with ^{13}C-glucose or ^{13}C palmitic acid. We found that late pregnant mouse hearts utilize approximately 30-50% less glucose than their non-pregnant counterparts by comparing the labeled isotopomer species of TCA intermediates in late pregnant mouse hearts perfused with ^{13}C-glucose to non-pregnant controls perfused with ^{13}C-glucose, as shown in Figure 2.7A. Conversely, pregnant mouse hearts perfused with ^{13}C-palmitic acid showed an approximately 20% increase in fat usage, compared to non-pregnant controls perfused with ^{13}C-palmitic acid (Figure 2.7A). To summarize this more clearly, we combined each labeled isotopomer species for a given metabolite in ^{13}C-glucose and

Figure 2.6: Incorporation of labeled carbons into glycolysis and TCA. (A) Wild-type, C57/bl6 hearts were perfused with unlabeled, ^{13}C-glucose or ^{13}C-palmitic acid modified KHB buffer for 25 minutes after equilibration with label-free media. Then, metabolites were extracted and samples were processed by mass spectrometry. Metabolites from glycolysis and the tricarboxylic acid (TCA) are plotted in the above graph. (Ctrl n=2; ^{13}C-glucose n=2; 13C-PA n=4). (B) Wild-type, C57/bl6 hearts were perfused with unlabeled or 13C-glucose modified KHB buffer for 45 minutes or 25 minutes after equilibration with label-free media. Then, metabolites were extracted and samples were processed by mass spectrometry. (Ctrl n=2; 13C-glucose 45 minute n=3, 25 minute n=2).

Figure 2.6 (Continued)

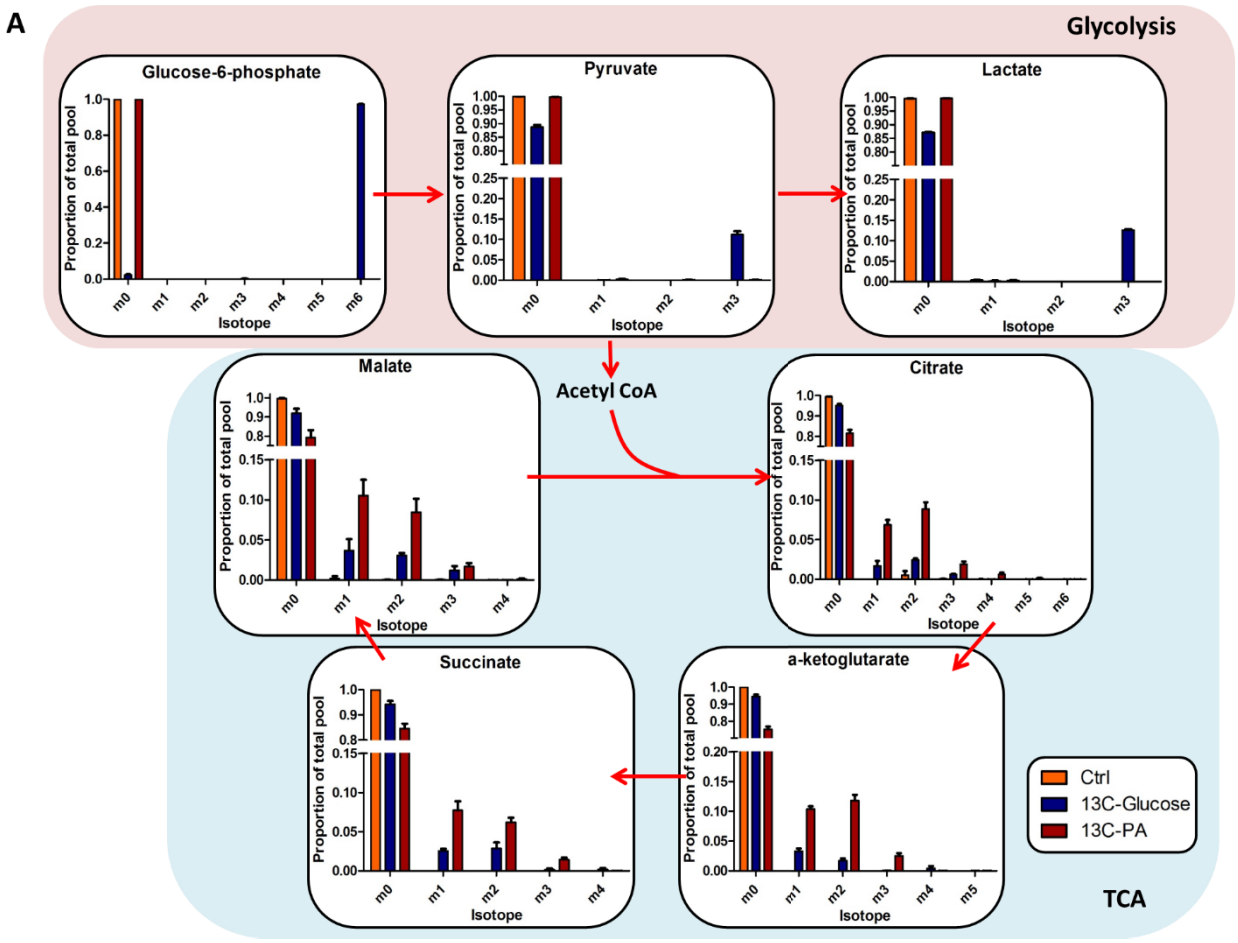

Figure 2.6 (Continued)

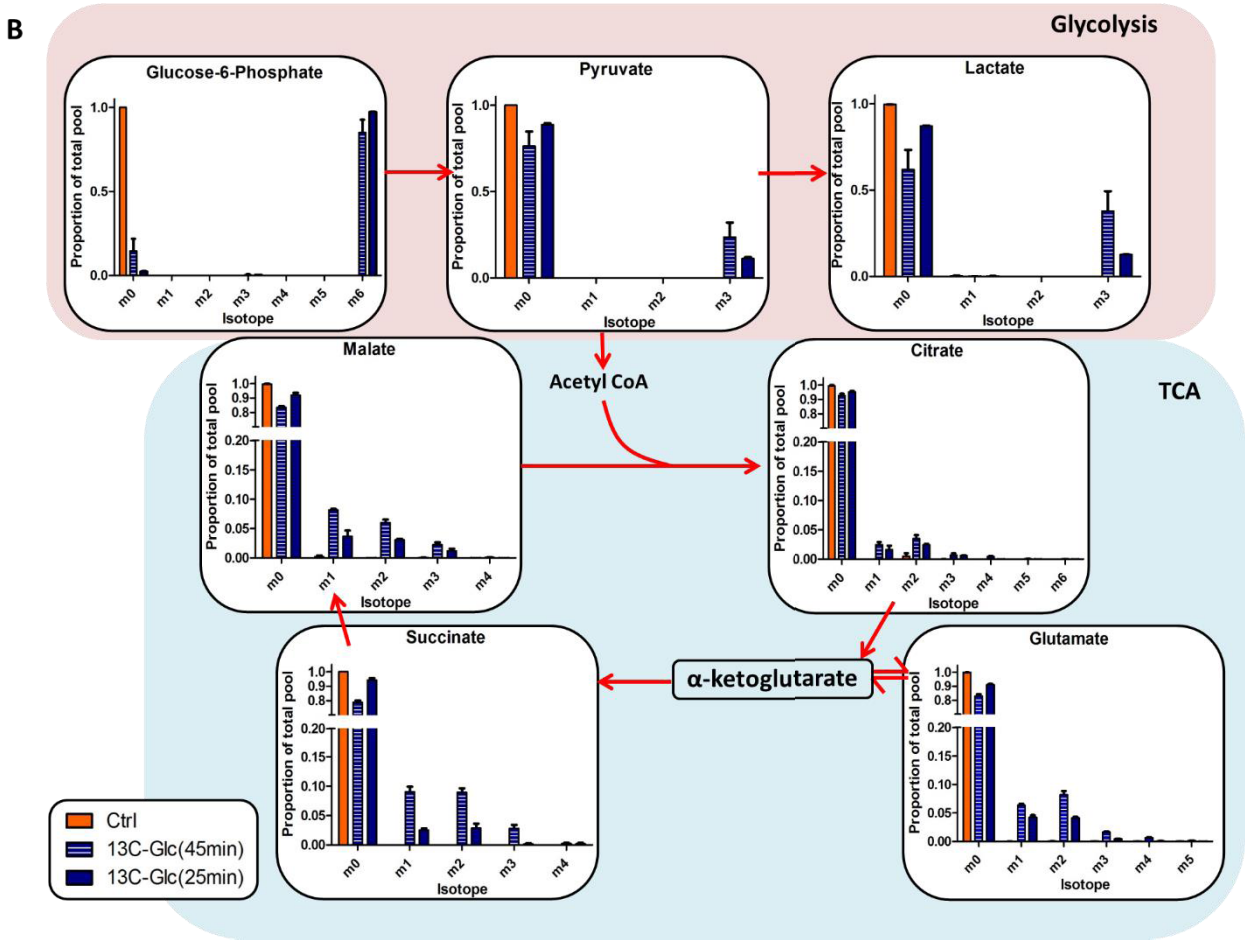

^{13}C-palmitic acid perfused hearts and compared late pregnancy to non-pregnant (Figure 2.7B and C). This observation is consistent among all the metabolites observed here of the TCA and confirms the general decrease in glucose utilization and increase in fatty acid utilization from other pregnant animals.

In an attempt to tease out metabolic flux specifically in cardiac cells, we isolated mouse adult cardiomyocytes and then incubated cells with labeled ^{13}C-glucose for 30 minutes. Adult cardiomyocytes are extremely sensitive to isolation, and if not carefully maintained, can overload with calcium and hypercontract to death. Thus, treatment of cells with an inhibitor of contraction, 2,3-butanedione 2-monoxime (BDM), in the labeling solution is necessary. However, this environment creates quiescent cells, and could greatly compromise their metabolic capacity. Figure 2.8 shows that 80-90% of each glycolytic intermediates, including glucose-6-phosphate and 3-phosphoglycerate, are labeled, suggesting saturation of glycolysis. However, very little incorporation of labeled glucose is exhibited in downstream TCA intermediates. In fact, the incorporation is predominantly anaplerotic due to the presence of the m3 isotopomer in oxaloacetate, fumarate, and malate, but the lack of the same species in succinate and α-ketoglutarate. We concluded that the limitations in labeling isolated cardiomyocytes would not allow us to assess the true metabolic phenotype of late pregnancy.

Discussion

We show here that in late pregnancy, there is an increase in serum triglyceride levels and an increase in uptake of fatty acids into mouse hearts. Furthermore, this increase in import parallels an increase in fat usage and a decrease in glucose usage. Previous reports have shown decreased glucose utilization and increased fat utilization in rats and dogs, but no mechanisms

Figure 2.7: Lower glucose utilization in late pregnant mouse hearts. Late pregnant (day 18) and non-pregnant (Ctrl) mouse hearts were perfused with ^{13}C-glucose (blue) or ^{13}C-palmitic acid (red) for 25 minutes after equilibration with label-free media. Then, metabolites were extracted and samples were processed by mass spectrometry. Various metabolites from glycolysis and the citric acid cycle (TCA) are shown (A). Percent change between non-pregnant and late pregnant mouse hearts was calculated for the prominently labeled isotopomers of the above metabolites from the TCA cycle (B). The percent change of all labeled isotopomer species between ^{13}C-glucose for Ctrl and D18, ^{13}C-palmitic acid for Ctrl and D18 were calculated for the metabolites of the TCA cycle (C). (^{13}C-glucose n=3; ^{13}C-PA n=3; ^{13}C-glucose D18 n=6; ^{13}C-PA D18 n=5, *p-value < 0.05)

Figure 2.7 (Continued)

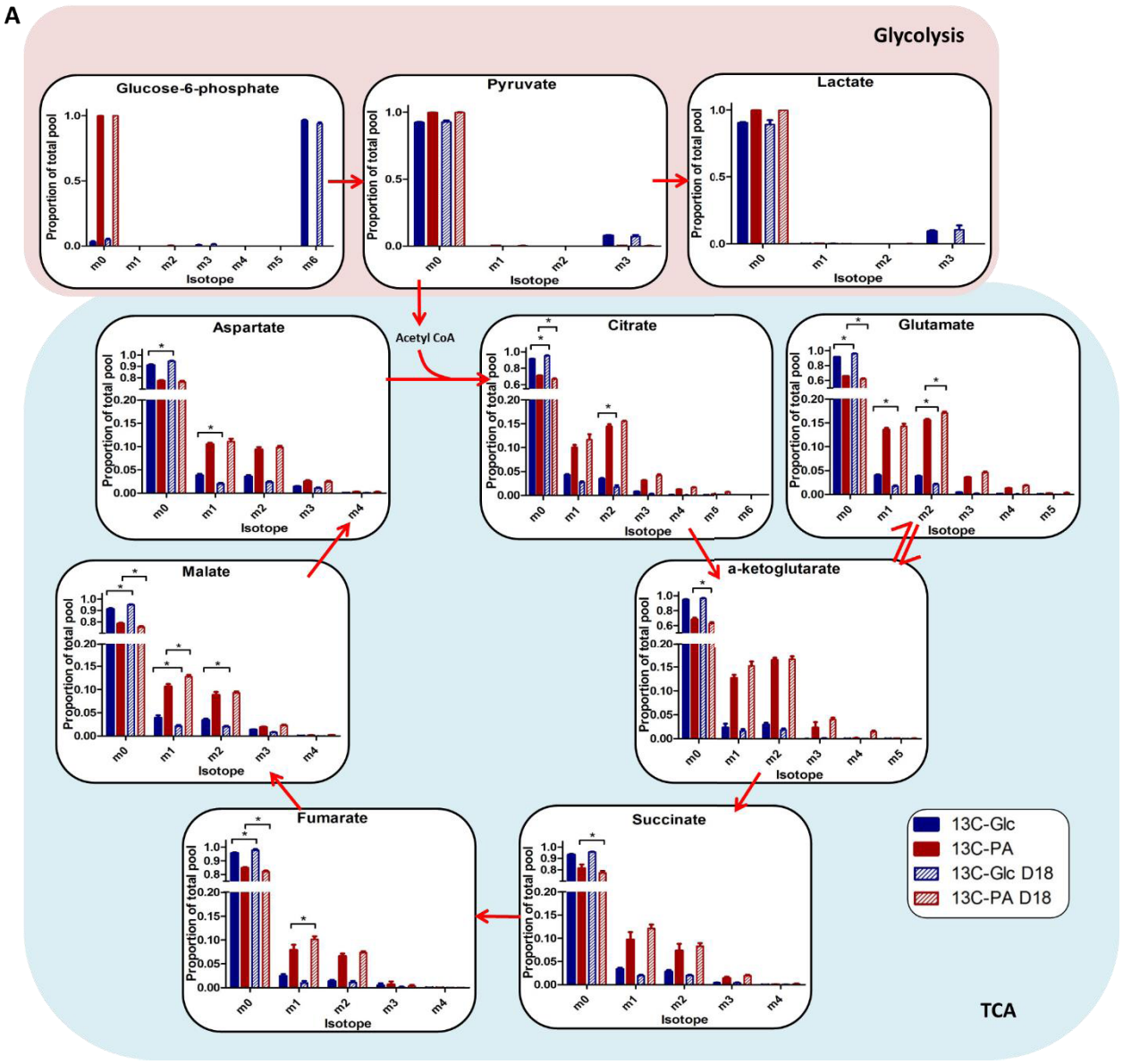

Figure 2.7 (Continued)

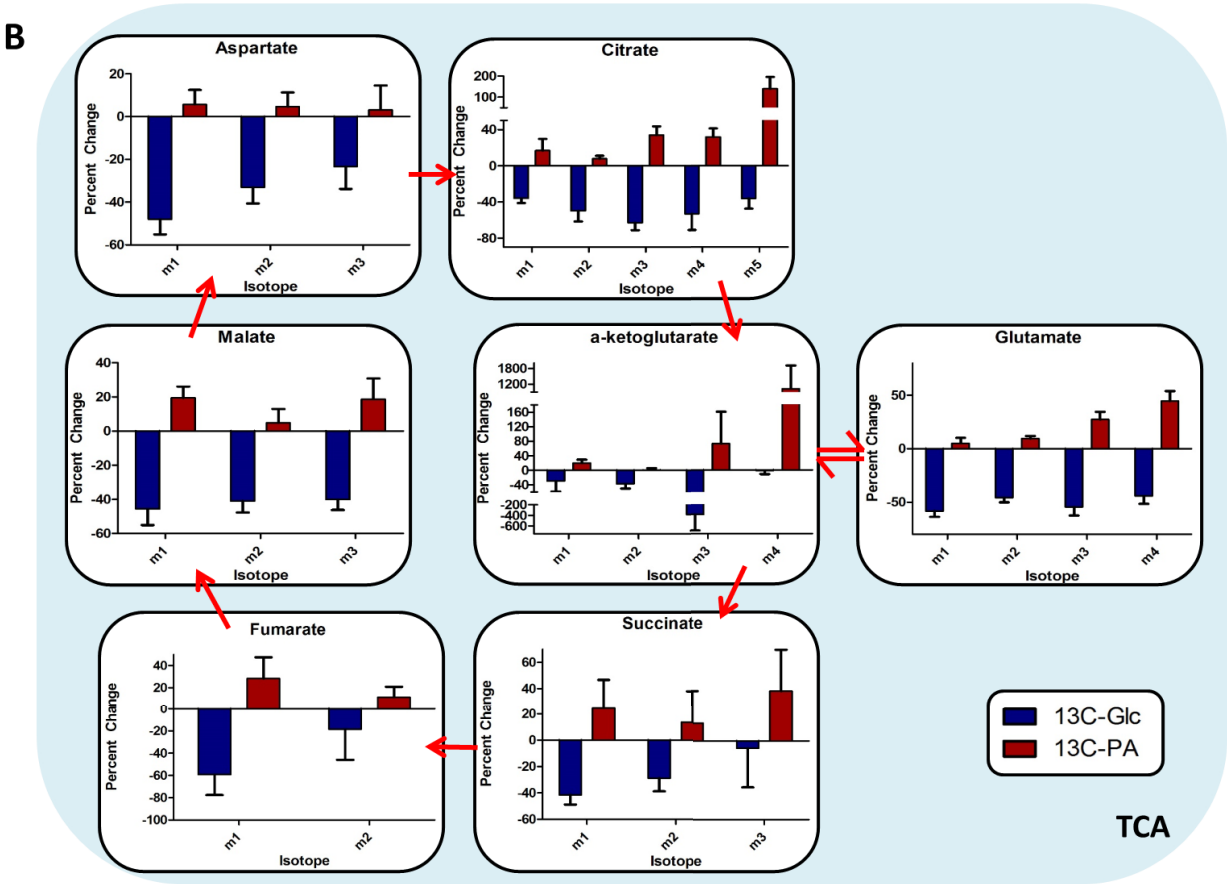

Figure 2.7 (Continued)

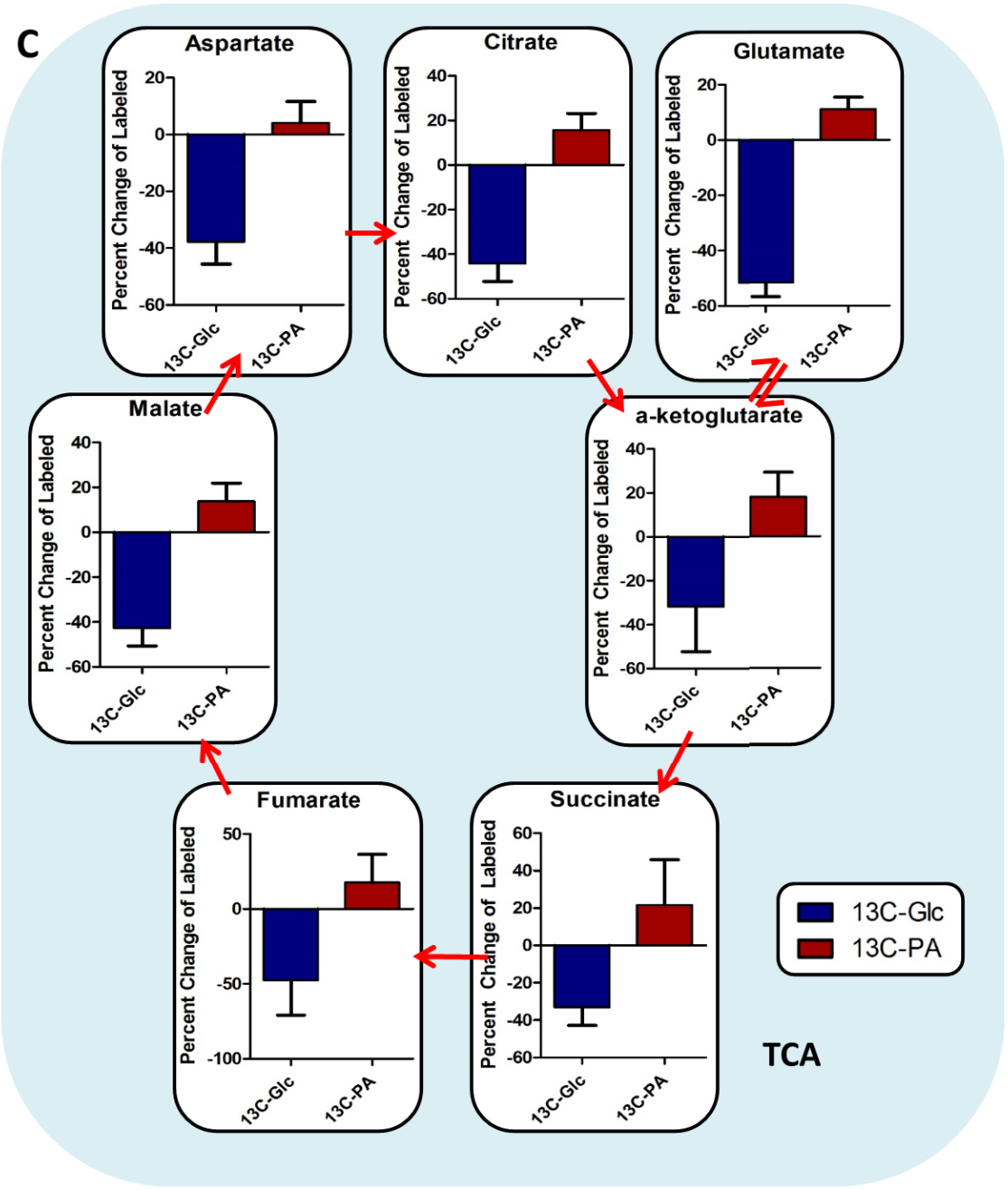

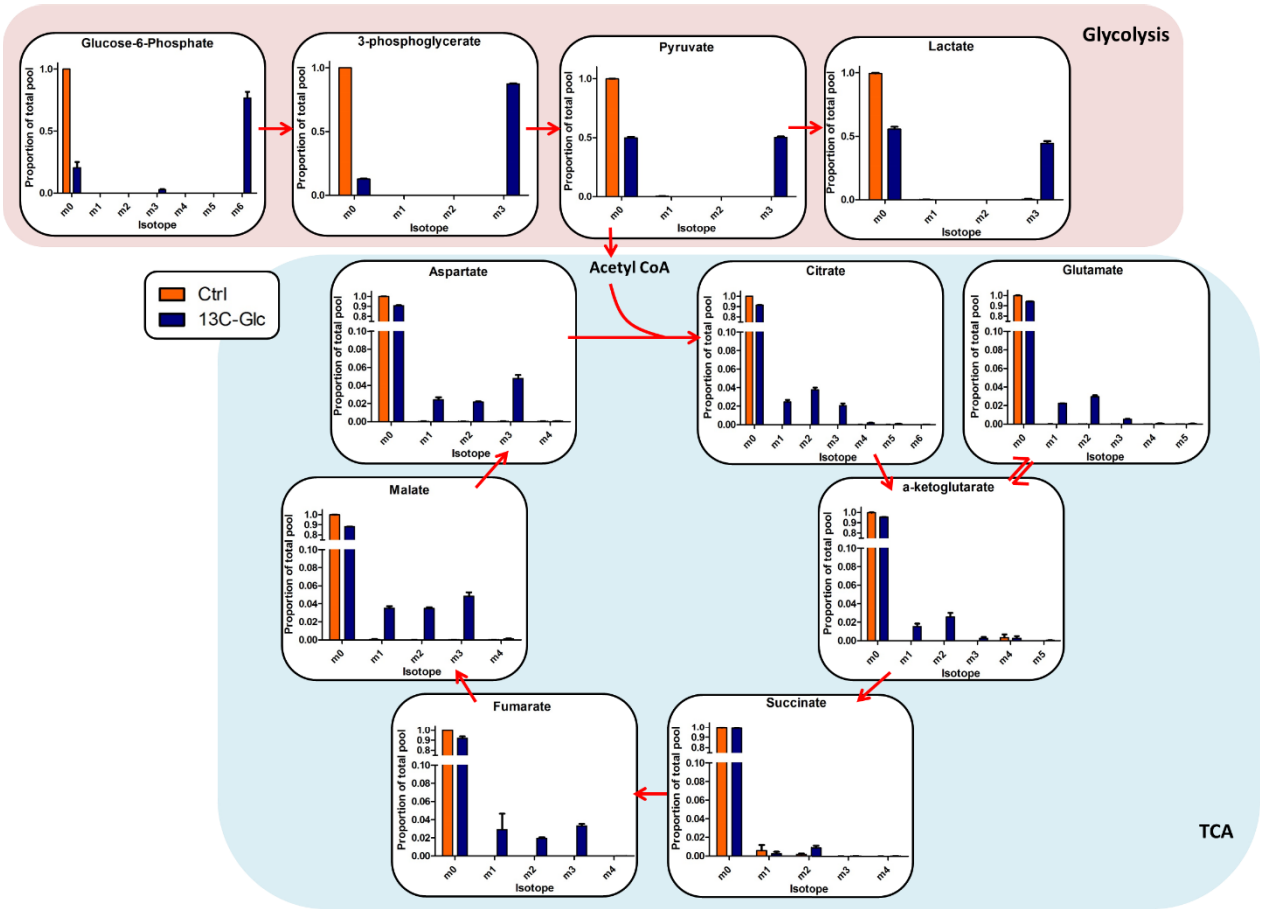

Figure 2.8: Metabolic flux analysis of isolated adult cardiomyocytes labeled with ^{13}C-glucose. Cardiomyocytes were isolated from wild-type mice and then incubated with ^{13}C-glucose for 30 minutes. Metabolites were isolated from the samples and were then analyzed by LC-MS.

have been proposed. Due to the dearth of studies on maternal cardiac changes during pregnancy in mice and the increasing value of using mouse models of diseases, we set out to better characterize the metabolic status of late pregnancy in mouse hearts. We used ^{13}C-metabolic flux analysis to directly characterize metabolite changes, a perspective that has not yet been studied in hearts from pregnant animals. We found that mouse hearts undergo a similar substrate switch in late gestation as other species.

Morphometric changes occur in pregnancy consistent with what was previously shown by others (Chung et al., 2012). Heart weight to tibia length increases approximately 10% in late pregnancy. Total RNA also increases in late pregnancy, suggesting increased transcription. There is no significant change in total DNA, but a trend towards an increase. If DNA is increased, this would suggest increased proliferation in late pregnancy, which we have not characterized. One group showed that in late pregnant rat hearts, there is no increase in Ki67, a marker of proliferation (Ciulla et al., 2013). However, those studies were in rats and it is possible that pregnant mouse hearts adapt differently. Furthermore, the ratio of total RNA to total DNA is unchanged – this would suggest that there is no cardiac hypertrophy. These results are puzzling, but more studies and greater sample sizes would need to be conducted to determine if total DNA content is truly upregulated in late pregnant mouse hearts.

The metabolic serum profiles were also assayed in pregnant rodents. Both mice and rats show higher serum triglycerides in late pregnancy, although rats show a much more drastic induction than mice do. There is no decrease in serum glucose levels in mouse pregnancies, but rats have a decreased, though not significant, serum glucose concentration in late pregnancy. Serum glucose levels were determined for non-fasted animals in all cases, but surprisingly, the concentrations are extremely low and comparable to fasted animals. This is likely due to a

collection artifact, as clotting protocol consisted of room temperature incubations and could have resulted in metabolically active red blood cells that took up glucose as a substrate source. Thus, measurements of glucose concentrations in plasma may yield more reliable values. We also found that rats have a much more drastic metabolic profile at late pregnancy than mice do, which is more consistent with what is observed in humans (Table 1.1). We assayed free fatty acids in mouse serum, and while there is no change in mid-pregnancy, there is decreased free fatty acid levels in late pregnancy. This is an interesting result, and it is unclear what causes increased triglyceride levels, but decreased free fatty acids. However, it is possible that increased uptake of free fatty acids into the late pregnant heart results in decreased serum concentrations. In humans (Table 1.1), an approximately 10% increase in free fatty acids is observed, while there is an almost 70% increase in triglycerides by late pregnant. Thus, it is clear that there are limitations of using the mouse models of pregnancy, as the serum profile of mouse pregnancies do not exactly recapitulate human serum profiles.

We move from the extracellular environment to the uptake of substrates into cardiac tissue. With the luciferase transgenic mouse, we found a 20% increase in fatty acid uptake. This is consistent with previously published findings in rats and dogs (Sugden and Holness, 1993a; Williams et al., 2008). However, previous studies did not use this *in vivo*, luciferase model to study fatty acid uptake in pregnancy. This model allows real-time uptake measurements, and observation of both the dynamics and saturation of fatty acid uptake in mouse hearts (Henkin et al., 2012). The heart weight to tibia length measurements do not increase in these mice as before. However, this could be confounded by other factors, such as the background of these mice (FVB/b6 mixed background compared to C57/bl6), the number of pups that were born in each litter (small litter sizes sometimes results in decreased adaptations), or perhaps slight errors in

measurements that may blunt small increases. Thus, we conclude that pregnant mouse hearts increase fatty acid uptake in late gestation. We also attempted to assay glucose uptake in late pregnant mice with ^{13}C-2-deoxyglucose injections, but were unsuccessful due to the technical problems.

Next, we used ^{13}C-tracer analysis to study the metabolic landscape in late pregnant mouse hearts. As described above, the new sensitivity of MS has facilitated detection of the isotopomers of many TCA and glycolytic intermediates. Pilot studies were conducted to determine optimal times of perfusion. We chose to conduct all late pregnancy experiments at 25 minutes of perfusion with labeled substrate due to the presence of ^{13}C in TCA intermediates at that time. It is worth noting, however, that results from 45 minutes of perfusion with ^{13}C-labeled glucose suggests that steady state has not been reached at 25 minutes. Furthermore, the lack of insulin and slightly elevated concentrations of lactate likely leads to underestimation of total glucose utilization in perfused hearts. In addition, the perfusion buffer also contains unlabeled pyruvate and lactate, which significantly dilutes out the contribution of labeled glucose to the TCA cycle. This confirms previous papers that pyruvate and lactate both contribute to acetyl CoA formation, but also prevents comparison between utilization of glucose and fat in these conditions. Future studies with ^{13}C-lactate of Langendorff-perfused hearts would illuminate the importance of lactate as an energy source in late pregnancy. Total lactate concentrations in the late pregnant mouse heart has also not been determined. If lactate levels are altered, this would be accompanied by changing transporter (MCT1 or MCT4) expression. Thus, it is next necessary to examine lactate uptake and oxidation pathways to determine its contribution in late pregnancy.

Late pregnant mouse hearts decline in glucose utilization and increase in fatty acid oxidation. This supports earlier findings in rats and dogs. The glucose usage decline is extremely

striking, while fatty acid oxidation increases, which while consistently, are not significant and not as prominent as glucose. This is the first study, as far as we know, to explore metabolic flux in late pregnant mouse hearts. Interestingly, we observed an increase by 20% in fatty acid uptake in the luciferase mouse studies, and for some TCA intermediates, similarly see a 20% increase in flux through β-oxidation, although the error are quite large for some. Thus, it would be revealing to look at total triglyceride content in late pregnant mouse hearts to determine if incoming fatty acids are being partitioned to triglyceride synthesis and storage. We attempted to tease out this finding in isolated cardiomyocytes, but due to the challenges of culturing these cells, did not further pursue this.

It is also evident from perfusion of ^{13}C-labeled substrates in late pregnant mouse hearts that there are intrinsic cardiac adaptations that occur in late pregnancy, independent of substrate availability. Both non-pregnant and late pregnant mouse hearts were exposed to the same substrate concentrations but consumed them very differently. Thus, it is not merely the presence of substrates in late pregnancy that determines what the heart uses but inherent changes in the myocardium itself that is determining substrate use. What these are and the factors responsible for regulating them will be further explored in Chapter 2.

Here, we found that in late pregnancy, heart weight and total RNA levels are increased. Furthermore, higher serum triglycerides characterize the late gestation environment in mouse and rat, although their serum glucose levels are contradictory. Mouse hearts in late pregnancy take up more fatty acids and have decreased glycolytic flux but higher fatty acid oxidation. This substrate switch is due to an intrinsic cardiac response to the late pregnant state, but it is not yet known what is responsible.

Materials and Methods

Animal studies. All animal studies were performed according to procedures approved by the Institutional Animal Care and Use Committee (IACUC) at Beth Israel Deaconess Medical Center (BIDMC). Mice were maintained on a standard rodent chow diet with 12 hours light and dark cycles with water and food ad libitum. Luciferase (Luc, Stock number 008450) and C57/bl6 mice were purchased from Jackson Laboratories (Bar Harbor, Maine). Luc mice (FVB background) were bred to C57/bl6 females to produce Luc.FVB/b6 mixed background progeny that were used for luciferase assays. Wild-type, three-month-old female C57/bl6 and female Luc.FVB/b6 mice undergoing estrus were mated with wild-type, C57/bl6 breeder males. The presence of a copulatory plug is denoted as day 0 of pregnancy. Pregnant females were singly placed in a new cage, and breeder diet (Formulab 5058) replaced the standard chow (Formulab 5008) they were previously on, unless delineated differently elsewhere. Breeder diet contains more fat and calories compared to standard chow. Timed pregnancies were carried out to day 11-12 (mid-pregnancy) and day 17-18 (late pregnancy) of gestation. Timed pregnant rats (Sprague Dawley) were obtained directly from Charles River.

Reagents and Materials. Unless otherwise stated, all reagents were from Sigma. ^{13}C-labeled substrates were from Cambridge Isotope Laboratories.

Organ Weight and Hypertrophy Assessment. At day 18 of pregnancy, mice were measured for body weight. Hearts were then harvested, rinsed in PBS to remove blood from ventricles, dried and weighed. Heart weight, body weight, and tibia length measurements were recorded. Hypertrophy was determined by calculating heart weight to body weight (HW/BW) and heart weight to tibia length (HW/TL) ratios.

DNA and RNA Isolation. Upon harvesting, mice tissues were immediately frozen in liquid nitrogen. 20 mg of heart tissue was used for the total RNA studies, and 20 mg for the total DNA studies. Total RNA was isolated from mouse tissue with the TRIzol (Invitrogen) and chloroform method. Total DNA was isolated using the DNeasy Blood and Tissue Kit (Qiagen). RNA and DNA concentrations were measured with the ThermoScientific NanoDrop spectrophotometer, and total RNA and DNA in the hearts were calculated by normalizing to total heart weight for each mouse.

Serum metabolite assays. Blood was collected from non-fasted mice or rats at mid- or late pregnancy via cheek puncture (mid-pregnancy) or terminal cardiac puncture (late pregnancy). Coagulation was allowed to occur for 30-45 minutes at room temperature, and then was centrifuged for 20 minutes at 2000g to obtain the serum fraction. Serum triglyceride (Cat. No. 100010303, Cayman, MI), glucose (Cat. No. 10009582 Cayman, MI), and free fatty acids (Cat. No. 700310, Cayman, MI) were measured.

***In vivo* fatty acid bioluminescence.** Bioluminescence studies were conducted at the Longwood Small Animal Imaging Facility (SAIF). Two days before imaging, chest hair was removed with a topical, depilatory cream. Protocol for injection and uptake was described briefly (Henkin et al., 2012). Mice were sedated with isoflourane and then intravenously injected (retro-orbital) with 100μL of 20 μM FFA-luciferin (Intrace Medical). Mice were placed in the supine position in the imaging chamber of the Xenogen IVIS-50 Bioluminescence Imaging System (Perkin Elmer). After data collection, hearts were removed and quickly imaged to obtain ex vivo uptake measurements. Flux analyses were performed and region of interest (ROI) were chosen with the Living Image Software from Xenogen.

Langendorff perfusion. Non-circulating, Langendorff perfusion was performed as described previously (Liao et al., 2001). Briefly, mice were sedated with ketamine and xylazine mixture. Hearts were removed and immediately placed in cold saline. Then, a cannula was placed into the aorta to undergo perfusion with non-labeled buffer for 20-25 minutes. The modified Krebs-Henseleit buffer (KHB) used contained 118 mM NaCl, 4.8 mM KCl, 2.5 mM $CaCl_2$, 1.2 mM KH_2PO_4, 1.2 mM $MgSO_4$, 25 mM $NaHCO_3$, 0.1 mM EDTA, 50 μM L-carnitine, 5 mM glucose, 0.4 mM palmitic acid conjugated to 2% BSA, 1.5 mM lactate, and 0.2 mM pyruvate, with the pH adjusted to 7.35. The buffer composition was chosen due to previously published reports (Khairallah et al., 2004; Vincent et al., 2004). The buffer was gassed with 95% CO_2/5% O_2 and maintained at 37^{o}C throughout the entirety of the experiment. A small tubing (PE-50) was used to pierce through the left ventricles to prevent fluid buildup. A balloon connected to a pressure transducer was then inserted into the left ventricle and inflated to measure ventricular function. The end-diastolic pressure, which was constant at around 5-10 mmHg, can be controlled by the inflation of the balloon. Hearts were paced at 420 beats per minute, and perfusion pressure was set at 80 mmHg for the whole study. After stable perfusion for 20 minutes, perfusate was switched to labeled substrates for 25 minutes.

Tissue preparations for mass spectrometry. After 25 minutes of labeling, the heart was immediately freeze clamped with tongs pre-chilled in liquid nitrogen. The tissue was pulverized with mortar and pestle, and the weight recorded. Metabolites were extracted with 80% methanol in H_2O with 0.1% formic acid. For the second and third extractions, a 40:40:20 ratio of methanol: acetonitrile: H_2O solution was used. All three extractions steps were completed with centrifugations at maximum speed for 5 minutes at 4^{o}C. Then, the samples were dried under nitrogen gas before processing by mass spectrometry.

Isolated adult cardiomyocytes from mouse hearts. Adult mouse hearts were excised and perfused via Langendorff perfusion, first with perfusion buffer (137 mM NaCl, 4 mM KCl, 1 mM $MgCl_2$, 10 mM HEPES, 0.33 mM NaH_2PO_4, 10mM glucose, 5 mM taurine, and 10 mM BDM), before switching to an enzyme buffer with collagenase D (Roche), collagenase B (Roche), and protease XIV for 10-15 minutes. Calcium was reloaded with concentrations of 0.06 mM, 0.25 mM, 0.60 mM, and 1.2 mM. Adult cardiomyocytes were plated on laminin-coated tissue culture plates for 2 hours in MEM (Invitrogen), 10% calf serum, BDM, 2mM glutamine, and 2mM ATP before switching to labeled media.

Labeled media treatment of cardiomyocytes and preparation for mass spectrometry. Adult cardiomyocytes were treated for 30 minutes with ^{13}C-labeled substrates in modified KHB buffer as described above. Then the cells were washed quickly in PBS twice and incubated with pre-chilled 80% methanol solution. After two more extractions with centrifugations at the highest speed for 10 minutes, nitrogen gas was used to dry the samples.

Measurement of ^{13}C-labeling pattern of cellular metabolites using liquid chromatography mass spectrometry (LC-MS). Samples were sent to the Metabolomics Core at the Penn Diabetes Research Center (DRC) for further processing. In brief, samples were resuspended in 100μL HPLC-grade water (for each well of a 6-well plate) or 1000μL HPLC-grade water for 40mg of heart tissue. Samples were analyzed via reverse phase ion-pairing chromatography coupled to an Exactive orbitrap mass spectrometer (ThermoFisher Scientific, San Jose, CA). The mass spectrometer was operated in negative ion mode with a scan rate of 1 Hz and resolving power of 100,000, scanning range being *m/z* 75-1000. The LC method has been described before (Lu et al., 2010), using a Synergy Hydro-RP column (100 mm × 2 mm, 2.5 μm particle size, Phenomenex, Torrance, CA) with a flow rate of 200 μL/min. The LC gradient was 0 min, 0% B;

2.5 min, 0% B; 5 min, 20% B; 7.5 min, 20% B; 13 min, 55% B; 15.5 min, 95% B; 18.5 min, 95% B; 19 min, 0% B; 25 min, 0% B. Solvent A is 97:3 water−methanol with 10 mM tributylamine and 15 mM acetic acid; solvent B is methanol. Other LC parameters were autosampler temperature 5°C, injection volume 10 μL, and column temperature 25 °C. The data analyses were performed using MAVEN software (Melamud et al., 2010). The metabolites, both unlabeled and the ^{13}C-labeled forms, were detected using the accurate mass with a 10 ppm m/z window. Data were corrected to remove the contribution from the nature isotope ^{13}C as described before (Munger et al., 2008). Labeling percentages were calculated from signal intensity using Excel.

Fractional abundance was calculated with the following equation:

$$\text{Fractional Abundance of each isotopomer} = \frac{m(0,1\ldots n)}{m0+m1+\cdots+mn}$$

References

Bell, R.M., Mocanu, M.M., and Yellon, D.M. (2011). Retrograde heart perfusion: the Langendorff technique of isolated heart perfusion. J Mol Cell Cardiol *50*, 940-950.

Brekke, E.M., Morken, T.S., Wideroe, M., Haberg, A.K., Brubakk, A.M., and Sonnewald, U. (2014). The pentose phosphate pathway and pyruvate carboxylation after neonatal hypoxic-ischemic brain injury. J Cereb Blood Flow Metab *34*, 724-734.

Buescher, J.M., Antoniewicz, M.R., Boros, L.G., Burgess, S.C., Brunengraber, H., Clish, C.B., DeBerardinis, R.J., Feron, O., Frezza, C., Ghesquiere, B., et al. (2015). A roadmap for interpreting C metabolite labeling patterns from cells. Curr Opin Biotechnol *34*, 189-201.

Ciulla, M.M., Acquistapace, G., Perrucci, G.L., Nicolini, P., Toffetti, L., Braidotti, P., Ferrero, S., Zucca, I., Aquino, D., Busca, G., et al. (2013). Immunohistochemical expression of oncological proliferation markers in the hearts of rats during normal pregnancy. Biomark Med *7*, 119-129.

Coggan, A.R. (1999). Use of stable isotopes to study carbohydrate and fat metabolism at the whole-body level. Proc Nutr Soc *58*, 953-961.

Des Rosiers, C., and Chatham, J.C. (2005). Myocardial phenotyping using isotopomer analysis of metabolic fluxes. Biochem Soc Trans *33*, 1413-1417.

Des Rosiers, C., Labarthe, F., Lloyd, S.G., and Chatham, J.C. (2011). Cardiac anaplerosis in health and disease: food for thought. Cardiovasc Res *90*, 210-219.

Des Rosiers, C., Lloyd, S., Comte, B., and Chatham, J.C. (2004). A critical perspective of the use of (13)C-isotopomer analysis by GCMS and NMR as applied to cardiac metabolism. Metab Eng *6*, 44-58.

Fan, T.W., and Lane, A.N. (2011). NMR-based stable isotope resolved metabolomics in systems biochemistry. J Biomol NMR *49*, 267-280.

Gelinas, R., Labarthe, F., Bouchard, B., Mc Duff, J., Charron, G., Young, M.E., and Des Rosiers, C. (2008). Alterations in carbohydrate metabolism and its regulation in PPARalpha null mouse hearts. Am J Physiol Heart Circ Physiol *294*, H1571-1580.

Henkin, A.H., Cohen, A.S., Dubikovskaya, E.A., Park, H.M., Nikitin, G.F., Auzias, M.G., Kazantzis, M., Bertozzi, C.R., and Stahl, A. (2012). Real-time noninvasive imaging of fatty acid uptake in vivo. ACS Chem Biol *7*, 1884-1891.

Hilfiker-Kleiner, D., Kaminski, K., Podewski, E., Bonda, T., Schaefer, A., Sliwa, K., Forster, O., Quint, A., Landmesser, U., Doerries, C., et al. (2007). A cathepsin D-cleaved 16 kDa form of prolactin mediates postpartum cardiomyopathy. Cell *128*, 589-600.

Intapad, S., and Alexander, B.T. (2013). Future cardiovascular risk: Interpreting the importance of increased blood pressure during pregnancy. Circulation *127*, 668-669.

Khairallah, M., Labarthe, F., Bouchard, B., Danialou, G., Petrof, B.J., and Des Rosiers, C. (2004). Profiling substrate fluxes in the isolated working mouse heart using 13C-labeled substrates: focusing on the origin and fate of pyruvate and citrate carbons. Am J Physiol Heart Circ Physiol *286*, H1461-1470.

King, J.C. (2000). Physiology of pregnancy and nutrient metabolism. Am J Clin Nutr *71*, 1218S-1225S.

Kolwicz, S.C., Jr., Olson, D.P., Marney, L.C., Garcia-Menendez, L., Synovec, R.E., and Tian, R. (2012). Cardiac-specific deletion of acetyl CoA carboxylase 2 prevents metabolic remodeling during pressure-overload hypertrophy. Circ Res *111*, 728-738.

Lauzier, B., Vaillant, F., Merlen, C., Gelinas, R., Bouchard, B., Rivard, M.E., Labarthe, F., Dolinsky, V.W., Dyck, J.R., Allen, B.G., et al. (2013). Metabolic effects of glutamine on the heart: anaplerosis versus the hexosamine biosynthetic pathway. J Mol Cell Cardiol *55*, 92-100.

Liao, R., Jain, M., Teller, P., Connors, L.H., Ngoy, S., Skinner, M., Falk, R.H., and Apstein, C.S. (2001). Infusion of light chains from patients with cardiac amyloidosis causes diastolic dysfunction in isolated mouse hearts. Circulation *104*, 1594-1597.

Liao, R., Podesser, B.K., and Lim, C.C. (2012). The continuing evolution of the Langendorff and ejecting murine heart: new advances in cardiac phenotyping. Am J Physiol Heart Circ Physiol *303*, H156-167.

Liu, L.X., and Arany, Z. (2014). Maternal cardiac metabolism in pregnancy. Cardiovasc Res *101*, 545-553.

Lu, W., Clasquin, M.F., Melamud, E., Amador-Noguez, D., Caudy, A.A., and Rabinowitz, J.D. (2010). Metabolomic analysis via reversed-phase ion-pairing liquid chromatography coupled to a stand alone orbitrap mass spectrometer. Anal Chem *82*, 3212-3221.

Luptak, I., Balschi, J.A., Xing, Y., Leone, T.C., Kelly, D.P., and Tian, R. (2005). Decreased contractile and metabolic reserve in peroxisome proliferator-activated receptor-alpha-null hearts can be rescued by increasing glucose transport and utilization. Circulation *112*, 2339-2346.

Melamud, E., Vastag, L., and Rabinowitz, J.D. (2010). Metabolomic analysis and visualization engine for LC-MS data. Anal Chem *82*, 9818-9826.

Metallo, C.M., and Vander Heiden, M.G. (2013). Understanding metabolic regulation and its influence on cell physiology. Mol Cell *49*, 388-398.

Munger, J., Bennett, B.D., Parikh, A., Feng, X.J., McArdle, J., Rabitz, H.A., Shenk, T., and Rabinowitz, J.D. (2008). Systems-level metabolic flux profiling identifies fatty acid synthesis as a target for antiviral therapy. Nat Biotechnol *26*, 1179-1186.

Nuutinen, E.M., Peuhkurinen, K.J., Pietilainen, E.P., Hiltunen, J.K., and Hassinen, I.E. (1981). Elimination and replenishment of tricarboxylic acid-cycle intermediates in myocardium. Biochem J *194*, 867-875.

Patten, I.S., Rana, S., Shahul, S., Rowe, G.C., Jang, C., Liu, L., Hacker, M.R., Rhee, J.S., Mitchell, J., Mahmood, F., et al. (2012). Cardiac angiogenic imbalance leads to peripartum cardiomyopathy. Nature *485*, 333-338.

Pound, K.M., Sorokina, N., Ballal, K., Berkich, D.A., Fasano, M., Lanoue, K.F., Taegtmeyer, H., O'Donnell, J.M., and Lewandowski, E.D. (2009). Substrate-enzyme competition attenuates upregulated anaplerotic flux through malic enzyme in hypertrophied rat heart and restores triacylglyceride content: attenuating upregulated anaplerosis in hypertrophy. Circ Res *104*, 805-812.

Reszko, A.E., Kasumov, T., David, F., Jobbins, K.A., Thomas, K.R., Hoppel, C.L., Brunengraber, H., and Des Rosiers, C. (2004). Peroxisomal fatty acid oxidation is a substantial source of the acetyl moiety of malonyl-CoA in rat heart. J Biol Chem *279*, 19574-19579.

Sugden, M.C., and Holness, M.J. (1993). Cardiac carbohydrate and lipid utilization during late pregnancy. Biochem Soc Trans *21 (Pt 3)*, 312S.

Vaillant, F., Lauzier, B., Poirier, I., Gelinas, R., Rivard, M.E., Robillard Frayne, I., Thorin, E., and Des Rosiers, C. (2014). Mouse strain differences in metabolic fluxes and function of ex vivo working hearts. Am J Physiol Heart Circ Physiol *306*, H78-87.

Vincent, G., Bouchard, B., Khairallah, M., and Des Rosiers, C. (2004). Differential modulation of citrate synthesis and release by fatty acids in perfused working rat hearts. Am J Physiol Heart Circ Physiol *286*, H257-266.

Vincent, G., Khairallah, M., Bouchard, B., and Des Rosiers, C. (2003). Metabolic phenotyping of the diseased rat heart using 13C-substrates and ex vivo perfusion in the working mode. Mol Cell Biochem *242*, 89-99.

Williams, J.G., Ojaimi, C., Qanud, K., Zhang, S., Xu, X., Recchia, F.A., and Hintze, T.H. (2008). Coronary nitric oxide production controls cardiac substrate metabolism during pregnancy in the dog. Am J Physiol Heart Circ Physiol *294*, H2516-2523.

Yi, L.Z., He, J., Liang, Y.Z., Yuan, D.L., and Chau, F.T. (2006). Plasma fatty acid metabolic profiling and biomarkers of type 2 diabetes mellitus based on GC/MS and PLS-LDA. FEBS Lett *580*, 6837-6845.

Zamboni, N., and Sauer, U. (2009). Novel biological insights through metabolomics and 13C-flux analysis. Curr Opin Microbiol *12*, 553-558.

Chapter 3:

Regulations of substrate switch in late pregnancy

Attributions: Laura Liu performed all experiments for this section unless otherwise noted. Dr. Glenn C. Rowe isolated mitochondria and performed the seahorse experiments. Dr. Barbara Kahn and Dr. Jack Lawler kindly provided the GLUT4 and CD36 deleted mouse tissues. Dr. Adam Wende generously donated the PDK4 KO mouse hearts, and Dr. Robert Harris provided the PDK4 antibody.

Abstract

Maternal cardiac metabolism defers to fetal preference for glucose by decreasing glucose consumption and increasing fatty acid oxidation. The factors responsible for this switch in late pregnancy has not been found. We determine here that mitochondrial biology is unchanged at the end of gestation. Furthermore, there are no alterations in the expression of enzymes in the triglyceride synthesis or turnover pathways or in the expression and localization of substrate transporters. Interestingly, we observed a muscle-specific induction of pyruvate dehydrogenase 4 (PDK4). PDK4 can regulate entry of pyruvate into the TCA cycle by phosphorylation of pyruvate dehydrogenase (PDH) and is crucial for connecting glycolysis, β-oxidation, and the TCA cycle. Furthermore, we found that treatment of isolated cardiomyocytes with the pregnancy hormone progesterone results in upregulation of PDK4. Mifepristone, an antagonist for the progesterone receptor, reverses this effect. Taken together, these studies point to PDK4 as a potential regulator of substrate switch in late pregnant mouse hearts.

Introduction

Fetal demands supersede maternal substrate usage during pregnancy. Late gestation is a state of insulin resistance and hyperlipidemia in the mother. The myocardium complies by decreasing glucose utilization and increasing fatty acid uptake and usage (Chapter 1). But what regulates this substrate switch? Metabolic pathways are regulated at many different points, including substrate availability, transporter localization, allosteric control of crucial enzymes, transcriptional control, post-translational modifications, and many more. What occurs during pregnancy has not been fully explored.

In this chapter, we seek to determine the regulator of substrate switch in late pregnancy. We will explore mitochondrial content and function, glucose transporter localization, and pyruvate dehydrogenase (PDH) regulation. Determining what controls substrate consumption in normal pregnancy will facilitate our understanding of whether cardiac diseases of pregnancy result from vulnerabilities in regulation.

Mitochondria in the heart

Over 95% of the ATP generated in the heart is derived from oxidative phosphorylation in the mitochondria, underscoring the importance of this organelle in fulfilling tissue energetic needs (Kolwicz et al., 2013). Disruption of mitochondrial processes, such as biogenesis, genome replication, or dynamics, can lead to diseased states. In fact, a hallmark of heart failure in humans and rodents is a decrease in mitochondrial copy number and content that is correlated with cardiac dysfunction (Bayeva et al., 2013). Certain physiological stimuli, such as exercise, can protect against age-related declines in mitochondria by promoting mitochondrial biogenesis (Holloszy and Booth, 1976). Thus, exploring the mitochondrial state of late pregnancy, especially with observed changes in substrate availability, will elucidate if adaptations have been made to this vital organelle.

Mitochondria have simple beginnings. Once a bacteria cell that was likely engulfed by a neighboring eukaryotic cell, they have evolved to become one of the most critical components of their host cell. It is an endo-symbiotic relationship, one in which over time the bacteria has lost its abilities to survive without its host, relying on it to transcribe and translate the majority of its genome (only 13 mitochondrial proteins are made in the mitochondria), and the host has become dependent on the ATP generated by its guest (relying on it for over 95% of its needs).

Cardiac mitochondria is different than that of other tissues (Song and Dorn, 2015). In most cells, mitochondria are dynamic, continuous, and form network structures. Elongation ("fusion") or fragmentation ("fission") is constantly occurring, depending on the needs of the cell. In the heart, however, mitochondria are completely different – they are short, small, fragmented and static. Fusion or fission seldom occur, and it takes over two weeks to complete a cycle (Beraud et al., 2009; Chen et al., 2011). This design is deliberate, it seems, as cardiac contractions would require tissue malleability, and long networks of mitochondria would hinder this. Though their phenotype differs from other cells types, fusion and fission do seem to have an important role as cardiac-specific ablation of genes involved in these processes can lead to cardiac dysfunction, respiratory abnormality, and cardiomyopathy (Chen et al., 2012a; Chen et al., 2012b; Chen et al., 2011; Kasahara et al., 2013; Papanicolaou et al., 2012a; Papanicolaou et al., 2012b; Song et al., 2015).

The metabolic pathways in the mitochondria are crucial to providing energy to the tissue (Stanley et al., 2005). β-oxidation, the tricarboxylic acid (TCA) cycle, and the electron transport chain (ETC) all reside in different parts of the mitochondria. The membrane duality of this organelle, with an inner mitochondrial membrane (IMM), surrounded by an outer mitochondrial membrane (OMM), is specifically created to facilitate these processes. β-oxidation and the TCA cycle occur in the mitochondrial matrix, the space inside the IMM. ETC complexes are on the IMM, and the proton gradient they create is in the space between the IMM and the OMM, entitled the intermembrane space (IMS). This double barrier also protects against any deleterious byproducts created from these metabolic pathways.

Since the principal function of the mitochondria is to provide ATP by oxidative phosphorylation, one way to assess mitochondrial capacity is by oxygen consumption in the

ETC. The ETC is made up of four complexes, each with the ultimate goal of pumping proteins from the matrix into the IMS to produce a proton gradient (Figure 3.1A). The driving force for electron transfer through the ETC is the free energy associated with reduction of oxygen to water. NADH and $FADH_2$ created from the TCA cycle, donate electrons to NADH-Q oxidoreductase (Complex I) and Q-cytochrome c oxidoreductase (Complex II), respectively. NADH donates two electrons to Complex I, which results in four protons transferred to the IMS. Complex II, on the other hand, contains succinate dehydrogenase, an enzyme in the TCA cycle that converts succinate to fumarate to generate $FADH_2$. Donation of electrons from $FADH_2$ does not contribute to formation of the proton gradient. Electrons from both complexes, traveling via electron carriers, arrive at Q-cytochrome c oxidoreductase (Complex III), where they are transferred to another carrier, cytochrome c. In this process, another four protons are transported to the IMS from the matrix. The fourth complex, cytochrome c oxidase, transfers electrons to reduce oxygen to water. The highly favorable reduction of oxygen drives the formation of the proton gradient, which is then used to drive ATP generation by the ATP synthase (Complex V), which is energetically unfavorable.

One common method to study mitochondrial respiration function is with inhibitors for the different complexes of the ETC on isolated mitochondria, concurrently with measurement of the oxygen consumption rate (Figure 3.1B). Doing so will allow targeting of dysfunction on the respiration of specific complexes (Readnower et al., 2012). We use this technique to assess mitochondrial respiration in isolated mitochondria from late pregnant hearts. Common inhibitors utilized include rotenone (complex I inhibitor), antimycin A (complex III inhibitor), and oligomycin (complex V inhibitor). First, basal respiration is assessed with ADP and energy

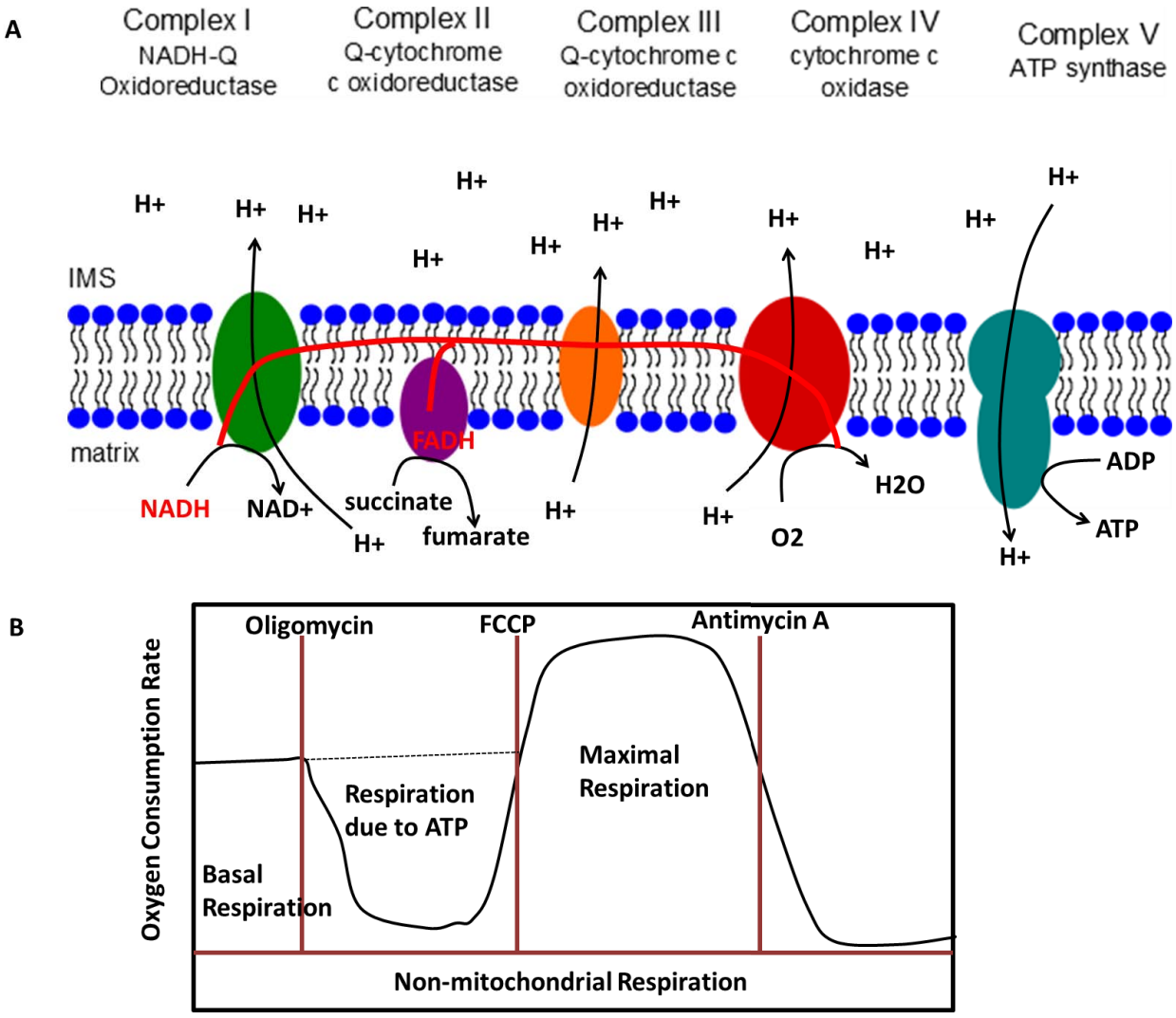

Figure 3.1: ETC and mitochondrial respiration. (A) The electrons donated from the products of the TCA cycle, NADH and FADH2, first travel to complex I and complex II of the ETC. The transfer of electrons through the ETC is coupled to the formation of the proton gradient in the IMS, and is driven by the free energy associated with the reduction of oxygen to water. Ultimately, this proton gradient drives the production of ATP by ATP synthase. (B) Oxygen consumption rate (OCR) is often used as a measure of mitochondrial functional capacity. Treatment of isolated mitochondria with inhibitors for the complexes of the ETC can be used to measure respiration under different conditions. First, in the presence of ADP and substrates, basal respiration is measured. Then, oligomycin, a complex V inhibitor, is added, leading to decreased respiration that is due to ATP production. Then, mitochondria are treated with FCCP, an uncoupler that will dissipate the proton gradient to lead to uninhibited electron transporter through the ETC and maximal oxygen consumption. Finally, antimycin A, a complex III inhibitor, shuts down respiration.

substrates. Then, mitochondria are treated with oligomyocin, which results in a decrease in the respiration due to ATP production. Next, uncouplers (FCCP, DNP), which completely dissipate the protein gradient to allow uninhibited electron transfer through the ETC, are used to determine maximal respiration status. Finally, antimycin A is added to fully shut down mitochondrial respiration (Figure 3.1B). Many groups have used this method to characterize cardiac mitochondria during heart failure (Nojiri et al., 2006; Sharov et al., 1998). While there have been some discrepancies, for the most part, decompensated heart failure is accompanied by impairments in complex I respiration (Rosca et al., 2013).

Alterations to mitochondrial capacity, copy number, biogenesis, and respiration are made in many physiological processes, such as heart failure or exercise (Doenst et al., 2010; Karamanlidis et al., 2011). Little has been studied about mitochondrial adaptations in the heart during pregnancy. One group found no difference in mitochondrial morphology with confocal microscopy studies (Bassien-Capsa et al., 2006). However, the increased workload of late pregnancy indicates that increased ATP demand could be accompanied by adaptations of the mitochondria to provide for this greater need.

Regulating substrate switch with transporter localization

Though substrate availability is a key determinant of usage in the heart, the import of substrates into the cell is still a highly regulated process (Schwenk et al., 2008). Two types of transporters are thought to be responsible for the majority of glucose and fat uptake, GLUTs (of which GLUT1 and GLUT4 are the most highly expressed in the heart) and CD36. Mice with deletion in cardiac CD36 decrease fatty acid uptake by approximately 70% and treatment of cells with an inhibitor of CD36, sulfo-N-succinimydyl-oleate (SSO), completely ablated fatty acid

uptake (Coburn et al., 2000; Coort et al., 2002; Habets et al., 2007). Furthermore, cardiac specific GLUT4 mice lack any insulin-stimulated glucose uptake, though their basal glucose uptake levels are normal, due to compensation by GLUT1 (Abel et al., 1999). There are similarities and differences in their regulation – both translocate when activated, and both respond to contraction and insulin. But they have very different means of storage and downstream effects. Assessing the expression and location of these transporters in late pregnant mouse hearts in the triglyceride-rich environment of late pregnancy can shed light on the role of CD36 and GLUT4 in substrate switch.

GLUT4 and CD36 have been well characterized to reside in intracellular vesicles until a stimulus induces their translocation to the sarcolemmal membrane (Steinbusch et al., 2011). There are two intracellular pools of GLUT4 – an endosomal pool and a non-endosomal pool that respond to different stimuli (Slot et al., 1991). Only 50% of CD36 transporters, on the other hand, are intracellular, while the majority of GLUT4 is intracellular until needed (Fischer et al., 1997; Luiken et al., 2004b; Luiken et al., 2002b). Furthermore, GLUT4 and CD36 occupy distinct subdomains of the sarcolemma – CD36 is thought to be in lipid raft-rich caveolae and GLUT4 has been characterized in caveolae and outside.

Though insulin and contraction can activate cellular localization of both transporters, their end goals are very different. Insulin signals for storage of substrates, whereas contraction promotes oxidation to generate ATP. Thus, different proteins respond to insulin and contraction. When insulin is secreted from pancreatic β-cells in response to feeding, it binds to insulin receptors on cardiomyocytes, which results in the phosphorylation of insulin receptor substrates 1 and 2 (IRS1/2) (Boucher et al., 2014). IRS1 activates the p85 regulatory component of phosphatidylinositol-3-phosphate (PI3K) (Luiken et al., 2002b). PI3K generates PI-3,4,5-

triphosphate (PIP3), which is responsible for inducing multiple kinases, including Akt/PKB and protein kinase C (PKC). These kinases directly inhibit AS160 (Akt substrate 160) to activate the rab GTPases that then promote GLUT4 and CD36 vesicle fission, transport, and finally fusion with the plasma membrane (Chen et al., 2008; Kramer et al., 2006a; Kramer et al., 2006b; Miinea et al., 2005; Roach et al., 2007).

On the other hand, increased contractile activity in cardiomyocytes signals an increased need for ATP (Luiken et al., 2004a). In this state, elevated levels of AMP, cAMP, and reactive oxygen species (ROS) work in concert to induce AMP-activated protein kinase (AMPK), protein kinase A (PKA), protein kinase D (PKD), and others (Zaha and Young, 2012). AMP can bind the regulatory γ-subunit of AMPK, exposing its catalytic α2-subunit to be phosphorylated by LKB1 (Jorgensen et al., 2004). Activated AMPK has many downstream actions, including increasing fatty acid oxidation. Furthermore, AMPK phosphorylates and inhibits AS160 in addition to activating the rab GTPases responsible for CD36 and GLUT4 vesicle translocation (Chen et al., 2008; Yang and Holman, 2005).

Diseased states show dysregulation of glucose and fatty acid utilization, and transporter location is similarly affected. For example, in diabetic cardiomyopathies, the increased presence of CD36 on the plasma membrane results in greater influx of fatty acids and ultimately lipotoxicity (Coort et al., 2004a; Coort et al., 2004c; Ouwens et al., 2007). Blocking CD36 with SSO in obese rats prevents buildup of excess lipids (Coort et al., 2004a). Skeletal muscle biopsies from humans with type 2 diabetes also have increased CD36 levels at the plasma membrane (Bonen et al., 2004). This parallels the increase in triglyceride levels in these patients. Ischemia/reperfusion (IR) also causes a substrate switch to increased glucose consumption that affect transporter localization. Rat hearts that underwent IR show 90% increased GLUT4 plasma

membrane levels during ischemia and 32% decrease in CD36 plasma membrane concentrations (Heather et al., 2013).

Triglyceride synthesis, storage and breakdown in the heart

The serum triglyceride environment of late pregnancy suggests that synthesis, storage, or breakdown of intracellular triglycerides could be altered to adequately meet energetic needs. How these pathways play in pregnant hearts have not been explored.

Upon uptake into cardiomyocytes, fats are activated to fatty acyl CoAs by long chain fatty acyl CoA synthetase (FACS). They then have two main fates: to continue on to β-oxidation or storage into triglycerides. In the healthy heart, the triglyceride pool has rapid turnover and thus is relatively limited. However, conditions where fatty acid oxidation is insufficient to keep up with increased fatty acid availability and uptake, such as diabetes, lead to increased triglyceride synthesis and lipid droplet formation. While this may be initially beneficial to keep harmful lipid intermediates away from the rest of the cell, long-term increases has been shown to adversely affect cardiac function. Thus, in the pregnancy state, could elevated serum triglycerides affect intracellular storage in the cell? We will explore expression of key proteins involved in these pathways in late pregnant mouse hearts.

The details of triglyceride synthesis and breakdown are explained in many excellent comprehensive reviews, so we will focus on the general principles here (Brindley et al., 2010; Kienesberger et al., 2013). Fats that enter the cell complete the Kennedy pathway to form triglycerides (Figure 3.2). This is dependent on a series of acylations and phosphorylations by many families of enzymes located near the mitochondria and the sarcoplasmic reticulum (SR). Proximity to these organelles allows rapid hydrolysis and usage when necessary. The enzymes in

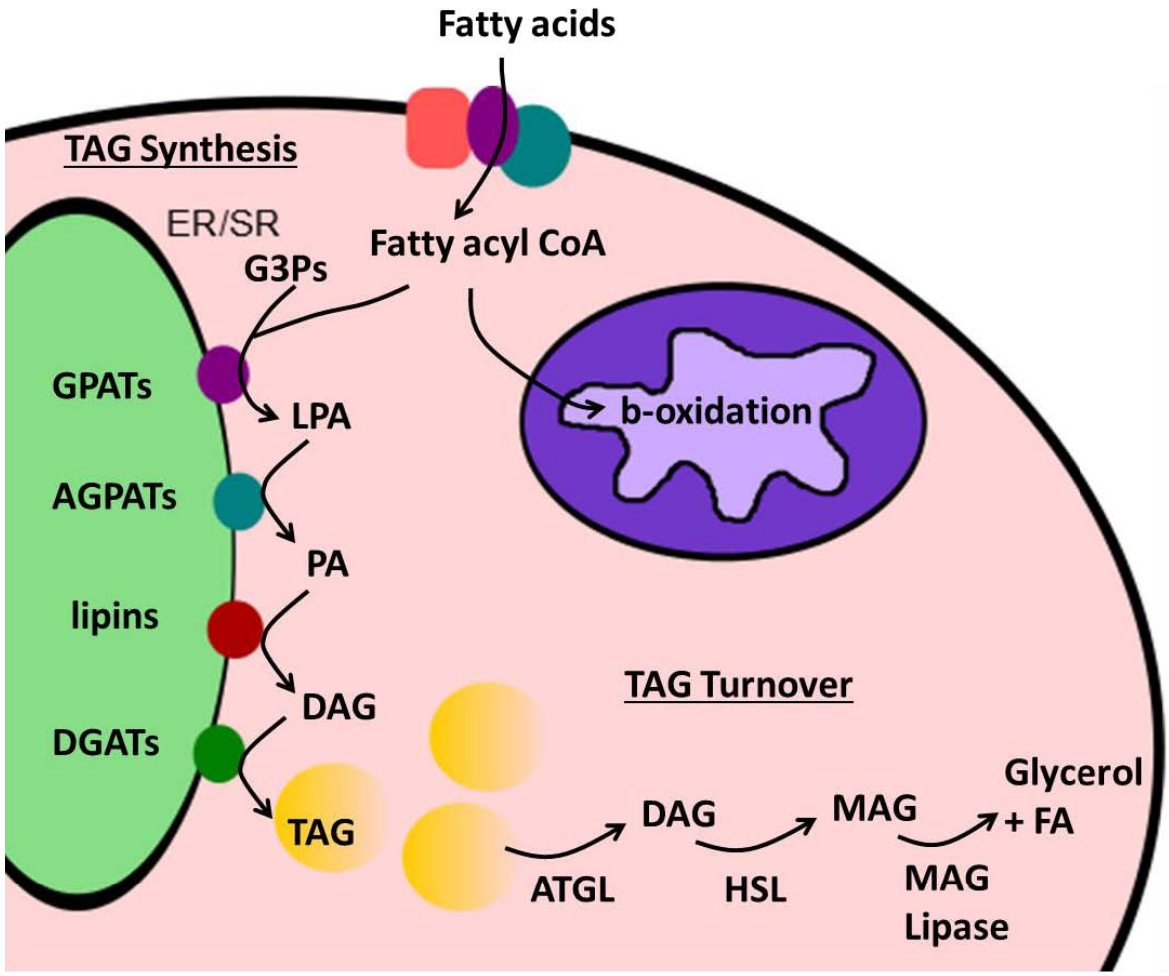

Figure 3.2: Triglyceride synthesis (Kennedy) and turnover pathways. Activated fatty acyl CoAs have two fates: to be oxidized in the mitochondria or undergo triglyceride synthesis by a series of enzymes located on the ER/SR surface. This includes a series of acylation and phosphorylation events by GPATs, AGPATs, lipins, and DGATs that ultimately results in the formation of triacylglycerols (TAG, triglycerides). When necessary, these TAGs can then be broken down in sequential hydrolysis reactions by ATGL, HSL, and MAG lipase to create glycerol and fatty acids.

the Kennedy pathway include glycerol-3-phosphate acyltransferases (GPATs), which catalyze the first step of esterification of fatty acids and glycerol-3-phosphate to form lysophosphatidic acid (LPA). A second esterification reaction by acylglycerol-3-phosphate acyltransferases (AGPATs) produces phosphatidic acid (PA), which is then converted to diacylglycerol (DAG) by lipins. The ultimate step is the formation of triglycerides by DAG acyltransferases (DGATs). Many of these proteins have been shown to be upregulated under physiological conditions that induce triglyceride formation. For example, GPATs levels are increased after fasting, in exercise-trained mice and in models of lipotoxic cardiomyopathy (Finck et al., 2002; Liu et al., 2009; Schoonderwoerd et al., 1990).

The myocardium is also capable of secreting lipoproteins by the actions of apolipoprotein B (apoB) and microsomal triglyceride transfer protein (MTTP) (Boren et al., 1998; Nielsen et al., 1998). After being made in the SR, lipoproteins are then processed through the trans-Golgi network for secretion. Consistent with their known roles, overexpression of apoB leads to elevated secretion and increased mtp expression is observed in diabetic states (Bartels et al., 2009; Nielsen et al., 2002).

The breakdown of triglycerides from lipid droplets occurs through a series of hydrolysis reactions (Figure 3.2). ATGL is the first enzyme to produce DAG through hydrolysis of TAG. Due to its rate-limiting role, it undergoes heavy regulation by many factors, including AMPK and periplipin-5. The hydrolysis of DAG by hormone-sensitive lipase (HSL) is then followed by the final hydrolysis of monoacylglycerol (MAG) lipase to form glycerol and fatty acids. The activity and expression of enzymes involved in triglyceride synthesis sand breakdown in hearts from late pregnant animals has not been examined.

Regulation of PDH by PDKs and PDPs

In late pregnant mouse hearts, there is a 50% decline in glucose utilization (Chapter 1). There are many regulatory points that result in decreased glucose flux. One of them is in the key enzyme complex that connects glycolysis to the TCA cycle - pyruvate dehydrogenase complex (PDC), which decarboxylates pyruvate to acetyl CoA (Figure 3.3). PDH is one of the components of the complex, also named E1 (Holness and Sugden, 2003; Zhang et al., 2014). PDH is located in the mitochondria and is strongly regulated by a family of kinases, pyruvate dehydrogenase kinases (PDKs), and a family of phosphatases, pyruvate dehydrogenase phosphatases (PDPs) (Holness and Sugden, 2003). There are four members of the PDK family, of which PDK2 and PDK4 have the highest expression in the heart. There are three serine sites (site 1: ser293; site 2: ser300; site3: ser232) on PDH that can be phosphorylated by PDK1-4, which have preferential activity towards each site. For example, PDK4 phosphorylates serine site 2 more so than others, while PDK1 is the only member that phosphorylates site 3. There are two members of the PDP family (PDP1-2), of which PDP2 has the greatest cardiac expression.

Regulation of PDH by PDK affords the cell metabolic flexibility in the face of different physiological conditions. For example, states of starvation, obesity, exercise, insulin resistance and diabetes all induce PDK4 in muscle (Holness et al., 2002; Lee, 2014; Pilegaard and Neufer, 2004). Induction of PDK4 inhibits PDH and prevents glucose utilization, while increasing fatty acid oxidation. In the case of starvation, this is to save the limited resources and convert to using fat as a substrate source. Thus, 48 hour fasted rats exhibit upregulation of PDK4 (Holness et al., 2002). PDK4-null mice that have been fasted have lower fatty acid oxidation and higher glucose use with decreased blood glucose and greater PDH activity (Jeoung and Harris, 2008). In times of excess energy supply, as in obesity and diabetes, however, PDK4 is also upregulated. Both

rats fed high fat diets and human type 2 diabetic patients induce PDK4 in skeletal muscle (Holness et al., 2000; Hwang et al., 2009; Kulkarni et al., 2012). In PDK4-deleted mice, high fat diet for 32 weeks protected against a pathological phenotype – mice have less fat accumulation and better glucose tolerance (Hwang et al., 2009). Thus, PDK4 has been at the center of therapeutics to increase metabolic flexibility during diseased states.

PDK4 itself is also regulated by many factors (Figure 3.3). In states of starvation, the

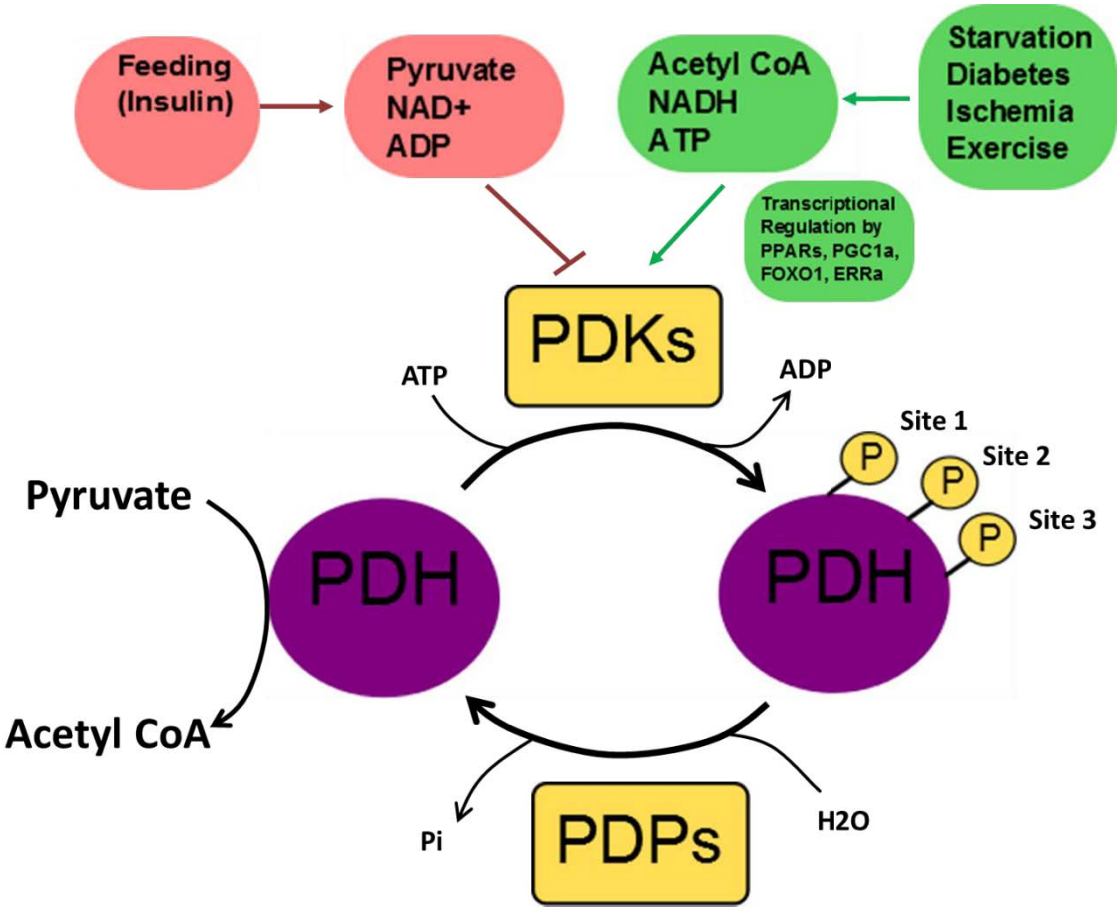

Figure 3.3: Regulation of PDH activity by PDKs and PDPs. PDH is responsible for decarboxylation of pyruvate to acetyl CoA. It is tightly regulated by families of PDKs (inhibition) and PDPs (activation), which themselves are highly regulated. PDKs are activated by states of starvation, diabetes, ischemia, and exercise. The environment is one of high acetyl CoA, NADH, and ATP. Many transcription factors and co-activators can induce its expression, including PPARs, PGC-1α, FOXO1, and ERRα. Furthermore, it is inhibited by fed states and insulin. Pyruvate, NAD+, and ADP can inhibit PDK.

high acetyl CoA to CoA and NADH to NAD+ ratios from fatty acid oxidation stimulate PDK4. In contrast, pyruvate inhibits PDK4. With less acetyl CoA conversion from pyruvate, less malonyl CoA is formed, lifting inhibition on fatty acid oxidation. Forkhead box O1 (FOXO1) and FOXO3 are transcription factors that also promote fatty acid utilization and PDK4 expression (Battiprolu et al., 2012). FOXO1 and PDK4 are both downstream of PPARδ/β. Thus, the influx of fats activate PPARδ/β signaling and shifts the transcriptional profile of the cell towards fatty acid usage. PGC-1α and ERRα also cooperatively induce PDK4 expression in response to exercise stimulation (Wende et al., 2005). Hormones can also affect PDK4 expression. Insulin, for example, strongly inhibits PDK4 in gastrocnemius muscle (Kim et al., 2006). Glucocorticoid receptors, on the other hand, can directly bind to the PDK4 promoter to stimulate expression (Connaughton et al., 2010).

There have also been studies in ovariectomized rats implanted with slow release progesterone or estrogen tablets that show increased PDK4 expression in skeletal muscle, suggesting that hormones of pregnancy can also affect substrate use in pregnant rodents as well (Campbell et al., 2003). Interestingly, two groups explored metabolism in pregnancy found no change in PDH activity or PDK4 expression in day 18 pregnant rat hearts (Nieuwenhuizen et al., 1998; Rimbaud et al., 2009), while decreased PDH expression was observed in dogs (Williams et al., 2008). However, the role of PDK4 in late pregnancy in mouse hearts is not clear.

Conclusion

Decreased glucose utilization in late pregnancy implicates alterations in metabolic regulation. However, whether the point of control is at mitochondrial phenotype, transporter translocation, triglyceride storage, pyruvate entry to the TCA cycle, or others has not been

explored. We seek to determine if late pregnant mouse hearts show differences in regulatory points compared to non-pregnant mice. Knowledge of this could point to new therapeutic perspectives to treat cardiac diseases of pregnancy.

Results

Normal mitochondrial phenotype in late pregnancy in mice

To determine if the substrate switch observed in late pregnancy is due to changes in mitochondria, we assessed the state of the mitochondria during late pregnancy. Mitochondrial DNA copy number (ratio of mito DNA to genomic DNA) is not different between late pregnancy and control (Figure 3.4A). Similarly, there is no change in gene expression of nuclear-encoded mitochondrial genes or in the expression of the proteins subunits in complexes of the ETC (Figure 3.4B and C). Mitochondrial morphology was assessed with mitotracker red staining, and no dramatic differences are apparent between late pregnant mouse hearts and non-pregnant controls (Figure 3.4D). However, electron microscopy (EM), the gold standard for assessing mitochondrial morphology was not performed and may better elucidate more subtle changes. Overall, this indicates that in late pregnancy, there are no dramatic changes in the number or morphology of cardiac mitochondria.

We further assayed if mitochondrial dynamics could be altered by examining gene expression of proteins involved in fusion and fission. No differences in the expression of mitochondrial fusion (Mfn1, Mfn2, Opa1) or fission (Drp1) was observed (Figure 3.5). Interestingly, PINK1 (PTEN-induced putative kinase 1), a quality control kinase that targets damaged mitochondria for degradation through mitophagy, is significantly decreased by approximately 25%. Furthermore, we observed a trend towards decreased expression of Parkin,

the E3 ubiquitin ligase that is recruited by PINK1 to the mitochondria, in late pregnant mouse hearts. Thus, this suggests that there is potentially decreased mitophagy in late pregnancy, while mitochondrial fission and fusion are not changed. However, further studies are necessary to confirm that mitophagy is indeed affected.

Though mitochondrial number is the same, mitochondrial function could still be altered. We performed oxygen consumption studies on isolated mitochondria of late pregnant mouse and

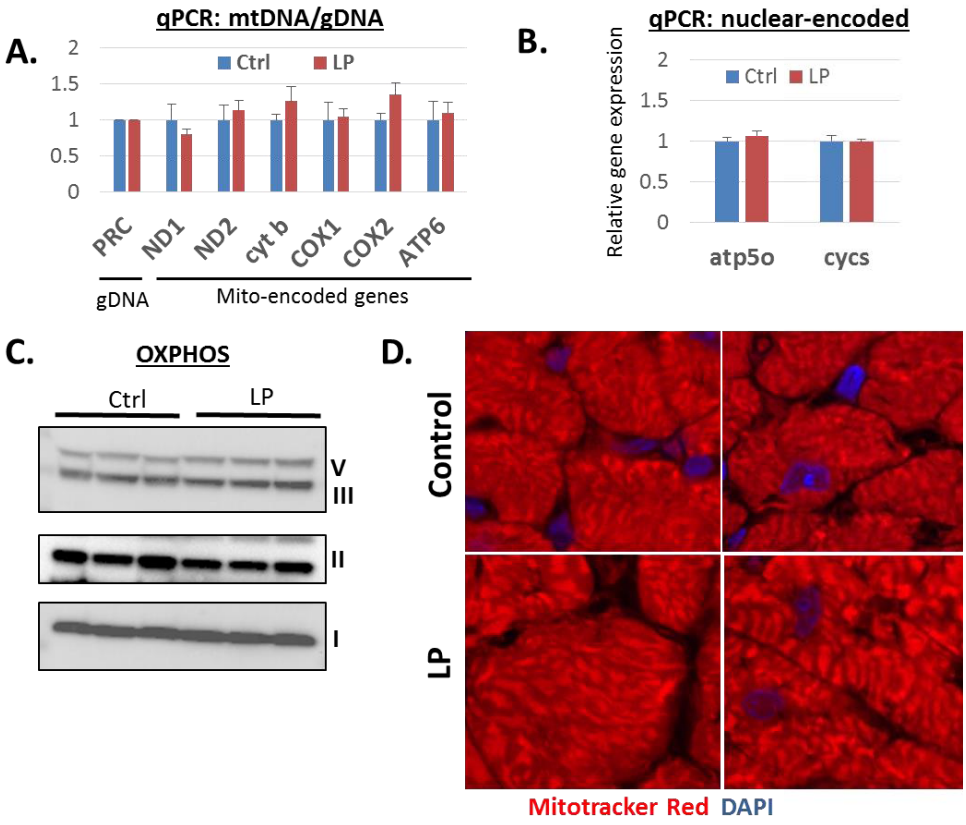

Figure 3.4: Mitochondrial DNA copy number, expression of oxidative phosphorylation proteins and morphology are unchanged in late pregnant mouse hearts. (A) DNA was isolated from mouse hearts and the ratio of mtDNA to gDNA was calculated for control (n=3) and late pregnant mouse hearts (n=3). (B) mRNA was isolated from mouse hearts, followed by qRT-PCR to assess expression of nuclear-encoded mitochondrial genes. (C) Western blot analysis of proteins subunits of ETC complexes from isolated mitochondria from late pregnant and control mouse hearts. (D) Mitochondrial morphology was examined by staining with mitotracker red on OCT frozen sections of hearts from late pregnant and control mice.

rat hearts, compared to non-pregnant control. Respiratory capacity does not change in late pregnancy, regardless of the conditions chosen (Figure 3.6). There is no difference in complex I or complex II respiration in rats. Furthermore, the choice of substrate (either pyruvate/malate or palmitoylcarnitine/malate) does not significantly affect the oxygen consumption rate in mice. It is worth noting that a trend towards decreased basal and maximal respiration is observed in late pregnant mouse hearts given pyruvate/malate as substrates, but the effect is not significant (Figure 3.6B).

The disadvantage of using isolated mitochondria from heart tissues is the potential for selecting a specific pool of mitochondria. Thus, we isolated adult cardiomyocytes from late pregnant mouse hearts, and treated the cells with saponin, a membrane permeabilizer. Consistent with the above findings, no alterations in respiration is observed (Figure 3.6E). We conclude that the mitochondrial biology of late pregnant mouse hearts is not distinctively different in number, function, and form from non-pregnant mouse hearts.

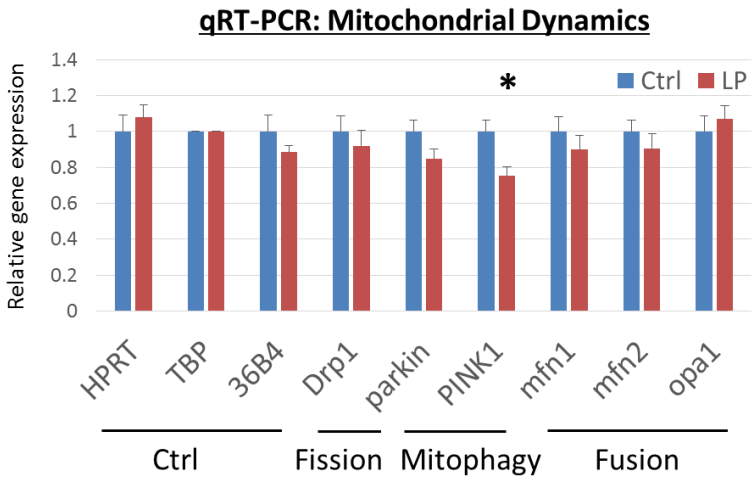

Figure 3.5: PINK1 is decreased in late pregnant mouse hearts. Quantitative, real-time PCR was performed from mRNA isolated from late pregnant mouse hearts, compared to non-pregnant controls (Ctrl: blue bars n=7; LP: red bars n=7, *p-value < 0.05).

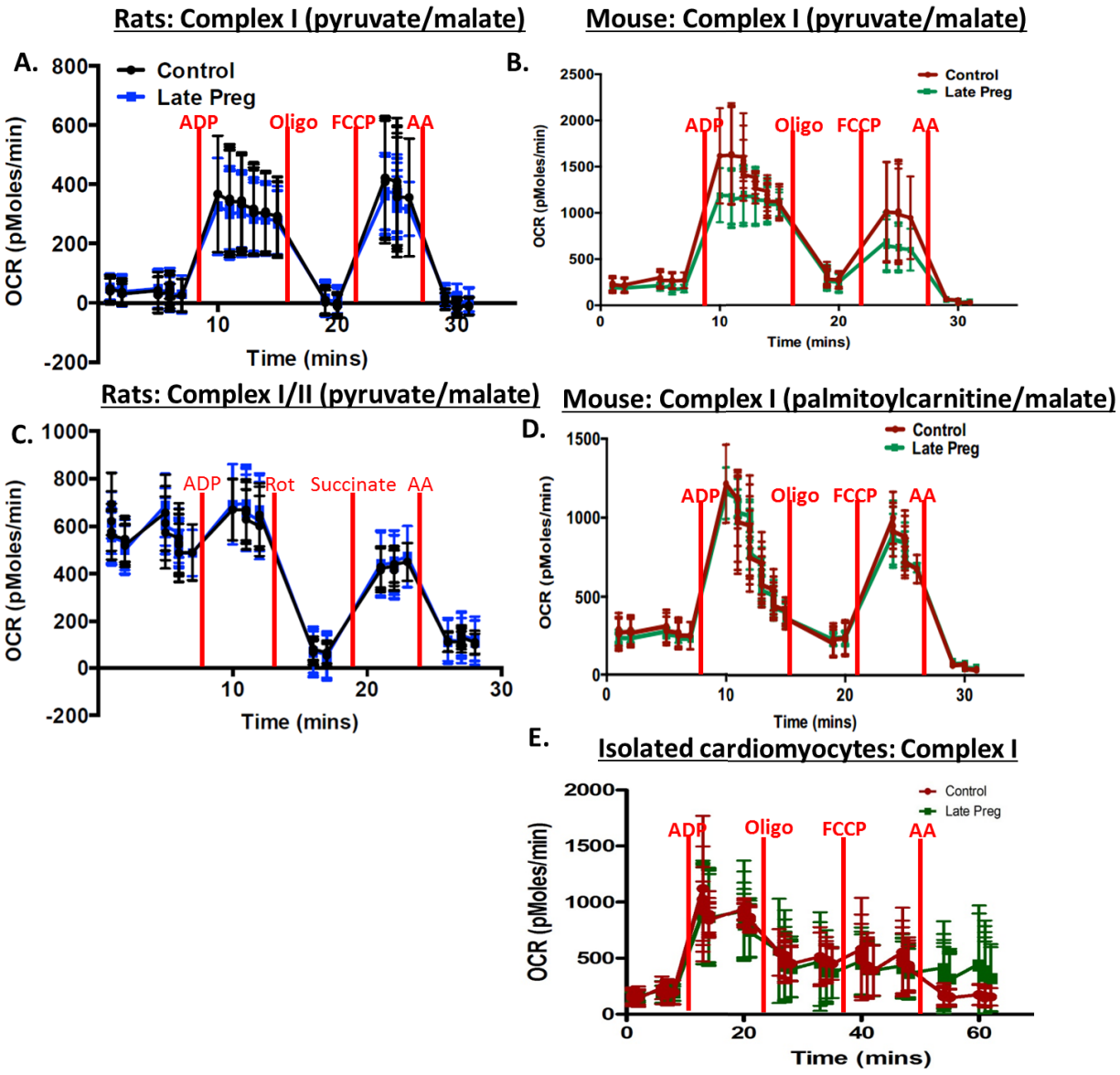

Figure 3.6: Mitochondrial respiration capacity is not significantly altered in late pregnant hearts. (A and C). Isolated mitochondria from late pregnant and control rat hearts were assayed for respiration by the Seahorse XF Flux Analyzer after inducing states 3 and 4 respiration. Complex I (A) and complex II respiration (C) were evaluated with pyruvate/malate as substrate (B and D). Isolated mitochondria from late pregnant and control mouse hearts were assayed for respiration. Complex I respiration was evaluated with pyruvate/malate (B) and palmitoylcarnitine/malate (D) as substrates. Adult cardiomyocytes were isolated from wild-type and late pregnant mice, and then treated with saponin to permeabilize the membrane before assessing respiration (E).

Substrate transporter localization and expression are unchanged in late pregnancy

Substrate switch often occurs concurrent with alterations in the expression of metabolic proteins. Quantitative, real-time PCR (qRT-PCR) demonstrated no change in the expression of genes involved in glucose uptake, GLUT1 or GLUT4, or lactate uptake, MCT1 and MCT4, in late pregnant mouse hearts (Figure 3.7A). However, CD36, the transporter that imports fatty acids, is moderately but significantly induced.

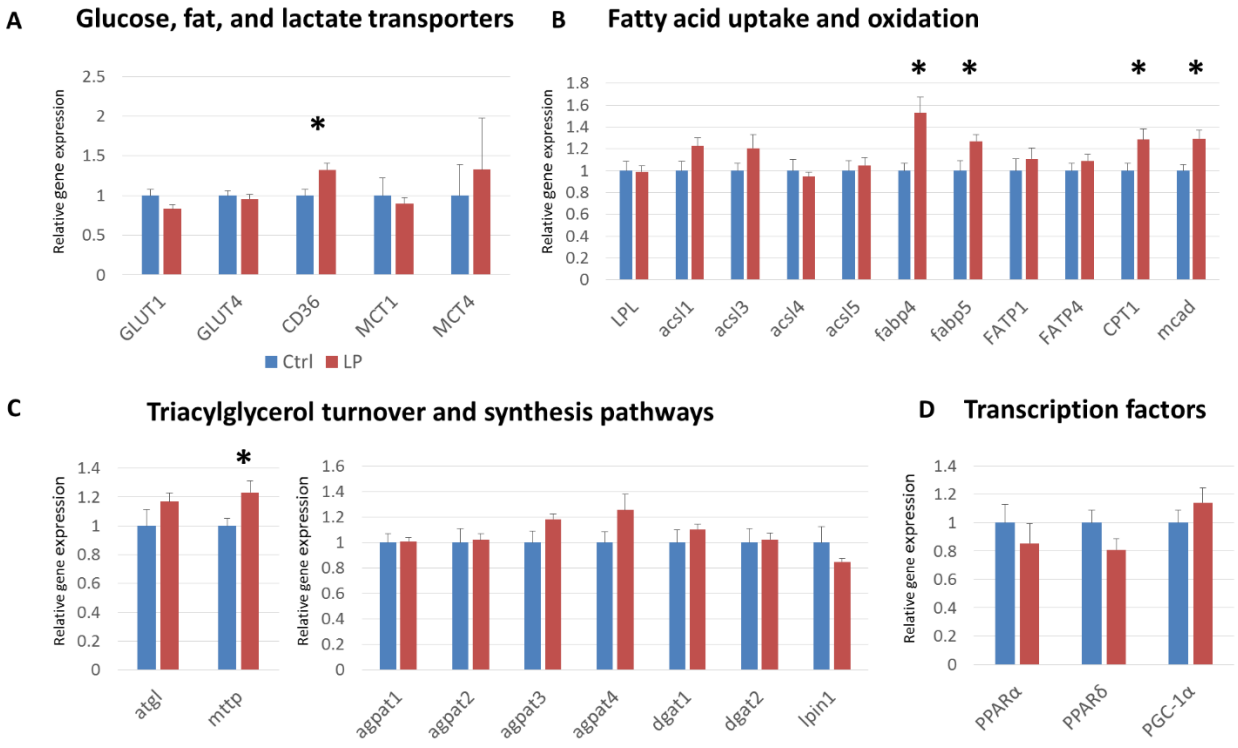

Figure 3.7: Moderate effects of pregnancy on fatty acid uptake and oxidation genes. Quantitative, real-time PCR was performed on mRNA isolated from late pregnant mouse hearts and then compared to non-pregnant controls. Genes for the following pathways were assayed: (A) substrate transporter expression; (B) fatty acid uptake and oxidation; (C) triacylglycerol breakdown and synthesis; (D) transcription factors. (Ctrl: blue bars n=7; LP: red bars n=7, *p-value < 0.05).

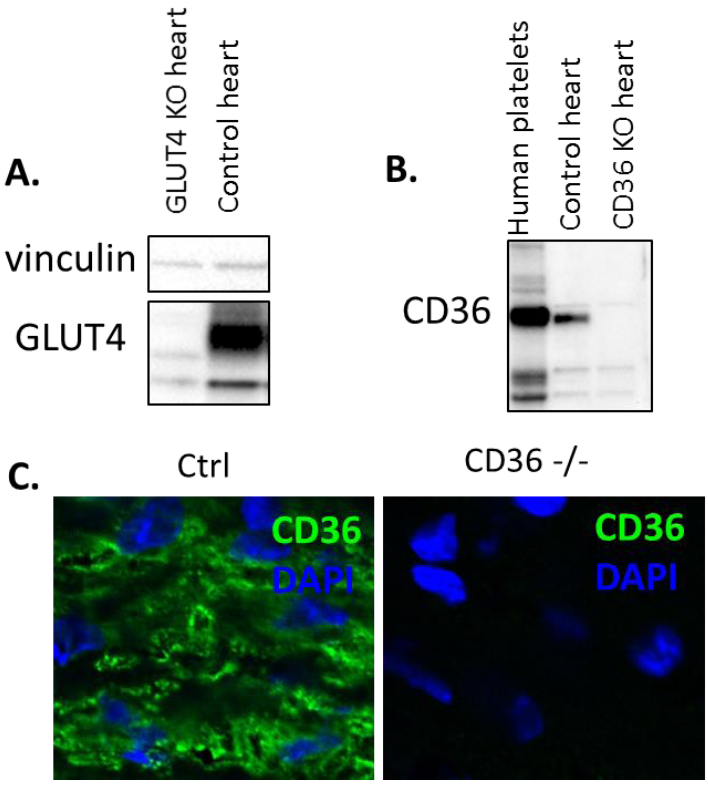

Figure 3.8: Antibody verification in GLUT4 and CD36 knockout animals. Total cell lysates were collected from GLUT4 and CD36 knock out mice hearts and antibodies were tested for GLUT4 (A) protein expression by Western, CD36 protein expression by Western (B), and CD36 immunofluorescence (C).

Western blot analysis of GLUT4 and CD36 demonstrated no difference in protein expression (Figure 3.9 and 3.10). Confirmation of these antibodies for western blot and histology were made in the hearts of GLUT4 and CD36-null mice (Figure 3.8), kindly provided by Dr. Barbara Kahn (GLUT4) and Dr. Jack Lawler (CD36). Other fatty acid uptake and oxidation genes, such as CPT1, MCAD, FABP4 and FABP5, are also mildly upregulated, while no change is observed for others, including ACSL and FATPs (Figure 3.7B). These results suggest that while no striking differences in gene expression are observed, there is a moderate signal for fatty acid oxidation.

A key regulatory point for substrate switch is the uptake of substrates. GLUT4 and CD36 allow entry of glucose and fatty acid through the plasma membrane. At basal states, these transporters reside predominantly in intracellular vesicles. Though there is no change in total protein expression of GLUT4 or CD36, their presence on the plasma membrane could be affected in late pregnancy. There is no evidence of transporter movement by histological analysis

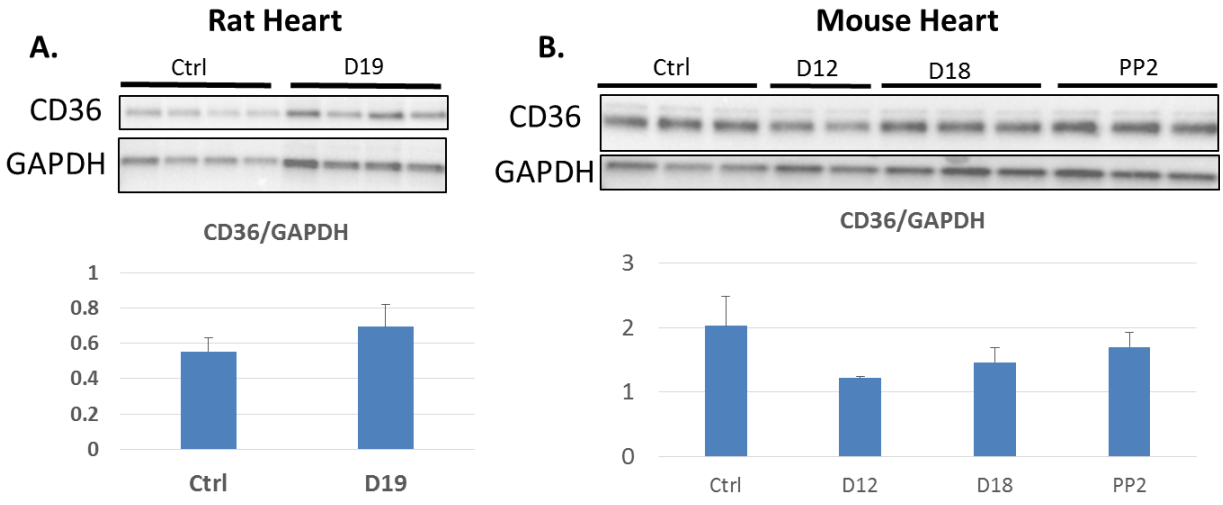

Figure 3.9: CD36 expression in mouse and rat pregnancies. (A) Total cell lysate was collected from day 19 of pregnancy and control rat hearts and then assayed by Western blot for CD36 expression. (B) Total cell lysate was collected from mouse hearts at day 12, day 18, and postpartum day 2 of pregnancy and then assayed by Western blot for CD36 expression. No significant changes were observed.

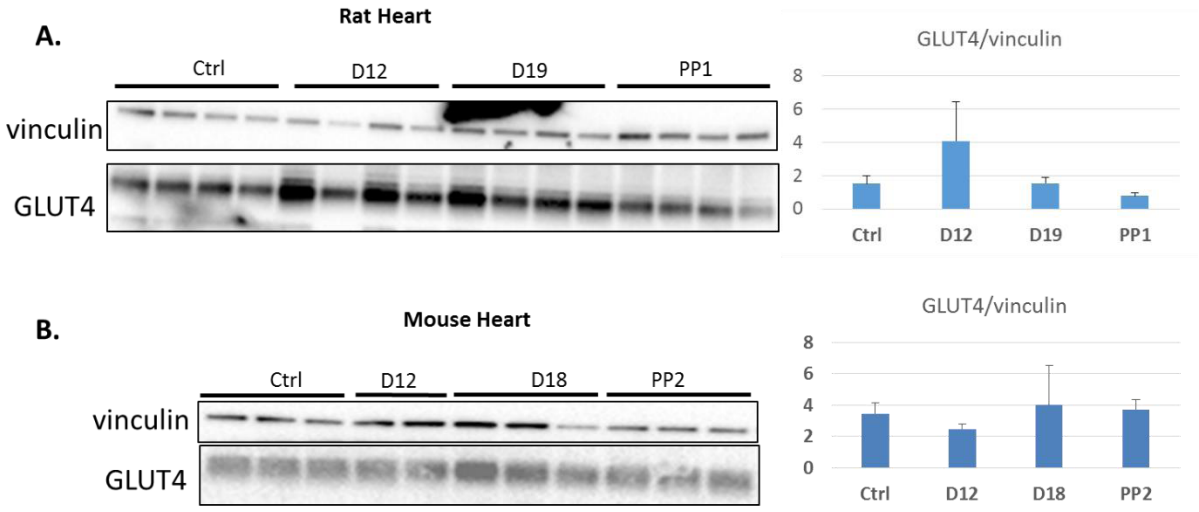

Figure 3.10: GLUT4 expression in mouse and rat pregnancies. (A) Total cell lysate was extracted from rat hearts at day 12, day 19, and postpartum day 1 of pregnancy and then assayed by Western blot for GLUT4 expression. (B) Total cell lysate was collected from mouse hearts at day 12, day 18, and postpartum day 2 of pregnancy and then assayed by Western blot for GLUT4 expression. No significance was observed.

(Figure 3.11A). Furthermore, subcellular fractionation studies on late pregnant mouse hearts showed no difference in GLUT4 localization (Figure 3.11B). We conclude that transporter localization is not a factor affecting the switch in energy source in late gestation.

Triglyceride synthesis and breakdown in late pregnancy

The increase in serum triglycerides suggests that triglyceride synthesis or storage pathways in the late pregnant heart could be activated. No change is observed in expression of AGPATs, DGATs, or lipin-1 (Figure 3.7C). Microsomal triglyceride transfer protein (mttp), which is involved in the export of triglycerides from the heart and known to be protective against lipotoxicity, is significantly induced by approximately 1.2-fold (Figure 3.7C). Furthermore, transcriptions factors responsible for the upregulation of fatty acid oxidation, such as PPARα, PPARδ, and PGC-1α also are not altered in late pregnancy (Figure 3.7D).

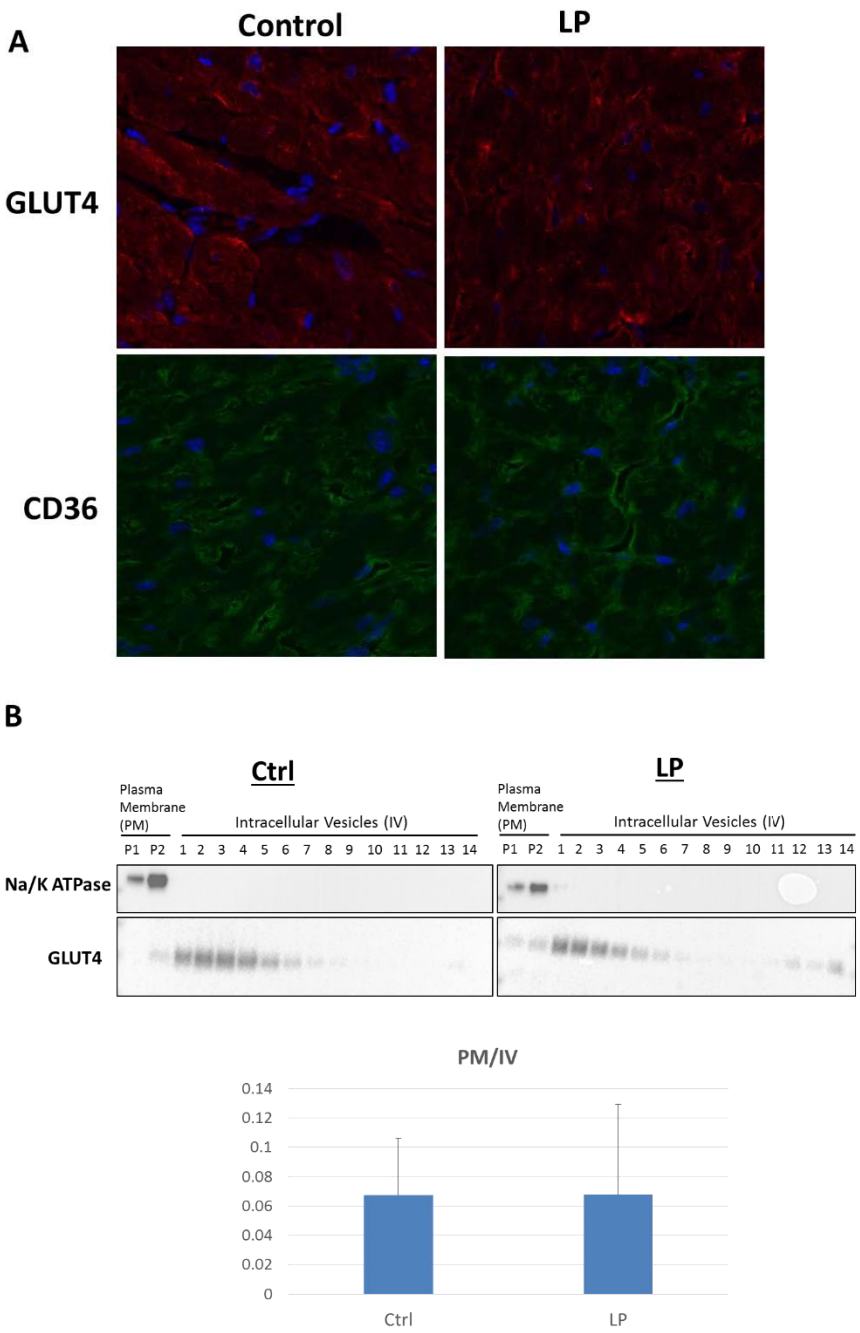

Figure 3.11: No change in localization of GLUT4 and CD36 in late pregnancy. (A) Mouse hearts were harvested from day 18 pregnant mice, compared to their non-pregnant controls. Histological analyses were conducted on OCT frozen mouse heart sections. GLUT4 and CD36 antibodies were used for staining. (B) Subcellular fractionation of late pregnant mouse hearts and their non-pregnant controls was conducted with different rounds of ultracentrifugation. The plasma membrane (PM, P1 and P2) was separated from intracellular vesicle fractions (IV, 1-14). Na/K ATPase was used as a plasma membrane marker. All fractions were blotted with GLUT4 to examine localization. Quantification of the abundance of GLUT4 on the PM versus IV (PM/IV) is shown (B). Ctrl (n=2), LP (n=3).

Late pregnancy promotes expression of PDK4

Approximately 50% decrease in flux from glycolysis was observed in the ^{13}C-tracer studies (Chapter 1). PDH controls the glycolytic contribution to the TCA cycle by converting pyruvate into acetyl CoA. As previously described, PDK4 can phosphorylate PDH to inhibit entry of carbons from glycolysis. We used qRT-PCR to assess the expression genes from the PDK family, the PDP family, and the FOXO family. There is a muscle-specific induction of PDK4 in late pregnancy (Figure 3.12). Consistent with this, a significant decrease in PDP1 and PDP2 is

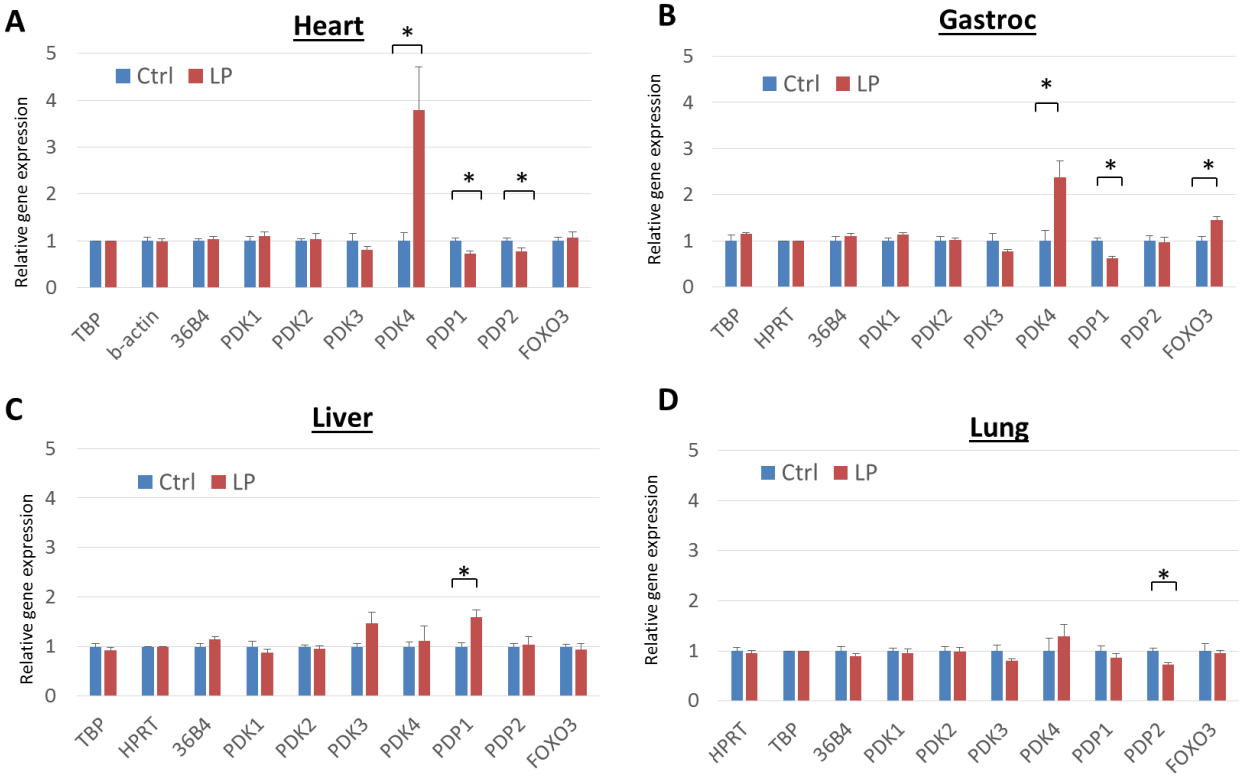

Figure 3.12: Muscle-specific induction of PDK4 in late pregnancy. Quantitative, real-time PCR was conducted on mRNA isolated from day 18 pregnant mouse tissues, including the heart, gastrocnemius, liver, and lung compared to their corresponding non-pregnant controls. (Ctrl n=7, LP n=7, *p-value < 0.05)

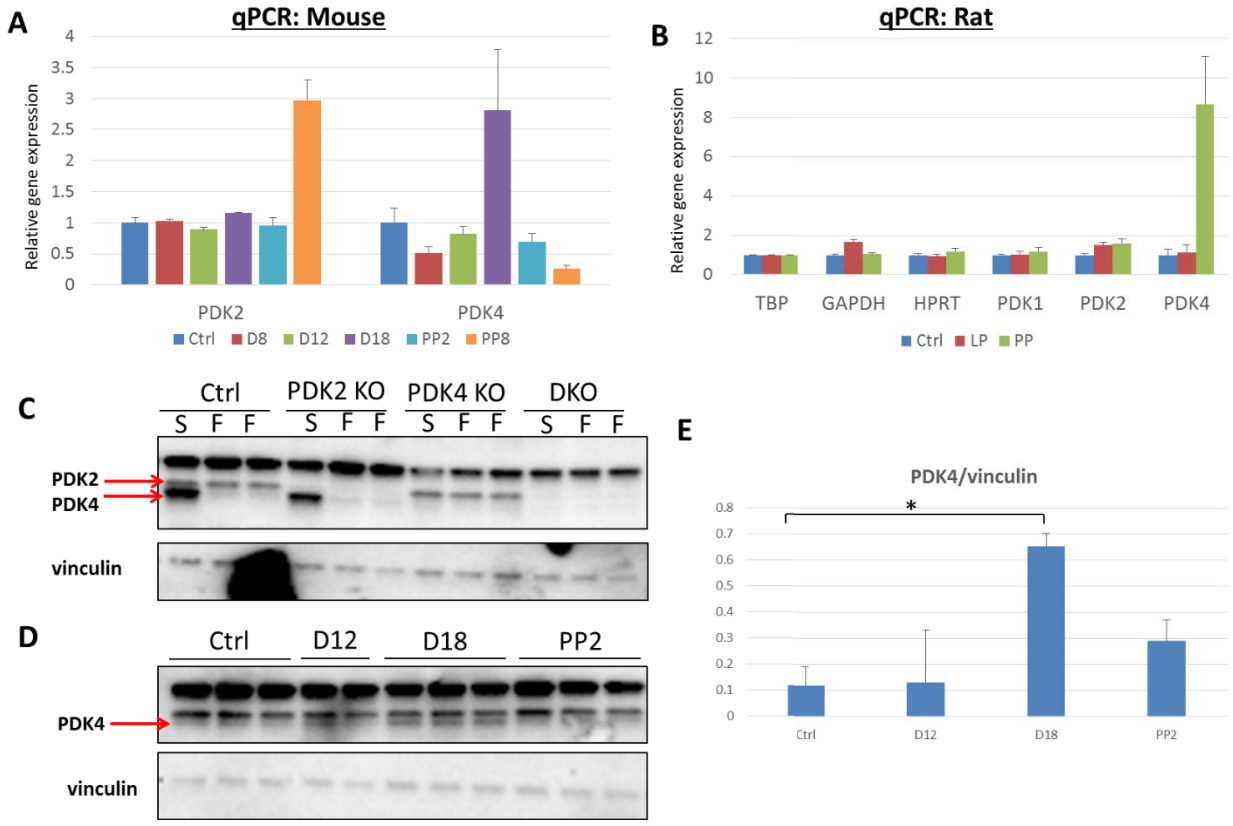

Figure 3.13: Induction of PDK4 expression is specific to late pregnancy. Hearts were harvested from different timed pregnancy samples from mice (A, days 8, 12, 18 of pregnancy and postpartum days 2 and 8) and rats (B, day 20 of pregnancy and postpartum day 1), mRNA was isolated and qRT-PCR was conducted to study gene expression. Verification of the PDK4 antibody was completed with PDK2 KO, PDK4 KO, and DKO (double knock out) mice (C) in starved (S) or fed (F) conditions. Western blot of PDK4 protein expression was conducted (D) with total cell lysates of timed pregnant mouse hearts. Quantification of PDK4 expression in late pregnancy is shown (E). (*p-value < 0.05).

observed in the heart, although only PDP2 is decreased in the skeletal muscle. FOXO3 is also significantly increased in gastrocnemius, but not in the heart.

A pregnancy time course evaluation of PDK4 expression shows that the response is targeted to late pregnancy, while downregulation is observed at postpartum day 8 (Figure 3.13A). Interestingly, this trend does not occur in rat pregnancies, as PDK4 is induced specifically at postpartum day 1 (Figure 3.13B). Protein expression of PDK4 shows an approximately 6-fold increase (Figure 3.13D and E). Verification of the antibody was completed on samples from PDK4-null mouse hearts, PDK2-null mouse hearts, and double knock out (DKO) hearts in the starved (S) and fed (F) conditions, kindly provided by Dr. Adam Wende (Figure 3.13C). Furthermore, downstream phosphorylation of PDH at serine 293 is shown in Figure 3.14, indicating that PDK4 activity is also upregulated. After observing PDK4 induction in late pregnancy, we re-analyzed the ^{13}C metabolic flux analysis of Langendorff perfused hearts

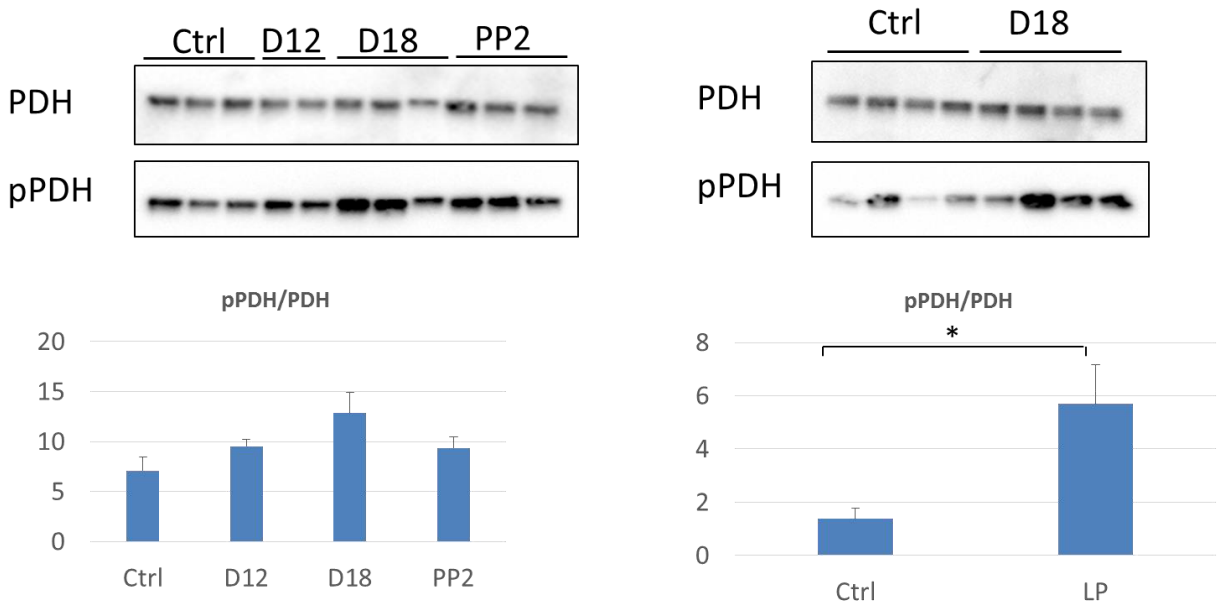

Figure 3.14: PDH is phosphorylated in late pregnancy. Western blot of late pregnant mouse hearts for phosphorylated (Serine 293) and total pyruvate dehydrogenase (PDH) in two sets of late pregnant mouse hearts. (*p-value < 0.05)

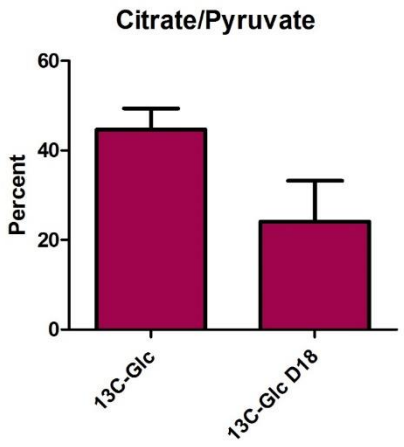

Figure 3.15: Pyruvate flux into the TCA cycle is inhibited during late pregnancy. From Langendorff perfused hearts data in Chapter 1, we determined the pyruvate flux into the TCA cycle. The presence of the m2 isotopomer of citrate (as a surrogate for acetyl CoA) was compared to the m3 isotopomer of pyruvate in non-pregnant and late pregnant mouse hearts to determine entry of pyruvate into the TCA cycle.

from Chapter 1 to specifically determine the input of labeled carbons from pyruvate into the TCA. There is a significant decrease in pyruvate entry into the TCA cycle (Figure 3.15).

Progesterone induces PDK4 in NRVMs

Induction of PDK4 specifically in late pregnancy suggests that the hormonal milieu could potentiate the response. Isolated neonatal ventricular myocytes (NRVMs) were used to determine the effects of hormones on PDK4 gene expression. Progesterone and estrogen have been well characterized to be elevated during late pregnancy. NRVMs were treated with physiological levels of progesterone and estrogen for 1-48 hours (Figure 3.16). Striking upregulation of PDK4 is observed after 4-8 hours of progesterone treatment. Furthermore, estrogen induces PDK4 but not as strongly as progesterone. Prolactin incubated on NRVMs did not induce PDK4 (data not

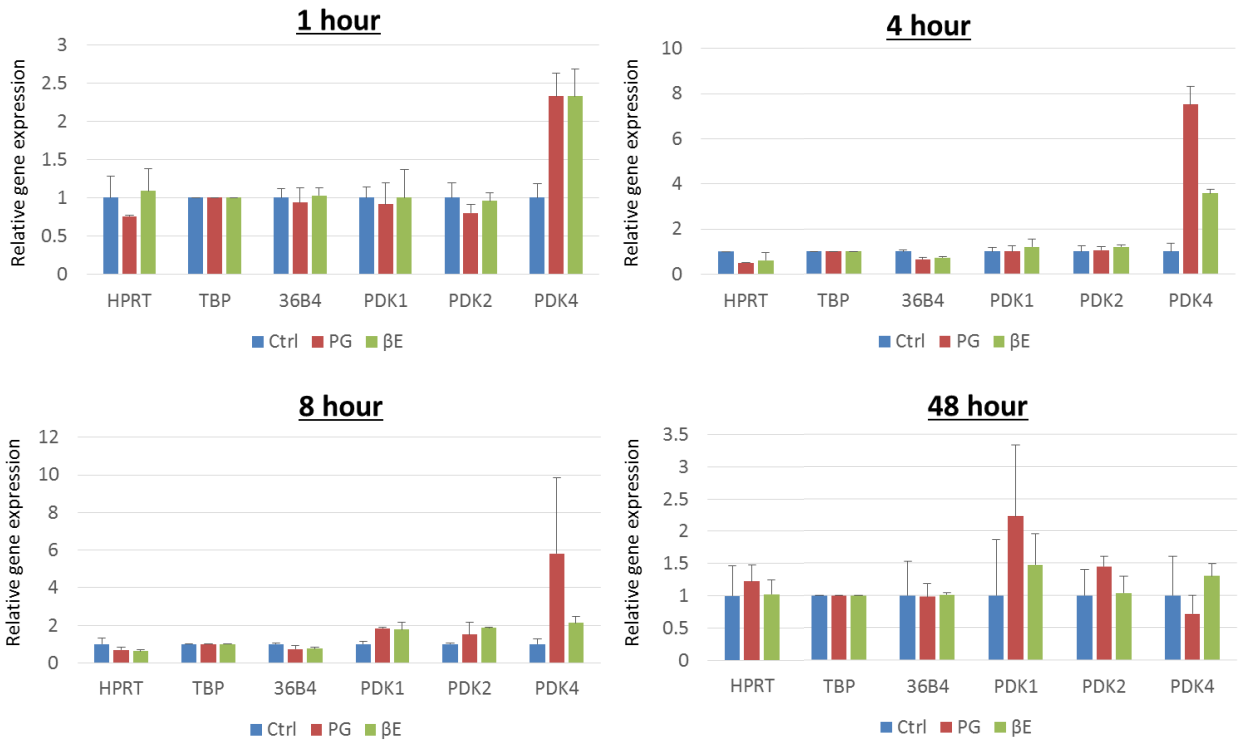

Figure 3.16: PDK4 is induced by progesterone at different time points in NRVMs. NRVMs were treated with 100 ng/mL of progesterone (PG) or 100 pg/mL β-estradiol (βE) for 1 hour, 4 hour, 8 hour, and 48 hours, and then assessed for gene expression with qRT-PCR.

shown). Treatment of isolated mouse adult cardiomyocytes, however, did not induce PDK4 (Figure 3.17), but the challenges of long-term culture of adult cardiomyocytes may contribute to the results presented here. MCF7s, a breast cancer cell line, also do not respond to progesterone treatment (Figure 3.18). C2C12s, a myoblast cell line that can be differentiated to myotubes, were also incubated with progesterone and estrogen. Mild induction of PDK4 is observed at 24 hours (Figure 3.19). This indicates that the striking PDK4 response to progesterone is cardiac specific.

The downstream effects of progesterone can be mediated through both progesterone receptor and non-receptor pathways. To determine if the progesterone receptor plays a role in PDK4 induction, we used a receptor antagonist, mifepristone (RU486) to pre-treat NRVMs for 1

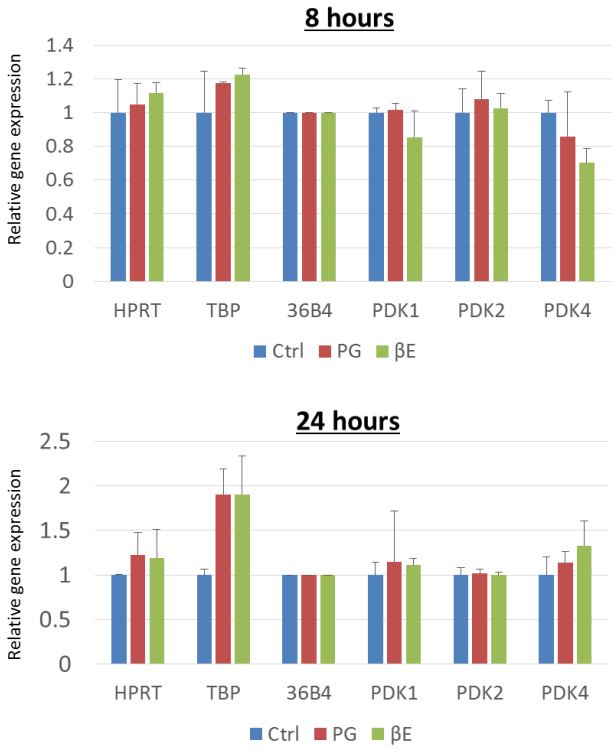

Figure 3.17: PDK4 is not induced in adult cardiomyocytes. Cardiomyocytes were isolated from C57/bl6 mice, and then treated with progesterone (PG) or β-estradiol (βE) for 8 or 24 hours in media containing MEM, insulin transferrin selenium (ITS), glutamine, NaHCO3, HEPES, 0.2% BSA, and blebbistatin. Then quantitative, real-time PCR was performed to assess gene expression.

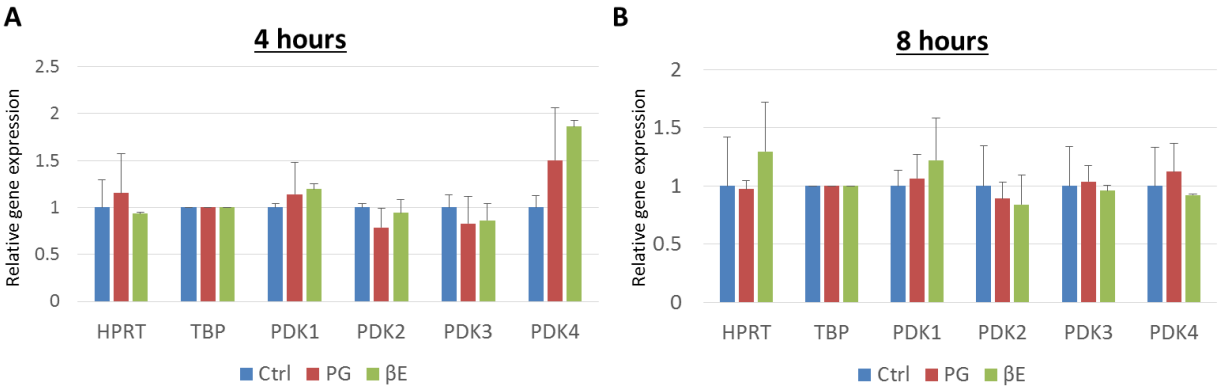

Figure 3.18: No change in PDK4 expression in MCF7 cells with progesterone. MCF7 cells were treated with 100 ng/mL progesterone (PG) or 100 pg/mL β-estradiol (βE) for 4 hours and 8 hours and then analyzed with qRT-PCR.

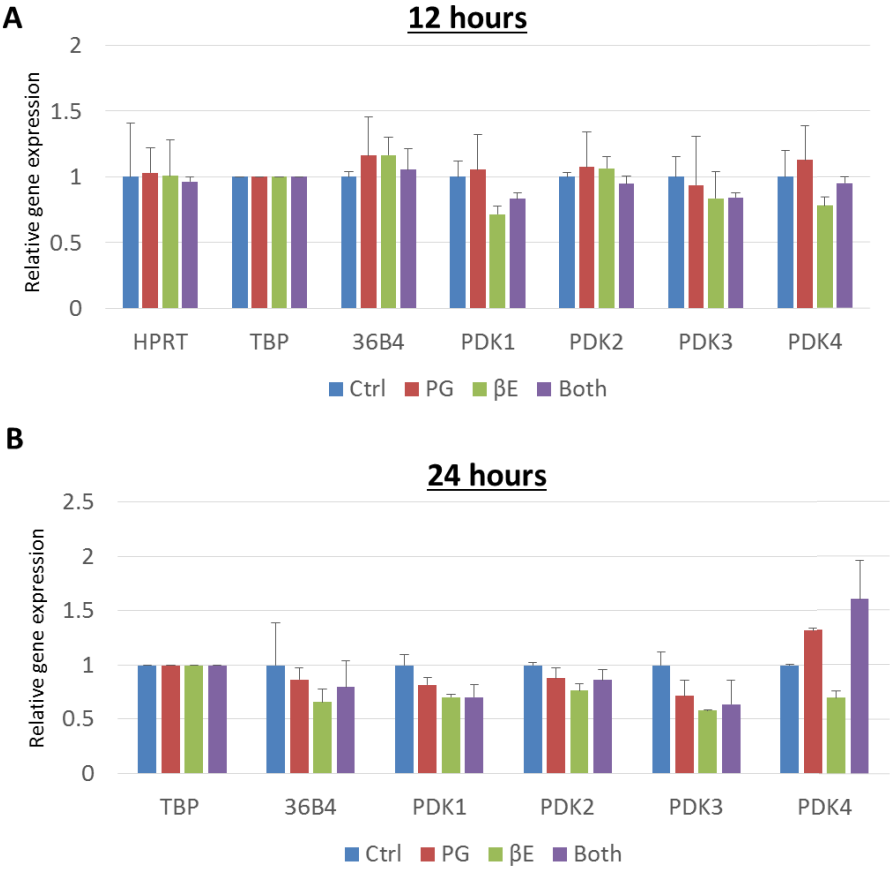

Figure 3.19: Mild effects of progesterone on PDK4 expression in C2C12s. C2C12 cells were treated with 100 ng/mL progesterone (PG) or 100 pg/mL β-estradiol (βE) for 12 hours and 24 hours and then analyzed with qRT-PCR.

hour, followed by progesterone incubation for 8 hours. Mifepristone attenuated the induction of PDK4 by approximately 50%, suggesting that progesterone-mediated effects is through the receptor (Figure 3.20). Antagonist alone also lead to an increase in PDK4 expression, not surprisingly because mifepristone in the absence of progesterone is known to behave as an agonist.

Discussion

Our study shows that in late pregnancy, PDK4, a crucial enzyme that governs the entry of glycolytic products into the TCA cycle, is upregulated in a muscle-specific manner. This is possibly in response to high serum progesterone levels. In addition, it occurs in the absence of changes in mitochondrial content and respiration capacity, GLUT4 and CD36 transporter expression and translocation, and factors involved in triglyceride synthesis and turnover.

We had hypothesized that due to the increased cardiac output in late pregnancy, the increased ATP demand would result in mitochondrial adaptations and enhanced respiration. The comparable respiration we observed in late pregnancy is also accompanied by lack of induction in genes involved in mitochondrial biogenesis, such as PGC-1α. This was surprising because in exercise, for example, increased work load results in mitochondrial biogenesis and greater respiratory capacity (Han and Kim, 2013; Tonkonogi et al., 2000). The only study on cardiac mitochondria of pregnancy stained late pregnant rat hearts with tetramethylrhodamine (TMRM), and then used confocal microscopy to quantify the length and width of mitochondria (Bassien-Capsa et al., 2006). They did not observe any differences. However, no group has assayed for respiration or proteins of the ETC complex. A previous study of cardiac-specific Ndufs4-null mice, which lack the ability to assemble complex I of the ETC, reported a heart failure phenotype in female mice with multiple pregnancies (Karamanlidis et al., 2013). This suggests

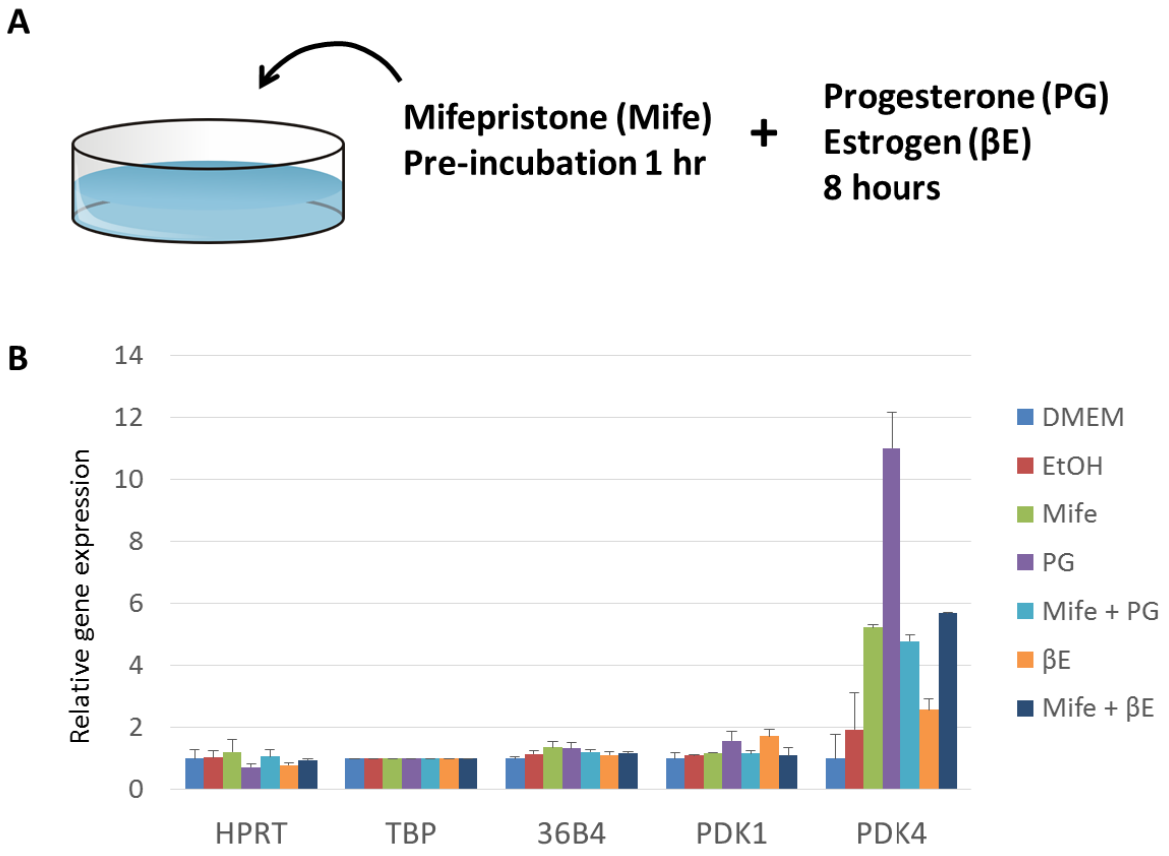

Figure 3.20: PDK4 induction by progesterone is mediated through the progesterone receptor. (A) Mifepristone, a known progesterone receptor antagonist, was pre-treated on NRVMs for 1 hour before addition of 100 ng/mL progesterone (PG) or 100 pg/mL β-estradiol (βE) for 8 hours. (B) After 9 hours of treatment, mRNA was isolated from NRVMs and assessed for gene expression by qRT-PCR.

that oxidative phosphorylation is vital for the increased demands of pregnancy. Overall, our results indicate that the increased work load of late pregnancy do not exceed the capabilities of the mitochondria and thus biogenesis is not necessary to satisfy demands.

There is a discrepancy between these results and subsequent data on PDK4 induction in late pregnant mouse hearts. An induction of PDK4 would prevent pyruvate input into the TCA cycle, and thus should lead to a decrease in respiration with pyruvate/malate as the substrate for isolated mitochondria. A trend towards decreased maximal and basal respiration can be seen in these isolated mitochondria that is consistent with PDH inhibition, but it is not significant. Thus, increasing sample size for each group may be necessary to observe a change. It is also possible that the technical process of mitochondrial isolation and centrifugation affected the phosphorylation state of PDH and resulted in loss of inhibition by PDK4. This ambiguity can be resolved by assessing the phospho-PDH state in isolated mitochondria. It is also worth noting that in our studies, maximal respiration with FCCP treatment is not greater than basal respiration (state 3), as would be expected. This commonly occurs in isolated mitochondria from the heart and could be due to limiting substrate concentrations in the assay solution.

Transporter translocation in response to insulin or contraction is well established to regulate substrate intake. Thus, we determined if differences in localization could contribute to the shift in usage. A modest, but significant induction in CD36 gene expression is observed, but GLUT4 is unchanged. However, protein expression did not detect differences in either transporter in late pregnancy. Previous studies found that increased CD36 expression in C2C12 cells induced PDK4 and FOXO1 expression, but this does not occur in late pregnancy (Nahle et al., 2008). There is also no change in localization of transporters. This suggests that transporter

localization does not regulate substrate switch in late pregnancy. It is worth noting that both mouse and rat hearts display parallel phenotypes.

Fatty acids that enter the cardiomyocyte have two fates: to continue on to β-oxidation in the mitochondria or be stored as a triglyceride. We did not detect any alterations in gene expression of factors in triglyceride storage or turnover in late pregnant mouse hearts. One modest increase was in the gene mttp. Interestingly, this protein is involved in the export of triglycerides and can be protective against lipotoxocity. It thus plays a role in preventing build-up of deleterious lipids that enter the heart during late pregnancy. There have been no reports of the effect of pregnancy on genetically manipulated mice with deletions in genes involved in triglyceride synthesis or break down, but it would be interesting to determine how metabolic flux is altered in these mice, and could elucidate the importance of the triglyceride pool as an energy resource in late pregnancy. Total triglyceride content and the presence of different lipid species in late pregnant mouse hearts have also not been characterized. Overall, we surmise that modest gene expression changes define the late pregnant heart. This is consistent with a previous study that studied the entire profile of late pregnant mouse hearts with microarray analysis (Chung et al., 2012a). If regulations in these pathways do occur, perhaps protein expression or posttranslational modifications should be examined.

A vital enzyme that connects glycolysis to the TCA cycle is PDH (Zhang et al., 2014). It is highly regulated by families of kinases (PDKs) and phosphatases (PDPs). Interestingly, we observe an increase in PDK4 in late pregnancy, the prominent isoform in the heart. This induction is strongest in the heart, compared to the gastrocnemius muscle, but is lacking in other tissues, like liver and lung. The phosphatase that reverses the inhibition, the PDP family, is oppositely regulated and is decreased in late pregnant mouse hearts. Consistent with this,

phospho-PDH at serine 293 to total PDH ratios were also increased in late pregnancy, indicative of increased PDK4 activity. Importantly, this induction is specific to the late pregnancy state in mice, as with PDK4 induction. PDH is also phosphorylated at two other serine sites (ser232 and ser300), though we have not explored the degree of phosphorylation in late pregnant mouse hearts. Furthermore, other post-translational modifications of PDH, such as acetylation, has been shown (Jing et al., 2013). Acetylation can affect the phosphorylation status and thus activity of PDH. We have not directly determined activity of PDH – the degree of phosphorylation can affect the activity and stringency of inhibition.

Interestingly, FOXO3 is upregulated in gastrocnemius muscle but not in cardiac muscle. FOXO1 has been shown to induce PDK4, so perhaps this indicates that PDK4 induction in skeletal muscle and cardiac muscle are via two different pathways. FOXO3 has not been greatly characterized in its role in PDK4 induction, although one study in colon cells found that overexpression of FOXO3 resulted in increased PDK4, but if the same is true in skeletal muscle is unknown (Ferber et al., 2012). Though we do not observe PDK4 differences in the liver and lung, PDP2 is significantly but oppositely changed in both tissues. Looking at downstream PDH phosphorylation states may shed light on the significance of these changes.

It is worth noting that mouse and rat physiology in pregnancy could be different. Two groups that examined late pregnant rat hearts found no change in PDH activity or PDK4 gene expression (Nieuwenhuizen et al., 1998; Rimbaud et al., 2009; Sugden and Holness, 1993a). In addition, they observed no GLUT4 or PGC-1α upregulation, but did see decreases in CPT-1 and mcad. In our rat heart samples, there was no induction in PDK4 at late pregnancy (D18), consistent with previous studies, but we did detect induction at postpartum day 1. Because a similar substrate switch was determined in late pregnant rat hearts by others, a PDK4-

independent mechanism must be present. It is possible that the "Randle cycle" is responsible, where increased concentrations of fatty acids can rapidly affect glucose utilization. Other potential mechanisms are further postulated in Chapter 4. Hence, it is important to be aware of differences in between rat and mouse hearts during pregnancy.

PDK4 upregulation is consistent with our ^{13}C-tracer analysis from Chapter 1, in which we observed decreased glucose and increased fatty acid utilization. To further extrapolate this from the data, we determined the amount of labeled citrate that forms from ^{13}C-glucose perfusion in late pregnant and control hearts, and found that there is a decrease in pyruvate entry into the TCA cycle. This is accomplished by substituting the m2 isotopomer species of citrate for acetyl CoA and comparing it to the m3 isotopomer of pyruvate. Ideally, the TCA contributed m2 isotopomer of citrate (which is the m2 isotopomer of oxaloacetate that combines with an unlabeled acetyl CoA) should be subtracted and account for, but we determined that these contributions were negligible. Thus, in order to establish if PDK4 is responsible for the substrate switch state observed at late gestation, it is necessary to determine metabolic flux in pregnant PDK4-null mice. We would expect mice without PDK4 to be unable to decrease glucose utilization. However, PDK2 is also highly expressed in hearts, as observed from the western blot with PDK antibody, and potential compensation could be made. Perhaps determining PDH activity in PDK2 and PDK4 KO mouse hearts will shed light on importance of the two in the heart. However, starved PDK4-deleted mice do not increase PDK2 expression, so compensation may not occur.

To further explore mechanistic details of PDK4 induction, we used the NRVMs model. The hormonal milieu is responsible for reprogramming maternal physiology during pregnancy. Thus, we sought to see if this is also true for PDK4 induction. Progesterone and estrogen are

both known to be elevated at late pregnancy (Chung and Leinwand, 2014; Chung et al., 2012b). Treatment of NRVMs with progesterone and estrogen showed that while both can upregulate PDK4, progesterone is a stronger and more consistent inducer. It is interesting to note that prolactin does not increase PDK4. One group found that in adipose cells, treatment with prolactin induced PDK4 expression via STAT5 (White et al., 2007). Progesterone receptor antagonist (mifepristone) treatment diminished the PDK4 effects. This induction is not observed in adult cardiomyocytes treated with progesterone. However, these cells in culture were treated with blebbistatin, an inhibitor of contractility (Kabaeva et al., 2008). This compromises the metabolic phenotype in isolated cells, and thus conclusions in adult cardiomyocytes are not reliable.

From these studies, we conclude that PDK4 is induced in late pregnant mouse hearts, and glucose utilization is decreased. Whether or not these two conclusions are causally linked is not clear. Future experiments to elucidate this will include using genetically manipulated mouse models with PDK4 deleted or inhibitors of PDK4, a commonly used one is dichloroacetate (DCA). Pregnancy in these mice followed by ^{13}C tracer analysis will allow us to conclude how important PDK4 induction is in late pregnancy. Furthermore, to explore if the *in vitro* data of progesterone induction of PDK4 in NRVMs is representative of *in vivo* phenotypes, we propose injecting progesterone or estrogen into ovariectomized mice to determine gene expression profiles of the heart.

Materials & Methods

Animal studies. All animal studies were performed according to procedures approved by the Institutional Animal Care and Use Committee (IACUC) at Beth Israel Deaconess Medical Center (BIDMC). Mice were maintained on a standard rodent chow diet with 12 hours light and dark cycles with water and food ad libitum. C57/bl6 mice were purchased from Jackson Laboratories (Bar Harbor, Maine). Wild-type, three-month-old female C57/bl6 undergoing estrus were mated with wild-type, C57/bl6 breeder males. The presence of a copulatory plug is denoted as day 0 of pregnancy. Pregnant females were singly placed in a new cage, and breeder diet (Formulab 5058) replaced the standard chow (Formulab 5008) they were previously on, unless delineated differently elsewhere. Breeder diet contains more fat and calories compared to standard chow. Timed pregnancies were carried out to day 11-12 (mid-pregnancy) and day 17-18 (late pregnancy) of gestation. Timed pregnant rats (Sprague Dawley) were obtained directly from Charles River.

Reagents and Materials. Unless otherwise stated, all reagents are from Sigma. GLUT4 and CD36 deleted mouse tissues were kindly provided by Dr. Barbara Kahn and Dr. Jack Lawler. PDK4 KO, PDK2 KO, and DKO mouse tissues were generously provided by Dr. Adam Wende. Dr. Robert Harris kindly gave us the PDK4 antibody.

Isolated mitochondria. Mitochondria were isolated from mouse and rat hearts as previously described. Hearts were rinsed in 2 mL of the mitochondrial isolation buffer (MIB) (70 mM sucrose, 210 mM mannitol, 5 mM HEPES, 1 mM EGTA, 0.5% (w/v) fatty acid free BSA, pH 7.2), and then transferred to 2 mL of fresh MIB. Tissue was homogenized with Teflon pedestal, programmed to drill at high speed with 3-4 dounces. Homogenate was spun at 1000 rpm for 10 minutes at 4^{o}C. Supernatant was transferred to a new tube and spun at 8000 rpm for 10 minutes

at 4°C. The pellet was resuspended in approximately 100µL of MIB. Samples were spun again as before. Pellet was then resuspended into 50µL of MIB and then brought up to 550 µL of mitochondrial assay solution (MAS) (70 mM sucrose, 220 mM mannitol, 10mM KH_2PO_4, 5 mM $MgCl_2$, 2 mM HEPES, 1 mM EGTA, and 0.2% (w/v) fatty acid free BSA, pH 7.2). Mitochondria was quantified using Bradford and approximately 2 µg of protein was loaded onto the Seahorse plate and spun at 2000 rpm for 10 minutes at room temperature.

Seahorse experiments. Mitochondrial respiratory function experiments were performed on a XF Flux Analyzer (Seahorse Biosciences). Isolated mitochondria was plated at 2µg per well and isolated cardiomyocytes were plated at 20,000 cells per well (Readnower et al., 2012). To assay complex I respiration, 10mM pyruvate and 2mM malate was used. State 3 respiration was induced with 4mM ADP, followed by state 4_o respiration with 3µM oligomycin. Then, 4µM of the uncoupler FCCP produced maximal respiration and lastly 2µM of rotenone and antimycin A was utilized to inhibit respiration. Fatty acid oxidation respiration rates were determined with 50µM palmitoylcarnitine and 0.5mM malate, which preceded the addition of the complex I respiration substrates. For isolated cardiomyocytes, 10µg/mL saponin was used to permeabilize the membrane, and then the inhibitors described were treated on cells.

Gene expression studies. Upon harvesting, mouse tissues were immediately frozen in liquid nitrogen. Total RNA was isolated from with the TRIzol (Invitrogen) and chloroform method. RNA concentrations were measured with the ThermoScientific NanoDrop spectrophotometer, 1 µg of RNA was used to synthesize cDNA with the High-Capacity cDNA Reverse Transcription kit (Applied Biosystems, CA). Gene expression was assayed with quantitative, real-time PCR using SYBR Green dye with specific primer set specially designed and the Bio-rad CFX 384

Touch Real-Time PCR Detection System. The primers used for mice and rats are listed in Tables 3.1 and 3.2.

Western blots. To determine protein expression, frozen mouse tissues were homogenized in the Qiagen TissueLyser for 10-15 minutes in RIPA lysis buffer, in the presence of phosphatase and protease inhibitors. Protein concentration was determined by the Bradford assay. Approximately 10 μg of protein were separated by SDS-PAGE, before transferred onto PVDF membrane. The primary antibodies were for immunoblot were: GLUT4 (Millipore), CD36 (Novus), PDK4 (a kind gift from Dr. Robert Harris), phospho-PDH at serine 293 (Novus), PDH (Cell signaling), Na^+/K^+ ATPase (Novus). Primary antibodies were incubated overnight at 1:1000. Three TBS-T washes were conducted before incubating with secondary antibody at 1:10,000 for 1 hour. Vinculin (Cell signaling) and GAPDH (Santa Cruz) were used as loading controls.

Histological studies. Hearts were excised from mice and rinsed in cold phosphate-buffer saline (PBS). Tissue was embedded in optimal cutting temperature (OCT) and then 10 μm sections were cut. Fixation with 4% PFA was carried out for 15-30 minutes. Blocking was with 3% BSA/PBS + 0.1% Triton-X for 1 hour at room temperature. Primary antibodies used were GLUT4 (Santa Cruz, 1:100 and 1:500) and CD36 (Cayman, 1:100 and 1:500).

Subcellular fractionation. Subcellular fractionation was carried out as previously described (Matsui et al., 2006; Zhou et al., 1998). Briefly, heart tissue was removed from mice and then immediately placed chilled HES buffer (20 mM HEPES, 250 mM sucrose, 1 mM EDTA) with protease inhibitors and then homogenized. Samples were then centrifuged at 2000g for 10 minutes at 4ºC. The supernatant is transferred to a new tube, where it is then centrifuged at 9000g for 20 minutes at 4ºC. The pellet (P1) is the plasma membrane fraction. The supernatant is ultracentrifuged at 180,000g for 90 minutes. The supernatant is the cytosol component and the

pellet is then resuspended in PBS and protease inhibitors and then loaded onto a 10-30% continuous sucrose gradient. It is then centrifuged further at 48,000 rpm for 55 minutes. The pellet (P2) is the plasma membrane, whereas the supernatant was separated in to 10-15 fractions and make up the intracellular vesicles.

Cells culture. C2C12 cells were purchased from ATCC and grown in DMEM, 10% fetal bovine serum (FBS) before differentiation for 2 days with insulin and transferrin and 2 days with 2% horse serum (HS). MCF-7 cells were grown in DMEM, 10% FBS before and during treatment.

Neonatal cardiomyocyte isolations. Neonatal cardiomyocyte isolations were carried out as previously described (Hajjar et al., 1997). Briefly, hearts of 1-2 day old Sprague Dawley neonates were excised and ventricles were isolated. Sequential incubations with collagenase type II (Worthington) were carried out in a 37ºC shaker. Cells were purified from non-cardiomyocytes via a crude, 1 hour pre-plating step. Cells were then incubated in DMEM, 10% HS, 5% FBS, and 1% penicillin-streptomycin (PS).

Adult cardiomyocyte isolations. Adult mouse hearts were excised and perfused via Langendorff perfusion, first with perfusion buffer (137 mM NaCl, 4 mM KCl, 1 mM $MgCl_2$, 10 mM HEPES, 0.33 mM NaH_2PO_4, 10mM glucose, 5 mM taurine, and 10 mM BDM), before switching to an enzyme buffer with collagenase D (Roche), collagenase B (Roche), and protease XIV for 10-15 minutes. Calcium was reloaded with concentrations of 0.06 mM, 0.25 mM, 0.60 mM, and 1.2 mM. Adult cardiomyocytes were plated on laminin-coated tissue culture plates for 2 hours in MEM (Invitrogen), 10% calf serum, BDM, 2 mM glutamine, and 2mM ATP before switching to labeled media.

Table 3.1 Mouse qRT-PCR primers	
PRC	GGAAGACTTTGATCCTGCTCCTG GGTTGGAAGAGGCTGGACACCTCC
TBP	CCCTATCACTCCTGCCACACCAGC GTGCAATGGTCTTTAGGTCAAGTTTACAGCC
β-actin	CCCTGTATGCCTCTGGTCGTACCAC GCCAGCCAGGTCCAGACGCAGGATG
36B4	GGAGCCAGCGAGGCCACACTGCTG CTGGCCACGTTGCGGACACCCTCC
ND1	GTGGCTCATCTACTCCACTGA TCGAGCGATCCATAACAATAA
ND2	ACCCACGATCAACTGAAGC TGTTTATAGTTGAGTACGATGGCC
cyt b	CATTTATTATCGCGGCCCTA TGTTGGGTTGTTTGATCCTG
COX1	CTAGCCGCAGGCATTACTAT TGCCCAAAGAATCAGAACAG
COX2	GCCGACTAAATCAAGCAACA CAATGGGCATAAAGCTATGG
ATP6	GACGAACATGAACCCTAAT TACGGCTCCAGCTCATAGT
GLUT1	GCCCCCGACAGAGAAGATG CAGTTCGGCTATAACACTGGTG
GLUT4	GTGACTGGAACACTGGTCCTA CCAGCCACGTTGCATTGTAG
CD36	GGCACAGACGCAGCCTCCTTTCCACC GGTGATGCAAAGGCATTGGCTGG
FATP1	TCAATGTACCAGGAATTACAGAAGG GAGTGAGAAGTCGCCTGCAC
FATP4	GCAAGTCCCATCAGCAACTG GGGGGAAATCACAGCTTCTC
CPT1	GGCACTGGCCGATGACGTGGAGCTC CAGGCAGAACTTGCCTTTGTCCCGG
mcad	CAGCTAGCACTGACGCCGTGCAG GCTCACGAGCTATGATCAGCCTCTG
Fabp4	GGGGCCAGGCTTCTATTCC GGAGCTGGGTTAGGTATGGG
Fabp5	TGAAAGAGCTAGGAGTAGGACTG CTCTCGGTTTTGACCGTGATG
acsl1	TGCCAGAGCTGATTGACATTC GGCATACCAGAAGGTGGTGAG
acsl3	CCAGCCATTGTTCATGGACTG TGGGACCAAAGAGACTATTTCCT
acsl4	CTCACCATTATATTGCTGCCTGT TCTCTTTGCCATAGCGTTTTTCT

Table 3.1 (continued)

acsl5	TCCTGACGTTTGGAACGGC CTCCCTCAATCCCCACAGAC
mttp	CTC TTG GCA GTG CTT TTT CTC T GAG CTT GTA TAG CCG CTC ATT
agpat1	TAA GAT GGC CTT CTA CAA CGG C CCA TAC AGG TAT TTG ACG TGG AG
Agpat2	CAG CCA GGT TCT ACG CCA AG TGA TGC TCA TGT TAT CCA CGG T
Agpat3	CTG CTT GCC TAC CTG AAG ACC GAT ACG GCG GTA TAG GTG CTT
Agpat4	CCA GTT TCT ATG TCA CCT GGT C GCA GAG TCT GGC ATT GAT CTT G
Lpin1	CAT GCT TCG GAA AGT CCT TCA GGT TAT TCT TTG GCG TCA ACC T
Dgat1	GCC TTA CTG GTT GAG TCT ATC AC GCA CCA CAG GTT GAC ATC C
Dgat2	GCG CTA CTT CCG AGA CTA CTT GGG CCT TAT GCC AGG AAA CT
Atgl	CAA CGC CAC TCA CAT CTA CGG GGA CAC CTC AAT AAT GTT GGC AC
PDK1	GGA CTT CGG GTC AGT GAA TGC TCC TGA GAA GAT TGT CGG GGA
PDK2	AGGGGCACCCAAGTACATC TGCCGGAGGAAAGTGAATGAC
PDK3	TCCTGGACTTCGGAAGGGATA ACCTCTCTCATGGTGTTAGCC
PDK4 **(same for rats)**	CCGCATTTCTACTCGGATGC CGATACTTCCAATGTGGCTTGG
PDP1	GCA CCC ATA GAG GAC CGG A CCT GCA TGA CCA TCA AAA ACC C
PDP2	ACT GTG TCC TAC TGG ATC TTC AA CAG GTT CCT ACT CGT GGC A
FOXO1	CCC AGG CCG GAG TTT AAC C GTT GCT CAT AAA GTC GGT GCT
FOXO3	GCA AGC CGT GTA CTG TGG A CGG GAG CGC GAT GTT ATC C

Table 3.2 Rat qRT-PCR primers	
HPRT	GGTGAAAAGGACCTCTCGAAG GCTTTTCCACTTTCGCTGATG
GAPDH	AACGACCCCTTCATTGACCTC CCTTGACTGTGCCGTTGAACT
PDK1	CGAGACGGCTTTGTGATTTG GTGATAGAGATGGGACGGAAC

References

Abel, E.D., Kaulbach, H.C., Tian, R., Hopkins, J.C., Duffy, J., Doetschman, T., Minnemann, T., Boers, M.E., Hadro, E., Oberste-Berghaus, C., et al. (1999). Cardiac hypertrophy with preserved contractile function after selective deletion of GLUT4 from the heart. J Clin Invest *104*, 1703-1714.

Bartels, E.D., Nielsen, J.M., Hellgren, L.I., Ploug, T., and Nielsen, L.B. (2009). Cardiac expression of microsomal triglyceride transfer protein is increased in obesity and serves to attenuate cardiac triglyceride accumulation. PLoS One *4*, e5300.

Bassien-Capsa, V., Fouron, J.C., Comte, B., and Chorvatova, A. (2006). Structural, functional and metabolic remodeling of rat left ventricular myocytes in normal and in sodium-supplemented pregnancy. Cardiovasc Res *69*, 423-431.

Battiprolu, P.K., Hojayev, B., Jiang, N., Wang, Z.V., Luo, X., Iglewski, M., Shelton, J.M., Gerard, R.D., Rothermel, B.A., Gillette, T.G., et al. (2012). Metabolic stress-induced activation of FoxO1 triggers diabetic cardiomyopathy in mice. J Clin Invest *122*, 1109-1118.

Bayeva, M., Gheorghiade, M., and Ardehali, H. (2013). Mitochondria as a therapeutic target in heart failure. J Am Coll Cardiol *61*, 599-610.

Beraud, N., Pelloux, S., Usson, Y., Kuznetsov, A.V., Ronot, X., Tourneur, Y., and Saks, V. (2009). Mitochondrial dynamics in heart cells: very low amplitude high frequency fluctuations in adult cardiomyocytes and flow motion in non beating Hl-1 cells. J Bioenerg Biomembr *41*, 195-214.

Bonen, A., Parolin, M.L., Steinberg, G.R., Calles-Escandon, J., Tandon, N.N., Glatz, J.F., Luiken, J.J., Heigenhauser, G.J., and Dyck, D.J. (2004). Triacylglycerol accumulation in human obesity and type 2 diabetes is associated with increased rates of skeletal muscle fatty acid transport and increased sarcolemmal FAT/CD36. FASEB J *18*, 1144-1146.

Boren, J., Veniant, M.M., and Young, S.G. (1998). Apo B100-containing lipoproteins are secreted by the heart. J Clin Invest *101*, 1197-1202.

Boucher, J., Kleinridders, A., and Kahn, C.R. (2014). Insulin receptor signaling in normal and insulin-resistant states. Cold Spring Harb Perspect Biol *6*.

Brindley, D.N., Kok, B.P., Kienesberger, P.C., Lehner, R., and Dyck, J.R. (2010). Shedding light on the enigma of myocardial lipotoxicity: the involvement of known and putative regulators of fatty acid storage and mobilization. Am J Physiol Endocrinol Metab *298*, E897-908.

Campbell, S.E., Mehan, K.A., Tunstall, R.J., Febbraio, M.A., and Cameron-Smith, D. (2003). 17beta-estradiol upregulates the expression of peroxisome proliferator-activated receptor alpha and lipid oxidative genes in skeletal muscle. J Mol Endocrinol *31*, 37-45.

Chen, L., Liu, T., Tran, A., Lu, X., Tomilov, A.A., Davies, V., Cortopassi, G., Chiamvimonvat, N., Bers, D.M., Votruba, M., et al. (2012a). OPA1 mutation and late-onset cardiomyopathy: mitochondrial dysfunction and mtDNA instability. J Am Heart Assoc *1*, e003012.

Chen, S., Murphy, J., Toth, R., Campbell, D.G., Morrice, N.A., and Mackintosh, C. (2008). Complementary regulation of TBC1D1 and AS160 by growth factors, insulin and AMPK activators. Biochem J *409*, 449-459.

Chen, Y., Csordas, G., Jowdy, C., Schneider, T.G., Csordas, N., Wang, W., Liu, Y., Kohlhaas, M., Meiser, M., Bergem, S., et al. (2012b). Mitofusin 2-containing mitochondrial-reticular microdomains direct rapid cardiomyocyte bioenergetic responses via interorganelle Ca(2+) crosstalk. Circ Res *111*, 863-875.

Chen, Y., Liu, Y., and Dorn, G.W., 2nd (2011). Mitochondrial fusion is essential for organelle function and cardiac homeostasis. Circ Res *109*, 1327-1331.

Chung, E., Heimiller, J., and Leinwand, L.A. (2012a). Distinct cardiac transcriptional profiles defining pregnancy and exercise. PLoS One *7*, e42297.

Chung, E., and Leinwand, L.A. (2014). Pregnancy as a cardiac stress model. Cardiovasc Res *101*, 561-570.

Chung, E., Yeung, F., and Leinwand, L.A. (2012b). Akt and MAPK signaling mediate pregnancy-induced cardiac adaptation. J Appl Physiol (1985) *112*, 1564-1575.

Coburn, C.T., Knapp, F.F., Jr., Febbraio, M., Beets, A.L., Silverstein, R.L., and Abumrad, N.A. (2000). Defective uptake and utilization of long chain fatty acids in muscle and adipose tissues of CD36 knockout mice. J Biol Chem *275*, 32523-32529.

Connaughton, S., Chowdhury, F., Attia, R.R., Song, S., Zhang, Y., Elam, M.B., Cook, G.A., and Park, E.A. (2010). Regulation of pyruvate dehydrogenase kinase isoform 4 (PDK4) gene expression by glucocorticoids and insulin. Mol Cell Endocrinol *315*, 159-167.

Coort, S.L., Hasselbaink, D.M., Koonen, D.P., Willems, J., Coumans, W.A., Chabowski, A., van der Vusse, G.J., Bonen, A., Glatz, J.F., and Luiken, J.J. (2004a). Enhanced sarcolemmal FAT/CD36 content and triacylglycerol storage in cardiac myocytes from obese zucker rats. Diabetes *53*, 1655-1663.

Coort, S.L., Luiken, J.J., van der Vusse, G.J., Bonen, A., and Glatz, J.F. (2004c). Increased FAT (fatty acid translocase)/CD36-mediated long-chain fatty acid uptake in cardiac myocytes from obese Zucker rats. Biochem Soc Trans *32*, 83-85.

Coort, S.L., Willems, J., Coumans, W.A., van der Vusse, G.J., Bonen, A., Glatz, J.F., and Luiken, J.J. (2002). Sulfo-N-succinimidyl esters of long chain fatty acids specifically inhibit fatty acid translocase (FAT/CD36)-mediated cellular fatty acid uptake. Mol Cell Biochem *239*, 213-219.

Doenst, T., Pytel, G., Schrepper, A., Amorim, P., Farber, G., Shingu, Y., Mohr, F.W., and Schwarzer, M. (2010). Decreased rates of substrate oxidation ex vivo predict the onset of heart failure and contractile dysfunction in rats with pressure overload. Cardiovasc Res *86*, 461-470.

Ferber, E.C., Peck, B., Delpuech, O., Bell, G.P., East, P., and Schulze, A. (2012). FOXO3a regulates reactive oxygen metabolism by inhibiting mitochondrial gene expression. Cell Death Differ *19*, 968-979.

Finck, B.N., Lehman, J.J., Leone, T.C., Welch, M.J., Bennett, M.J., Kovacs, A., Han, X., Gross, R.W., Kozak, R., Lopaschuk, G.D., et al. (2002). The cardiac phenotype induced by PPARalpha overexpression mimics that caused by diabetes mellitus. J Clin Invest *109*, 121-130.

Fischer, Y., Thomas, J., Sevilla, L., Munoz, P., Becker, C., Holman, G., Kozka, I.J., Palacin, M., Testar, X., Kammermeier, H., et al. (1997). Insulin-induced recruitment of glucose transporter 4 (GLUT4) and GLUT1 in isolated rat cardiac myocytes. Evidence of the existence of different intracellular GLUT4 vesicle populations. J Biol Chem *272*, 7085-7092.

Habets, D.D., Coumans, W.A., Voshol, P.J., den Boer, M.A., Febbraio, M., Bonen, A., Glatz, J.F., and Luiken, J.J. (2007). AMPK-mediated increase in myocardial long-chain fatty acid uptake critically depends on sarcolemmal CD36. Biochem Biophys Res Commun *355*, 204-210.

Hajjar, R.J., Schmidt, U., Kang, J.X., Matsui, T., and Rosenzweig, A. (1997). Adenoviral gene transfer of phospholamban in isolated rat cardiomyocytes. Rescue effects by concomitant gene transfer of sarcoplasmic reticulum Ca(2+)-ATPase. Circ Res *81*, 145-153.

Han, G.S., and Kim, S.R. (2013). Effects of endurance exercise on mitochondrial function in mice. J Phys Ther Sci *25*, 1317-1319.

Heather, L.C., Pates, K.M., Atherton, H.J., Cole, M.A., Ball, D.R., Evans, R.D., Glatz, J.F., Luiken, J.J., Griffin, J.L., and Clarke, K. (2013). Differential translocation of the fatty acid transporter, FAT/CD36, and the glucose transporter, GLUT4, coordinates changes in cardiac substrate metabolism during ischemia and reperfusion. Circ Heart Fail *6*, 1058-1066.

Holloszy, J.O., and Booth, F.W. (1976). Biochemical adaptations to endurance exercise in muscle. Annu Rev Physiol *38*, 273-291.

Holness, M.J., Kraus, A., Harris, R.A., and Sugden, M.C. (2000). Targeted upregulation of pyruvate dehydrogenase kinase (PDK)-4 in slow-twitch skeletal muscle underlies the stable modification of the regulatory characteristics of PDK induced by high-fat feeding. Diabetes *49*, 775-781.

Holness, M.J., Smith, N.D., Bulmer, K., Hopkins, T., Gibbons, G.F., and Sugden, M.C. (2002). Evaluation of the role of peroxisome-proliferator-activated receptor alpha in the regulation of cardiac pyruvate dehydrogenase kinase 4 protein expression in response to starvation, high-fat feeding and hyperthyroidism. Biochem J *364*, 687-694.

Holness, M.J., and Sugden, M.C. (2003). Regulation of pyruvate dehydrogenase complex activity by reversible phosphorylation. Biochem Soc Trans *31*, 1143-1151.

Hwang, B., Jeoung, N.H., and Harris, R.A. (2009). Pyruvate dehydrogenase kinase isoenzyme 4 (PDHK4) deficiency attenuates the long-term negative effects of a high-saturated fat diet. Biochem J *423*, 243-252.

Jeoung, N.H., and Harris, R.A. (2008). Pyruvate dehydrogenase kinase-4 deficiency lowers blood glucose and improves glucose tolerance in diet-induced obese mice. Am J Physiol Endocrinol Metab *295*, E46-54.

Jing, E., O'Neill, B.T., Rardin, M.J., Kleinridders, A., Ilkeyeva, O.R., Ussar, S., Bain, J.R., Lee, K.Y., Verdin, E.M., Newgard, C.B., Gibson, B.W., Kahn, C.R. (2013). Sirt3 regulates metabolic flexibility of skeletal muscle through reversible enzymatic deacetylation. Diabetes. 62(10): 3404-17.

Jorgensen, S.B., Viollet, B., Andreelli, F., Frosig, C., Birk, J.B., Schjerling, P., Vaulont, S., Richter, E.A., and Wojtaszewski, J.F. (2004). Knockout of the alpha2 but not alpha1 5'-AMP-activated protein kinase isoform abolishes 5-aminoimidazole-4-carboxamide-1-beta-4-ribofuranosidebut not contraction-induced glucose uptake in skeletal muscle. J Biol Chem *279*, 1070-1079.

Kabaeva, Z., Zhao, M., and Michele, D.E. (2008). Blebbistatin extends culture life of adult mouse cardiac myocytes and allows efficient and stable transgene expression. Am J Physiol Heart Circ Physiol *294*, H1667-1674.

Karamanlidis, G., Bautista-Hernandez, V., Fynn-Thompson, F., Del Nido, P., and Tian, R. (2011). Impaired mitochondrial biogenesis precedes heart failure in right ventricular hypertrophy in congenital heart disease. Circ Heart Fail *4*, 707-713.

Karamanlidis, G., Lee, C.F., Garcia-Menendez, L., Kolwicz, S.C., Jr., Suthammarak, W., Gong, G., Sedensky, M.M., Morgan, P.G., Wang, W., and Tian, R. (2013). Mitochondrial complex I deficiency increases protein acetylation and accelerates heart failure. Cell Metab *18*, 239-250.

Kasahara, A., Cipolat, S., Chen, Y., Dorn, G.W., 2nd, and Scorrano, L. (2013). Mitochondrial fusion directs cardiomyocyte differentiation via calcineurin and Notch signaling. Science *342*, 734-737.

Kienesberger, P.C., Pulinilkunnil, T., Nagendran, J., and Dyck, J.R. (2013). Myocardial triacylglycerol metabolism. J Mol Cell Cardiol *55*, 101-110.

Kim, Y.I., Lee, F.N., Choi, W.S., Lee, S., and Youn, J.H. (2006). Insulin regulation of skeletal muscle PDK4 mRNA expression is impaired in acute insulin-resistant states. Diabetes *55*, 2311-2317.

Kolwicz, S.C., Jr., Purohit, S., and Tian, R. (2013). Cardiac metabolism and its interactions with contraction, growth, and survival of cardiomyocytes. Circ Res *113*, 603-616.

Kramer, H.F., Witczak, C.A., Fujii, N., Jessen, N., Taylor, E.B., Arnolds, D.E., Sakamoto, K., Hirshman, M.F., and Goodyear, L.J. (2006a). Distinct signals regulate AS160 phosphorylation in response to insulin, AICAR, and contraction in mouse skeletal muscle. Diabetes *55*, 2067-2076.

Kramer, H.F., Witczak, C.A., Taylor, E.B., Fujii, N., Hirshman, M.F., and Goodyear, L.J. (2006b). AS160 regulates insulin- and contraction-stimulated glucose uptake in mouse skeletal muscle. J Biol Chem *281*, 31478-31485.

Kulkarni, S.S., Salehzadeh, F., Fritz, T., Zierath, J.R., Krook, A., and Osler, M.E. (2012). Mitochondrial regulators of fatty acid metabolism reflect metabolic dysfunction in type 2 diabetes mellitus. Metabolism *61*, 175-185.

Lee, I.K. (2014). The role of pyruvate dehydrogenase kinase in diabetes and obesity. Diabetes Metab J *38*, 181-186.

Liu, L., Shi, X., Bharadwaj, K.G., Ikeda, S., Yamashita, H., Yagyu, H., Schaffer, J.E., Yu, Y.H., and Goldberg, I.J. (2009). DGAT1 expression increases heart triglyceride content but ameliorates lipotoxicity. J Biol Chem *284*, 36312-36323.

Luiken, J.J., Coort, S.L., Koonen, D.P., Bonen, A., and Glatz, J.F. (2004a). Signalling components involved in contraction-inducible substrate uptake into cardiac myocytes. Proc Nutr Soc *63*, 251-258.

Luiken, J.J., Coort, S.L., Koonen, D.P., van der Horst, D.J., Bonen, A., Zorzano, A., and Glatz, J.F. (2004b). Regulation of cardiac long-chain fatty acid and glucose uptake by translocation of substrate transporters. Pflugers Arch *448*, 1-15.

Luiken, J.J., Koonen, D.P., Willems, J., Zorzano, A., Becker, C., Fischer, Y., Tandon, N.N., Van Der Vusse, G.J., Bonen, A., and Glatz, J.F. (2002). Insulin stimulates long-chain fatty acid utilization by rat cardiac myocytes through cellular redistribution of FAT/CD36. Diabetes *51*, 3113-3119.

Matsui, T., Nagoshi, T., Hong, E.G., Luptak, I., Hartil, K., Li, L., Gorovits, N., Charron, M.J., Kim, J.K., Tian, R., et al. (2006). Effects of chronic Akt activation on glucose uptake in the heart. Am J Physiol Endocrinol Metab *290*, E789-797.

Miinea, C.P., Sano, H., Kane, S., Sano, E., Fukuda, M., Peranen, J., Lane, W.S., and Lienhard, G.E. (2005). AS160, the Akt substrate regulating GLUT4 translocation, has a functional Rab GTPase-activating protein domain. Biochem J *391*, 87-93.

Nahle, Z., Hsieh, M., Pietka, T., Coburn, C.T., Grimaldi, P.A., Zhang, M.Q., Das, D., and Abumrad, N.A. (2008). CD36-dependent regulation of muscle FoxO1 and PDK4 in the PPAR delta/beta-mediated adaptation to metabolic stress. J Biol Chem *283*, 14317-14326.

Nielsen, L.B., Bartels, E.D., and Bollano, E. (2002). Overexpression of apolipoprotein B in the heart impedes cardiac triglyceride accumulation and development of cardiac dysfunction in diabetic mice. J Biol Chem *277*, 27014-27020.

Nielsen, L.B., Veniant, M., Boren, J., Raabe, M., Wong, J.S., Tam, C., Flynn, L., Vanni-Reyes, T., Gunn, M.D., Goldberg, I.J., et al. (1998). Genes for apolipoprotein B and microsomal triglyceride transfer protein are expressed in the heart: evidence that the heart has the capacity to synthesize and secrete lipoproteins. Circulation *98*, 13-16.

Nieuwenhuizen, A.G., Schuiling, G.A., Bonen, A., Paans, A.M., Vaalburg, W., and Koiter, T.R. (1998). Glucose consumption by various tissues in pregnant rats: effects of a 6-day euglycaemic hyperinsulinaemic clamp. Acta Physiol Scand *164*, 325-334.

Nojiri, H., Shimizu, T., Funakoshi, M., Yamaguchi, O., Zhou, H., Kawakami, S., Ohta, Y., Sami, M., Tachibana, T., Ishikawa, H., et al. (2006). Oxidative stress causes heart failure with impaired mitochondrial respiration. J Biol Chem *281*, 33789-33801.

Ouwens, D.M., Diamant, M., Fodor, M., Habets, D.D., Pelsers, M.M., El Hasnaoui, M., Dang, Z.C., van den Brom, C.E., Vlasblom, R., Rietdijk, A., et al. (2007). Cardiac contractile dysfunction in insulin-resistant rats fed a high-fat diet is associated with elevated CD36-mediated fatty acid uptake and esterification. Diabetologia *50*, 1938-1948.

Papanicolaou, K.N., Kikuchi, R., Ngoh, G.A., Coughlan, K.A., Dominguez, I., Stanley, W.C., and Walsh, K. (2012a). Mitofusins 1 and 2 are essential for postnatal metabolic remodeling in heart. Circ Res *111*, 1012-1026.

Papanicolaou, K.N., Ngoh, G.A., Dabkowski, E.R., O'Connell, K.A., Ribeiro, R.F., Jr., Stanley, W.C., and Walsh, K. (2012b). Cardiomyocyte deletion of mitofusin-1 leads to mitochondrial fragmentation and improves tolerance to ROS-induced mitochondrial dysfunction and cell death. Am J Physiol Heart Circ Physiol *302*, H167-179.

Pilegaard, H., and Neufer, P.D. (2004). Transcriptional regulation of pyruvate dehydrogenase kinase 4 in skeletal muscle during and after exercise. Proc Nutr Soc *63*, 221-226.

Readnower, R.D., Brainard, R.E., Hill, B.G., and Jones, S.P. (2012). Standardized bioenergetic profiling of adult mouse cardiomyocytes. Physiol Genomics *44*, 1208-1213.

Rimbaud, S., Sanchez, H., Garnier, A., Fortin, D., Bigard, X., Veksler, V., and Ventura-Clapier, R. (2009). Stimulus specific changes of energy metabolism in hypertrophied heart. J Mol Cell Cardiol *46*, 952-959.

Roach, W.G., Chavez, J.A., Miinea, C.P., and Lienhard, G.E. (2007). Substrate specificity and effect on GLUT4 translocation of the Rab GTPase-activating protein Tbc1d1. Biochem J *403*, 353-358.

Rosca, M.G., Tandler, B., and Hoppel, C.L. (2013). Mitochondria in cardiac hypertrophy and heart failure. J Mol Cell Cardiol *55*, 31-41.

Schoonderwoerd, K., Broekhoven-Schokker, S., Hulsmann, W.C., and Stam, H. (1990). Properties of phosphatidate phosphohydrolase and diacylglycerol acyltransferase activities in the isolated rat heart. Effect of glucagon, ischaemia and diabetes. Biochem J *268*, 487-492.

Schwenk, R.W., Luiken, J.J., Bonen, A., and Glatz, J.F. (2008). Regulation of sarcolemmal glucose and fatty acid transporters in cardiac disease. Cardiovasc Res *79*, 249-258.

Sharov, V.G., Goussev, A., Lesch, M., Goldstein, S., and Sabbah, H.N. (1998). Abnormal mitochondrial function in myocardium of dogs with chronic heart failure. J Mol Cell Cardiol *30*, 1757-1762.

Slot, J.W., Geuze, H.J., Gigengack, S., James, D.E., and Lienhard, G.E. (1991). Translocation of the glucose transporter GLUT4 in cardiac myocytes of the rat. Proc Natl Acad Sci U S A *88*, 7815-7819.

Song, M., and Dorn, G.W., 2nd (2015). Mitoconfusion: noncanonical functioning of dynamism factors in static mitochondria of the heart. Cell Metab *21*, 195-205.

Song, M., Mihara, K., Chen, Y., Scorrano, L., and Dorn, G.W., 2nd (2015). Mitochondrial fission and fusion factors reciprocally orchestrate mitophagic culling in mouse hearts and cultured fibroblasts. Cell Metab *21*, 273-285.

Stanley, W.C., Recchia, F.A., and Lopaschuk, G.D. (2005). Myocardial substrate metabolism in the normal and failing heart. Physiol Rev *85*, 1093-1129.

Steinbusch, L.K., Schwenk, R.W., Ouwens, D.M., Diamant, M., Glatz, J.F., and Luiken, J.J. (2011). Subcellular trafficking of the substrate transporters GLUT4 and CD36 in cardiomyocytes. Cell Mol Life Sci *68*, 2525-2538.

Sugden, M.C., and Holness, M.J. (1993). Cardiac carbohydrate and lipid utilization during late pregnancy. Biochem Soc Trans *21 (Pt 3)*, 312S.

Tonkonogi, M., Walsh, B., Svensson, M., and Sahlin, K. (2000). Mitochondrial function and antioxidative defence in human muscle: effects of endurance training and oxidative stress. J Physiol *528 Pt 2*, 379-388.

Wende, A.R., Huss, J.M., Schaeffer, P.J., Giguere, V., and Kelly, D.P. (2005). PGC-1alpha coactivates PDK4 gene expression via the orphan nuclear receptor ERRalpha: a mechanism for transcriptional control of muscle glucose metabolism. Mol Cell Biol *25*, 10684-10694.

White, U.A., Coulter, A.A., Miles, T.K., and Stephens, J.M. (2007). The STAT5A-mediated induction of pyruvate dehydrogenase kinase 4 expression by prolactin or growth hormone in adipocytes. Diabetes *56*, 1623-1629.

Yang, J., and Holman, G.D. (2005). Insulin and contraction stimulate exocytosis, but increased AMP-activated protein kinase activity resulting from oxidative metabolism stress slows endocytosis of GLUT4 in cardiomyocytes. J Biol Chem *280*, 4070-4078.

Zaha, V.G., and Young, L.H. (2012). AMP-activated protein kinase regulation and biological actions in the heart. Circ Res *111*, 800-814.

Zhang, S., Hulver, M.W., McMillan, R.P., Cline, M.A., and Gilbert, E.R. (2014). The pivotal role of pyruvate dehydrogenase kinases in metabolic flexibility. Nutr Metab (Lond) *11*, 10.

Zhou, M., Sevilla, L., Vallega, G., Chen, P., Palacin, M., Zorzano, A., Pilch, P.F., and Kandror, K.V. (1998). Insulin-dependent protein trafficking in skeletal muscle cells. Am J Physiol *275*, E187-196.

Chapter 4:

Discussion

In this thesis, we determined the metabolic state and regulations of late pregnancy in mice. We observed higher serum triglyceride levels, concurrent with increased uptake of fatty acids in late pregnancy. In the heart, this coincides with intrinsic cardiac alterations that results in decreased glucose utilization and moderate increase in fatty acid utilization. How this substrate switch occurs was then explored. We found that the mitochondrial biology of late gestation is not significantly different from the non-pregnant state. Furthermore, there is no alteration in GLUT4 and CD36 transporter status or gene expression of factors involved in the triglyceride synthesis or turnover pathway. Interestingly, we found that pyruvate dehydrogenase kinase 4 (PDK4) is induced by ~4-fold in late pregnant mouse hearts. PDK4 is a crucial regulatory enzyme that can affect glycolytic product input into the TCA cycle by phosphorylation of pyruvate dehydrogenase (PDH). Pyruvate dehydrogenase phosphatases, activators of PDH through dephosphorylation, was oppositely regulated and significantly decreased. This effect is specific to heart and skeletal muscle in late gestation. Lastly, we determined that the pregnancy hormone progesterone can promote PDK4 upregulation by the progesterone receptor in isolated cardiomyocytes. These studies demonstrate that the substrate switch of late pregnancy could be promoted by PDH inhibition via PDK4.

Increased uptake and β-oxidation of fats in late pregnant mouse hearts

The continuous contraction of the heart muscle results in high metabolic demands. With low energy reserves available, it is especially important that it is never lacking for substrate source. Fortunately, the heart is extremely flexible and can utilize many different substrates depending on the condition. For example, in the increased workload of exercise, the myocardium uses abundant lactate sources to fulfill its needs (Gertz et al., 1988; Stanley, 1991). During times

of metabolic inflexibility, however, as in pathological states, it has been evident that compromises in meeting energy needs is strongly linked to cardiac dysfunction. Thus, the importance of maintaining sufficient cardiac metabolism during both physiological and pathological states is critical to ensuring that contractile function can be preserved.

In pregnancy, maternal physiology drastically changes. Systemic insulin resistance shifts maternal substrate usage to increase fat usage in order to facilitate fetal preferences for glucose (King, 2000). In addition, cardiac output, which peaks by early to mid-trimester, is sustained to the end of pregnancy (Melchiorre et al., 2012). Thus, both fetal needs and greater ATP demands on the maternal myocardium indicates that adaptations must occur to sustain this for the duration of pregnancy. However, the metabolic phenotype of the heart during pregnancy has not been greatly explored.

Previously published work demonstrated that late pregnant dog and rat hearts decrease glucose utilization and increase fatty acid oxidation (Sugden and Holness, 1993a; Williams et al., 2008). We confirm these findings using two novel techniques, which have not been used before to study cardiac metabolism during pregnancy. With a luciferase-based *in vivo*, real-time bioluminescence imaging system, we were able to detect both faster dynamics and greater overall uptake in fatty acids in late pregnant mouse hearts. This, however, is not paralleled by an increase in CD36 transporter expression or localization. This raises an interesting point: while we observe an increase in the source and sink of fatty acids in late pregnancy, the means by which they enter the cell is not altered. This indicates that there must be an increase in the rate of uptake, which we do discern in the bioluminescence studies. The second technique we utilized was ^{13}C-substrate tracer analysis on ex vivo perfused pregnant mouse hearts. This is the first study that we know of to characterize cardiac metabolism during pregnancy by directly studying

flux through glycolysis and the TCA cycle. With this tool, we corroborate the findings of previous groups. We can also conclude from perfused hearts that there are intrinsic cardiac adaptations that occur in late pregnancy, independent of the substrate environment of the cell.

Both the sensitivity and speed in the simultaneous detection of many intermediates, and the flexibility in assaying many different conditions make ^{13}C-tracer analysis a valuable tool to study cardiac metabolism. Here, we scrutinize only glucose and fatty acids as substrate sources for the late pregnant mouse heart. However, it is well-known that the healthy heart utilize pyruvate and lactate as well, and thus labeling of these substrates will elucidate if other carbohydrate sources is compensating for the decrease in glucose usage that we observe (Khairallah et al., 2004). Furthermore, our perfusion buffer contains only one type of fatty acid, palmitic acid. The most common fatty acid is oleate and using either labeled oleate or a cocktail of labeled fatty acids may be closer to physiology.

Metabolic dysfunction in pregnancy-related cardiac diseases

Peripartum cardiomyopathy (PPCM), diagnosed by the onset of heart failure in late gestation or immediately postpartum, is a disease with unknown etiology. Recent work by our lab and others have led to the hypothesis that PPCM is caused by pathological capillary adaptations in the heart (Halkein et al., 2013; Hilfiker-Kleiner et al., 2007; Patten et al., 2012). Two common models for PPCM, for example, is the cardiac PGC-1α- and the STAT3-deleted mice. Both models develop heart failure during late pregnancy and have pointed to vascular insufficiency and metabolic deficiency as a potential underlying cause of PPCM. PGC-1α is a transcriptional co-activator that regulates angiogenesis and mitochondrial biogenesis and respiration (Arany et al., 2008; Arany et al., 2005). In the skeletal muscle, PGC-1α coordinates

with ERRα to increase PDK4 expression during exercise or starvation (Wende et al., 2005). Assessment of whole-body PGC-1α knockout mice found not only significant deficiencies in ATP levels, but also cardiac dysfunction. STAT3 has been well-characterized to be involved in paracrine-mediated angiogenesis and has been found to protect against ischemia reperfusion in cardiomyocytes by upregulation of antioxidant enzymes. In addition, recent studies have determined that STAT3 is also present in the mitochondria and isolated mitochondria from mice with deleted STAT3 in the heart show reduced respiration (Wegrzyn et al., 2009). Thus, in both mouse models, significant metabolic inadequacies exist that could play a role in predisposal to PPCM.

We hypothesize that ablation of PGC-1α and STAT3 in late pregnancy may compromise the ability of the heart to induce PDK4 and switch substrate preferences. To test this hypothesis, cardiac PDK4 expression levels in both PGC-1α and STAT3 deficient mice during late pregnancy should be established. ^{13}C tracer studies of metabolic flux with Langendorff perfused hearts from each of these models can determine substrate utilization under this pathological setting. We expect to observe that fatty acid uptake and utilization is decreased in these mice and glucose utilization is increased compared to wild-type mice during late pregnancy.

In addition, mating to cardiac-specific PDK4 overexpressing transgenic mice should rescue the cardiac dysfunction defects observed in late pregnancy. PDK4 overexpressing mice have been formerly characterized to have elevated fatty acid oxidation and diminished glucose utilization (Chambers et al., 2011; Zhao et al., 2008). Furthermore, they are protected against ischemia reperfusion and triglyceride accumulations with high fat diet. These studies would delineate the importance of maintaining the switch in substrate usage that occurs in late pregnancy and how dysregulation could lead to cardiac diseases, such as PPCM.

Mitochondrial function during late pregnancy

We hypothesized the increased demand for ATP must result in adaptations in the machinery that generates ATP, namely the mitochondria. Furthermore, women with mitochondrial diseases are more prone to complications during pregnancy, such as preterm delivery or preeclampsia though the sample size of this study is limited (Say et al., 2011). In addition, female mice with deletion of a complex I protein, Ndufs4, develop heart failure after multiple pregnancies (Karamanlidis et al., 2013). These studies suggest that vulnerabilities in mitochondrial ability to adjust to energetic needs leads to pathological conditions.

In this study, we found no significant differences in isolated mitochondrial function during late pregnancy compared to non-pregnant controls. Furthermore, the number per unit weight of the heart and mitochondrial morphology were not changed. This is consistent with a previous study that found no change in the size of mitochondria with confocal microscopy (Bassien-Capsa et al., 2006). PINK1, an enzyme that promotes mitophagy, is significantly decreased in late pregnant mouse hearts, but further studies are necessary to determine if mitophagy itself is affected as well. In addition, because we utilized a rather crude method of assaying mitochondria number and morphology during pregnancy, we may not be able to detect subtle changes in mitochondria. More stringent characterization can be made with electron microscopy (EM), which is the gold standard in characterizing mitochondrial dimensions, or by determining citrate synthase activity. Thus, we conclude that the mitochondria can withstand the increased demands during pregnancy. However, if preexisting defects are already present, then the machinery cannot sustain the added stress and demand of pregnancy, leading to cardiac diseases.

Metabolic substrate uptake during late pregnancy

Metabolic uptake in cardiomyocytes is controlled in multiple ways, including serum availability, endothelial transport, and availability of metabolic transporters. We investigated and found no changes in the expression and localization of the glucose transporter GLUT4 and the fatty acid transporter CD36. Previous work showed no difference in GLUT4 expression in late pregnant rat hearts, but localization has not been explored (Nieuwenhuizen et al., 1998; Rimbaud et al., 2009). We find here no difference in transporter localization during pregnancy. This is surprising given the increase in fatty acid uptake.

There are, however, modest increases in the proteins involved in fatty acid uptake, such as FABP4 and FABP5. These proteins are known to be expressed in the endothelium and mice with deletions are deficit in fatty acid uptake (Elmasri et al., 2009; Maeda et al., 2005; Masouye et al., 1997). Determining their expression levels in isolated cardiac endothelial cells from late pregnant mouse hearts would be more informative, as the induction may be diluted out by non-endothelial cells in the heart. If an increase in endothelial expression is observed, it would suggest increased transport of fatty acids through the endothelium to cardiomyocytes.

The role of PDK4 in cardiac metabolic switch in late pregnancy

PDK4 has been extremely well-characterized for its role in metabolic regulation by phosphorylation and thus inhibition of PDH. We found a marked upregulation of PDK4 in late pregnant mouse hearts and a concomitant decrease in PDP2. This indicates that PDH is inhibited so that glycolytic product entry into the TCA is diminished. It is also consistent with our finding in ^{13}C-metabolic flux analysis of late pregnant mouse hearts that intrinsic cardiac alterations

occur. Earlier work in pregnant rats and dogs showed divergent results. One group found no change in PDK4 expression in late pregnancy, while another showed decreased gene expression of PDH (Rimbaud et al., 2009; Sugden et al., 1992; Williams et al., 2008). However, PDH is regulated at post-translationally, but they did not explore the phosphorylation profile of PDH. In our studies, we determined that one serine phosphorylation site (293) is increased in late pregnant mouse hearts, but did not assay two other potential sites (232 and 300). Furthermore, other post-translational modifications of PDH, including acylation, was not characterized. Acetylation can affect the phosphorylation status and thus activity of PDH (Jing et al., 2013). This, along with directly examining the activity of PDH, would be informative to understanding the duration and degree of inhibition.

In order to determine if PDK4 is responsible for the substrate switch we observe in late pregnancy, future studies with PDK4-null mice or PDK4 inhibitors at late gestation and ex vivo perfusion of ^{13}C-labeled substrates should be conducted. PDK4 knockout mice at baseline have normal serum profiles, but after fasting, have reduced serum glucose and increased fatty acid levels (Jeoung and Harris, 2008, 2010). Diaphragms from these mice increase in glucose utilization and decrease in fat oxidation. However, metabolic flux in hearts have not been directly determined. Treatment with PDK4 inhibitors can provide another method to study the role of PDK4 in substrate switch. These inhibitors are under consideration as therapeutics for many diseases, including diabetes and certain cancers. One commonly used inhibitor is dichloroacetate (DCA), which is a pyruvate mimetic. First, we would determine the substrate usage state in both PDK4-null mice and wild-type mice in non-pregnancy. We would expect the phenotype to be similar to that of the diaphragm, with more glucose than fat usage. Then, null mice or wild-type treated with DCA in late pregnancy would be compared to their non-pregnant

controls in Langendorff perfusion studies of ^{13}C-labeled substrates. We hypothesize that mice with re-activation of PDH would exhibit a substrate consumption profile comparable to their corresponding controls. This would confirm that upregulation of PDK4 is responsible for the change in substrate use in late pregnancy.

One interesting point worth exploring is the state of neonates from PDK4-deleted pregnant females. Since glucose is the primary substrate source of the fetus, and the predicted serum profile in mice with PDK4 ablation is lower serum glucose but due to usage by the heart, less glucose will be shunted to the fetus. Will this result in decreased litter or neonate size? Furthermore, how can this affect future offspring health? This has not been reported in published literature.

Many hormones can regulate PDK4, including insulin, glucocorticoids, and thyroid hormone (Attia et al., 2010; Connaughton et al., 2010). PPARα and PGC-1α have already been well-characterized to directly activate PDK4 gene expression under different stimuli. In the heart, no studies have been done to determine the effects of pregnancy-related sex hormones on PDK4 expression. One group did find that implantation of progesterone and estrogen slow-release tablets into ovariectomized rats led to an upregulation of PDK4 in gastrocnemius, although slightly more so with estrogen than progesterone (Campbell et al., 2003). Bioinformatics characterization of the PDK4 promoter showed an estrogen receptor binding site in a distal enhancer region. However, most studies have focused on more proximal regions and thus it is unclear what role this site plays in regulating PDK4 expression. Future luciferase experiments can illuminate the direct effects of progesterone on the PDK4 promoter activity. It would be interesting to investigate if there is a site for progesterone transcriptional control in this region.

The importance of selecting a good model organism in the study of pregnancy

In our studies, we included characterizations of rat metabolic phenotypes during pregnancy. It has become apparent that rat and mouse physiology differs more drastically than we expected. For example, the serum triglyceride and glucose profiles of late pregnancy in mouse and rat contrast each other. While mice show a modest 1.4-fold increase, pregnant rats increase serum triglycerides by almost 7-fold. Serum glucose is even more prominent. No change is observed in mice but a 40% decrease occurs in late pregnant rats. Furthermore, many previously published studies were completed in rats, and we have found that mouse physiology do not always match. For example, the increase in PDK4 expression is not supported by previous studies in rats (Rimbaud et al., 2009). In addition to this, expression of C/EBPβ is different in mice and rat hearts in late pregnancy and postpartum day 1 (Appendix). However, there are similarities in substrate switch preferences in all species examined so far. Furthermore, substrate transporter localization are both unchanged in rats and mice. Thus, this underscores the importance of choosing the correct model to study metabolism during pregnancy and warns against making overarching conclusions based on the results of one model.

Limitations

Langendorff perfusion and metabolic flux studies

Langendorff perfusion of ^{13}C-labeled substrates in late pregnant mouse hearts demonstrated relative decreases in glucose oxidation and increases in fat usage. While this system offers immense control to be able to study different conditions, the environment can be vastly different from the whole-body system, but recognition of this can facilitate the

interpretation of results. The perfusion buffer composition is pivotal to ensuring that the correct conditions have been chosen. It is thus important to select perfusates that closely match the environment that the heart is used to seeing, however, that is difficult when studying physiological adaptations. For example, we chose to use non-pregnant concentrations of substrates to perfuse both non-pregnant and late pregnant mouse hearts as a starting point. Our perfusion buffer also lacks insulin and uses slightly elevated concentrations of lactate, which likely leads to underestimations of total glucose usage in the non-pregnant and late pregnant mouse heart. Other hormones, especially those elevated in pregnancy, such as progesterone and estrogen, were also not included. Despite these limitations, the intrinsic cardiac changes we observe in late pregnant mouse hearts suggests that the effects are not transient nor affected by the increased triglyceride environmental of late pregnancy.

It is also important to clarify parameters of metabolic flux analysis to ensure that the conclusions and inferences made from the data are correct. First, flux analysis is often performed in systems at steady state, in which metabolic flux and metabolite concentrations are constant, or more realistically, at pseudo-steady state, where minimal changes occur. While glycolysis can reach saturation in minutes, the TCA cycle often can take hours for true steady state to be reached. We found that in 45 minutes of perfusion, an increase in labeled isotopomer species of TCA intermediates was detected compared to 25 minutes of perfusion, which indicates that steady state was not reached at 25 minutes. Thus, dynamic metabolic flux analysis of non-steady state conditions may more realistically show the utilization of different substrates. Furthermore, we did not perfuse hearts with ^{13}C-palmitic acid for longer than 30 minutes and so cannot conclude if steady state was reached with ^{13}C-palmitic acid. It would be important to establish this for proper interpretation of our flux analysis. Secondly, the measurements determined here

with ^{13}C-labeling is the relative metabolic rate of substrate utilization and not absolute rates. Using radioactively labeled substrates, such as ^{14}C-glucose, followed by detection for $^{14}CO_2$, on the other hand, would provide absolute rates of substrate utilization.

In addition to exogenous glucose and fat as energy substrates for the heart, other endogenous sources, such as stored triglycerides and glycogen exist. Previous studies have found that the triglyceride pool in cardiomyocytes can contribute significantly to fat oxidation and that exogenous triglycerides can cycle through the triglyceride pool before being oxidized (Banke et al., 2010). We did not measure the triglyceride pool in late pregnant and non-pregnant mouse hearts, but it is possible that the endogenous pool contributes energy substrates. If the triglyceride pool is greater in late pregnant mouse hearts than non-pregnant mouse hearts, then the contribution of endogenous triglycerides can affect our analysis. We assume here that ^{13}C-palmitic acid concentrations is the predominant supply for β-oxidation, but if the triglyceride pool in the heart is also a contributor, then our analysis would be underestimating fatty acid utilization in late pregnant mouse hearts. In addition, if our measurements were not performed at steady state of label incorporation, then the transit time through the triglyceride pool could also affect our conclusions. If this is so, then first order kinetics models cannot be used to determine metabolic rates and other models such as second order kinetics may be more applicable and necessary to properly calculate rates.

Fatty acid uptake

We observed an increase in fatty acid uptake into late pregnant mouse hearts in the luciferase transgenic mice after injection of a free fatty acid (FFA) conjugated to luciferin probe (luc-FFA). The luc-FFA probe was a non-esterified, 16 carbon fatty acid designed to mimic

physiological conditions and enter through fatty acid transporters (Henkin et al., 2012). Nutrient serum analysis revealed an approximately 50% decrease in fatty acid concentrations in late pregnancy in mice. Thus, the diminished endogenous pool of FFA can affect the proportion of labeled fat in the serum after injection of the probe. On the other hand, blood volume in pregnancy is also significantly altered and can increase by 30% by day 17.5 of pregnancy in mice (Kulandavelu et al., 2006), which would offset the error introduced by lower endogenous FFA levels. To formally test the final effect, measurements of FFA concentrations in serum after injection could be made, though we have not performed these studies.

PDK4 induction in late pregnant mouse hearts

In late pregnant mouse hearts, PDK4 expression is upregulated, as is a similar increase in phosphorylated PDH. The phospho-antibody specifically recognizes serine 293 of PDH, which corresponds to site 1. PDK family members have varying capacities to phosphorylate the three serine sites of PDH, and PDP isoforms similarly have different activities levels towards each site (Patel and Korotchkina, 2006). Thus, expression levels of these enzymes can control both the rate and duration of activation and inactivation of PDH in different tissues. In our studies, we determined only phosphorylation of site 1, and did not assay for site 2, which corresponds to serine 300, or site 3 (serine 232). PDK4 can phosphorylate both sites 1 and 2 of PDH, which could affect the degree of PDH inhibition. In addition to phosphorylation conditions, the activity of PDH can also be directly measured to determine how it may correspond to the level of phosphorylation in mouse hearts. These direct assays are planned for the near future.

A notable species-specific discordance was observed between rats and mice in terms of PDK4 upregulation. While we observed an increase in PDK4 expression in late pregnancy in

mice, we do not observe a similar induction in rats in late pregnancy, though decreased glucose utilization is still present. This suggests that a PDK4-independent mechanism is in effect in rats at late pregnancy. A potential explanation is the "Randle cycle" (or "glucose-fatty acid cycle"). Elevated fatty acid oxidation results in a rapid increase in the ratios of acetyl CoA/CoA, NADH/NAD+ and concentration of citrate, which results in quick changes of decreased PDH activity, pyruvate oxidation, and also inhibition of phosphofructokinase 1 and 2 (PFK1, PFK2) in the heart. Thus, the drastic increase in serum triglycerides at late pregnancy in rats could shut down glycolysis in the absence of PDK4 upregulation. Furthermore, the increase in fatty acids could activate transcription factors, such as PPARα or PPARδ, which would upregulate genes involved in fatty acid oxidation and uptake, though we did not observe this in mice. It is also possible that AMPK is phosphorylated and activated, which would lead to decreases in malonyl CoA concentrations and subsequent augmentation of fatty acid oxidation. However, whether or not this occurs has not been explored. Abnormal glucose tolerance and increased insulin secretion in the insulin resistant state can also dramatically alter substrate usage. In mice fed high fat diets for 2 weeks, fatty acid oxidation is increased in absence of changes in PDH activity or PDK4 expression (Wright et al., 2009). In those circumstances, impaired GLUT4 translocation is potentially responsible for the reduction in glycolysis and increase in fatty acid oxidation, though again we did not see this in mice.

Contribution of glycolytic ATP to ion homeostasis

Decreased glycolytic flux can dramatically affect the function of ion channels located at the sarcolemmal and sarcoplasmic membranes. Many glycolytic and glycogenolytic proteins are localized at the sarcolemma or the sarcoplasmic reticulum (SR) in order for ion channels at these

sites to preferentially use ATP produced from glycolysis. Thus, glycolysis plays an important role to ensure that these channels, such as the SR Ca^{2+} ATPase, ATP-sensitive K^+ channel, and Na^+/K^+ ATPase, are functioning at optimal levels and that ion homeostasis is maintained. In late pregnancy, we observe a decrease in glucose utilization, suggesting decreased ATP produced by glycolysis. How this affects ion channels that rely on this glycolytic ATP has not been extensively explored. One previous study found that the α1-subunit of Na^+/K^+ ATPase was decreased by approximately 20% in late pregnant rat hearts, leading to increased concentrations of sodium at steady state (Elzwiei et al., 2013). However, whether this is an effect of decreased glycolytic flux has not been studied. Furthermore, under stressful conditions, such as in ischemia, glycolytic ATP is important to maintain calcium levels by improving the activity of the SR Ca^{2+} ATPase (Aasum et al., 1998; Zima et al., 2006). These studies suggest that potentially decreased glycolysis in late pregnancy could modify the activity of ion channels, ion homeostasis, and electrophysiological properties in the heart.

Cardiac LPL

Another key regulatory point in the uptake of fatty acids is the cardiac lipoprotein lipase (LPL). LPL is made by parenchymal cells, such as cardiomyocytes, and then transferred to the luminal surface of endothelial cells via heparin sulfate proteoglycans (HSPG) and glycosylphosphatidylinositol anchored high density lipoprotein binding protein (GPIHBP1), where it can then hydrolyze triglycerides to liberate free fatty acids. Mice with cardiac-specific deletion of LPL not only have increased plasma triglyceride levels and decreased fatty acid content and oxidation, but surprisingly, also have altered gene expression consistent with decreased fatty acid uptake and oxidation, such as reduced expression of CPT1, CD36, PDK4,

FATP1, and PPARγ (Augustus et al., 2004; Augustus et al., 2006). Furthermore, basal glucose uptake and oxidation in LPL-null hearts was significantly upregulated, along with modest increases in GLUT4 gene expression. Consistent with this, positron emission tomography (PET) studies of human patients with LPL deficiency show elevated glucose uptake (Khan et al., 2011). These drastic phenotypes suggest that LPL plays a pivotal role in controlling substrate usage in the heart. In our studies, we found no change in expression of cardiac LPL in late pregnancy, but have not explored the activity levels of LPL. The increased serum triglyceride concentrations of late pregnancy indicates that LPL may be an important factor in fatty acid uptake. Furthermore, usage of palmitate or Luc-FFA overlooks the contribution of LPL as FFA can enter the cell without the need for LPL, and perhaps measurements with labeled very low density lipoproteins (VLDL) will more closely mimic the physiological environment in late pregnancy. Injection of VLDL in LPL-deficient mice determined a decrease in the uptake of lipoproteins (Augustus et al., 2006). Mice overexpressing LPL in the heart were found to decrease FFA oxidation and increase triglyceride oxidation (Yagyu et al., 2003, Pillutla et al., 2005). Thus, future experiments will examine the role of LPL in pregnant mouse hearts.

Conclusion

Profound metabolic reprogramming occurs in pregnancy. However, much still remains to be explored in the metabolic changes of the maternal heart during pregnancy. Deeper understanding of these regulations could have significant impacts on the pregnancy-related cardiac diseases, such as PPCM, preeclamptic heart failure, and others, of which predisposition could likely result from aberrant metabolism.

References

Aasum, E., Lathrop, D.A., Henden, T., Sundset, R., Larsen, T.S. (1998). The role of glycolysis in myocardial calcium control. *J Mol Cell Cardiol.*30: 1703-1712.

Arany, Z., Foo, S.Y., Ma, Y., Ruas, J.L., Bommi-Reddy, A., Girnun, G., Cooper, M., Laznik, D., Chinsomboon, J., Rangwala, S.M., et al. (2008). HIF-independent regulation of VEGF and angiogenesis by the transcriptional coactivator PGC-1alpha. Nature *451*, 1008-1012.

Arany, Z., He, H., Lin, J., Hoyer, K., Handschin, C., Toka, O., Ahmad, F., Matsui, T., Chin, S., Wu, P.H., et al. (2005). Transcriptional coactivator PGC-1 alpha controls the energy state and contractile function of cardiac muscle. Cell Metab *1*, 259-271.

Attia, R.R., Connnaughton, S., Boone, L.R., Wang, F., Elam, M.B., Ness, G.C., Cook, G.A., and Park, E.A. (2010). Regulation of pyruvate dehydrogenase kinase 4 (PDK4) by thyroid hormone: role of the peroxisome proliferator-activated receptor gamma coactivator (PGC-1 alpha). J Biol Chem *285*, 2375-2385.

Augustus, A., Yagyu, H., Haemmerle, G., Bensadoun, A., Vikramadithyan, R.K., Park, S.Y., Kim, J.K., Zechner, R., and Goldberg, I.J. (2004). Cardiac-specific knock-out of lipoprotein lipase alters plasma lipoprotein triglyceride metabolism and cardiac gene expression. J Biol Chem *279*, 25050-25057.

Augustus, A.S., Buchanan, J., Park, T.S., Hirata, K., Noh, H.L., Sun, J., Homma, S., D'Armiento, J., Abel, E.D., and Goldberg, I.J. (2006). Loss of lipoprotein lipase-derived fatty acids leads to increased cardiac glucose metabolism and heart dysfunction. J Biol Chem *281*, 8716-8723.

Bassien-Capsa, V., Fouron, J.C., Comte, B., and Chorvatova, A. (2006). Structural, functional and metabolic remodeling of rat left ventricular myocytes in normal and in sodium-supplemented pregnancy. Cardiovasc Res *69*, 423-431.

Campbell, S.E., Mehan, K.A., Tunstall, R.J., Febbraio, M.A., and Cameron-Smith, D. (2003). 17beta-estradiol upregulates the expression of peroxisome proliferator-activated receptor alpha and lipid oxidative genes in skeletal muscle. J Mol Endocrinol *31*, 37-45.

Chambers, K.T., Leone, T.C., Sambandam, N., Kovacs, A., Wagg, C.S., Lopaschuk, G.D., Finck, B.N., and Kelly, D.P. (2011). Chronic inhibition of pyruvate dehydrogenase in heart triggers an adaptive metabolic response. J Biol Chem *286*, 11155-11162.

Connaughton, S., Chowdhury, F., Attia, R.R., Song, S., Zhang, Y., Elam, M.B., Cook, G.A., and Park, E.A. (2010). Regulation of pyruvate dehydrogenase kinase isoform 4 (PDK4) gene expression by glucocorticoids and insulin. Mol Cell Endocrinol *315*, 159-167.

Elmasri, H., Karaaslan, C., Teper, Y., Ghelfi, E., Weng, M., Ince, T.A., Kozakewich, H., Bischoff, J., and Cataltepe, S. (2009). Fatty acid binding protein 4 is a target of VEGF and a regulator of cell proliferation in endothelial cells. FASEB J *23*, 3865-3873.

Elzwiei, F., Bassien-Capsa, V., St-Louis, J., Chorvatova, A. (2013). Regulation of the sodium pump during cardiac adaptation to pregnancy. *Exp Physiol*. 98.1: 183-192.

Gertz, E.W., Wisneski, J.A., Stanley, W.C., and Neese, R.A. (1988). Myocardial substrate utilization during exercise in humans. Dual carbon-labeled carbohydrate isotope experiments. J Clin Invest *82*, 2017-2025.

Halkein, J., Tabruyn, S.P., Ricke-Hoch, M., Haghikia, A., Nguyen, N.Q., Scherr, M., Castermans, K., Malvaux, L., Lambert, V., Thiry, M., et al. (2013). MicroRNA-146a is a therapeutic target and biomarker for peripartum cardiomyopathy. J Clin Invest *123*, 2143-2154.

Henkin, A.H., Cohen, A.S., Dubikovskaya, E.A., Park, H.M., Nikitin, G.F., Auzias, M.G., Kazantzis, M., Bertozzi, C.R., and Stahl, A. (2012). Real-time noninvasive imaging of fatty acid uptake in vivo. ACS Chem Biol *7*, 1884-1891.

Hilfiker-Kleiner, D., Kaminski, K., Podewski, E., Bonda, T., Schaefer, A., Sliwa, K., Forster, O., Quint, A., Landmesser, U., Doerries, C., et al. (2007). A cathepsin D-cleaved 16 kDa form of prolactin mediates postpartum cardiomyopathy. Cell *128*, 589-600.

Jeoung, N.H., and Harris, R.A. (2008). Pyruvate dehydrogenase kinase-4 deficiency lowers blood glucose and improves glucose tolerance in diet-induced obese mice. Am J Physiol Endocrinol Metab *295*, E46-54.

Jeoung, N.H., and Harris, R.A. (2010). Role of pyruvate dehydrogenase kinase 4 in regulation of blood glucose levels. Korean Diabetes J *34*, 274-283.

Jing, E., O'Neill, B.T., Rardin, M.J., Kleinridders, A., Ilkeyeva, O.R., Ussar, S., Bain, J.R., Lee, K.Y., Verdin, E.M., Newgard, C.B., Gibson, B.W., Kahn, C.R. (2013). Sirt3 regulates metabolic flexibility of skeletal muscle through reversible enzymatic deacetylation. Diabetes. 62(10): 3404-17.

Khan, R.S., Schulze, P.C., Bokhari, S., and Goldberg, I.J. (2011). A sweet heart: increased cardiac glucose uptake in patients with lipoprotein lipase deficiency. J Nucl Cardiol *18*, 1107-1110.

Karamanlidis, G., Lee, C.F., Garcia-Menendez, L., Kolwicz, S.C., Jr., Suthammarak, W., Gong, G., Sedensky, M.M., Morgan, P.G., Wang, W., and Tian, R. (2013). Mitochondrial complex I deficiency increases protein acetylation and accelerates heart failure. Cell Metab *18*, 239-250.

Khairallah, M., Labarthe, F., Bouchard, B., Danialou, G., Petrof, B.J., and Des Rosiers, C. (2004). Profiling substrate fluxes in the isolated working mouse heart using 13C-labeled substrates: focusing on the origin and fate of pyruvate and citrate carbons. Am J Physiol Heart Circ Physiol *286*, H1461-1470.

King, J.C. (2000). Physiology of pregnancy and nutrient metabolism. Am J Clin Nutr *71*, 1218S-1225S.

Kulandavelu, S., Qu, D., and Adamson, S.L. (2006). Cardiovascular function in mice during normal pregnancy and in the absence of endothelial NO synthase. Hypertension *47*, 1175-1182.

Maeda, K., Cao, H., Kono, K., Gorgun, C.Z., Furuhashi, M., Uysal, K.T., Cao, Q., Atsumi, G., Malone, H., Krishnan, B., et al. (2005). Adipocyte/macrophage fatty acid binding proteins control integrated metabolic responses in obesity and diabetes. Cell Metab *1*, 107-119.

Masouye, I., Hagens, G., Van Kuppevelt, T.H., Madsen, P., Saurat, J.H., Veerkamp, J.H., Pepper, M.S., and Siegenthaler, G. (1997). Endothelial cells of the human microvasculature express epidermal fatty acid-binding protein. Circ Res *81*, 297-303.

Melchiorre, K., Sharma, R., and Thilaganathan, B. (2012). Cardiac structure and function in normal pregnancy. Curr Opin Obstet Gynecol *24*, 413-421.

Nieuwenhuizen, A.G., Schuiling, G.A., Bonen, A., Paans, A.M., Vaalburg, W., and Koiter, T.R. (1998). Glucose consumption by various tissues in pregnant rats: effects of a 6-day euglycaemic hyperinsulinaemic clamp. Acta Physiol Scand *164*, 325-334.

Patel, M.S., and Korotchkina, L.G. (2006). Regulation of the pyruvate dehydrogenase complex. Biochem Soc Trans *34*, 217-222.

Patten, I.S., Rana, S., Shahul, S., Rowe, G.C., Jang, C., Liu, L., Hacker, M.R., Rhee, J.S., Mitchell, J., Mahmood, F., et al. (2012). Cardiac angiogenic imbalance leads to peripartum cardiomyopathy. Nature *485*, 333-338.

Pillutla, P., Hwang, Y.C., Augustus, A., Yokoyama, M., Yagyu, H., Johnston, T.P., Kaneko, M., Ramasamy, R., and Goldberg, I.J. (2005). Perfusion of hearts with triglyceride-rich particles reproduces the metabolic abnormalities in lipotoxic cardiomyopathy. Am J Physiol Endocrinol Metab *288*, E1229-1235.

Rimbaud, S., Sanchez, H., Garnier, A., Fortin, D., Bigard, X., Veksler, V., and Ventura-Clapier, R. (2009). Stimulus specific changes of energy metabolism in hypertrophied heart. J Mol Cell Cardiol *46*, 952-959.

Stanley, W.C. (1991). Myocardial lactate metabolism during exercise. Med Sci Sports Exerc *23*, 920-924.

Sugden, M.C., Changani, K.K., Bentley, J., and Holness, M.J. (1992). Cardiac glucose metabolism during pregnancy. Biochem Soc Trans *20*, 195S.

Sugden, M.C., and Holness, M.J. (1993). Cardiac carbohydrate and lipid utilization during late pregnancy. Biochem Soc Trans *21 (Pt 3)*, 312S.

Wegrzyn, J., Potla, R., Chwae, Y.J., Sepuri, N.B., Zhang, Q., Koeck, T., Derecka, M., Szczepanek, K., Szelag, M., Gornicka, A., et al. (2009). Function of mitochondrial Stat3 in cellular respiration. Science *323*, 793-797.

Wende, A.R., Huss, J.M., Schaeffer, P.J., Giguere, V., and Kelly, D.P. (2005). PGC-1alpha coactivates PDK4 gene expression via the orphan nuclear receptor ERRalpha: a mechanism for transcriptional control of muscle glucose metabolism. Mol Cell Biol *25*, 10684-10694.

Williams, J.G., Ojaimi, C., Qanud, K., Zhang, S., Xu, X., Recchia, F.A., and Hintze, T.H. (2008). Coronary nitric oxide production controls cardiac substrate metabolism during pregnancy in the dog. Am J Physiol Heart Circ Physiol *294*, H2516-2523.

Wright, J.J., Kim, J., Buchanan, J., Boudina, S., Sena, S., Bakirtzi, K., Ilkun, O., Theobald, H.A., Cooksey, R.C., Kandror, K.V., et al. (2009). Mechanisms for increased myocardial fatty acid utilization following short-term high-fat feeding. Cardiovasc Res *82*, 351-360.

Yagyu, H., Chen, G., Yokoyama, M., Hirata, K., Augustus, A., Kako, Y., Seo, T., Hu, Y., Lutz, E.P., Merkel, M., et al. (2003). Lipoprotein lipase (LpL) on the surface of cardiomyocytes increases lipid uptake and produces a cardiomyopathy. J Clin Invest *111*, 419-426.

Zhao, G., Jeoung, N.H., Burgess, S.C., Rosaaen-Stowe, K.A., Inagaki, T., Latif, S., Shelton, J.M., McAnally, J., Bassel-Duby, R., Harris, R.A., et al. (2008). Overexpression of pyruvate dehydrogenase kinase 4 in heart perturbs metabolism and exacerbates calcineurin-induced cardiomyopathy. Am J Physiol Heart Circ Physiol *294*, H936-943.

Zima, A.V., Kockskamper, J., Blatter, L.A. (2006). Cytosolic energy reserves determine the effect of glycolytic sugar phosphates on sarcoplasmic reticulum Ca2+ release in cat ventricular myocytes. *J Physiol*. 15;577(Pt 1): 281-93.

Appendix:

An unknown role for C/EBPβ in late pregnant rat hearts

Introduction

During pregnancy, the heart undergoes physiological remodeling that is similar to the "eccentric" hypertrophy observed in athletes. This is characterized by wall thickening and volume overload (Bamfo et al., 2007). After pregnancy, there is a rapid reversal of cardiac hypertrophy. By 12-24 weeks postpartum, systolic function and left ventricular mass have returned to normal (Gonzalez et al., 2007). Other changes such as cardiac output and systemic resistance have been found to persist for up to a year.

CCAAT-enhancer-binding protein β (C/EBPβ) is a transcription factor that plays a critical role in a number of different biological processes, including adipogenesis, osteoclast differentiation, inflammatory responses, and apoptosis induction. In the heart, heterozygous deletion of C/EBPβ protects from heart failure when pressure overloaded (Bostrom et al., 2010). In exercise models of swimming, cardiac C/EBPβ expression is downregulated (Bostrom et al., 2010). This decrease has been directly linked to the increased hypertrophy observed in response to exercise through the negative regulation of CITED4 by C/EBPβ. Although the role of C/EBPβ in exercise induced hypertrophy has been well characterized, it is unclear if this transcription factor also plays a role in pregnancy-induced physiological hypertrophy, or potentially postpartum reversal of hypertrophy.

Here we investigate the role of C/EBPβ in cardiac hypertrophy during and immediately after pregnancy. We hypothesize that C/EBPβ plays a similar role in pregnancy-induced hypertrophy as it does in exercise-induced cardiac hypertrophy. Therefore, we tested if C/EBPβ expression is decreased during pregnancy. Furthermore, as cardiac hypertrophy is reversed in the postpartum state, we hypothesized that C/EBPβ expression might also increase postpartum to play a role in the reversal of cardiac hypertrophy. We also explored the effects of conditioned

media from human placental explants of term deliveries on its ability to induce C/EBPβ to determine if these effects are mediated through placental secretion of hormones or cytokines. One previous study found that C/EBPβ is induced in mid-pregnancy in the heart, but unchanged in late gestation and postpartum (Chung et al., 2012b). This suggests that perhaps pregnancy-induced hypertrophy has a distinct signaling mechanism compared to exercise-induced hypertrophy.

Results

C/EBPβ expression is selectively induced in the hearts of late pregnant and early postpartum rats

Hearts from rats at different stages of gestation, including mid-pregnancy (D12), late pregnancy (D20), and postpartum day 1 (PP1) were assayed for C/EBPβ expression. There was no change observed in mid-pregnancy, but in late pregnancy, a post-transcriptional induction was

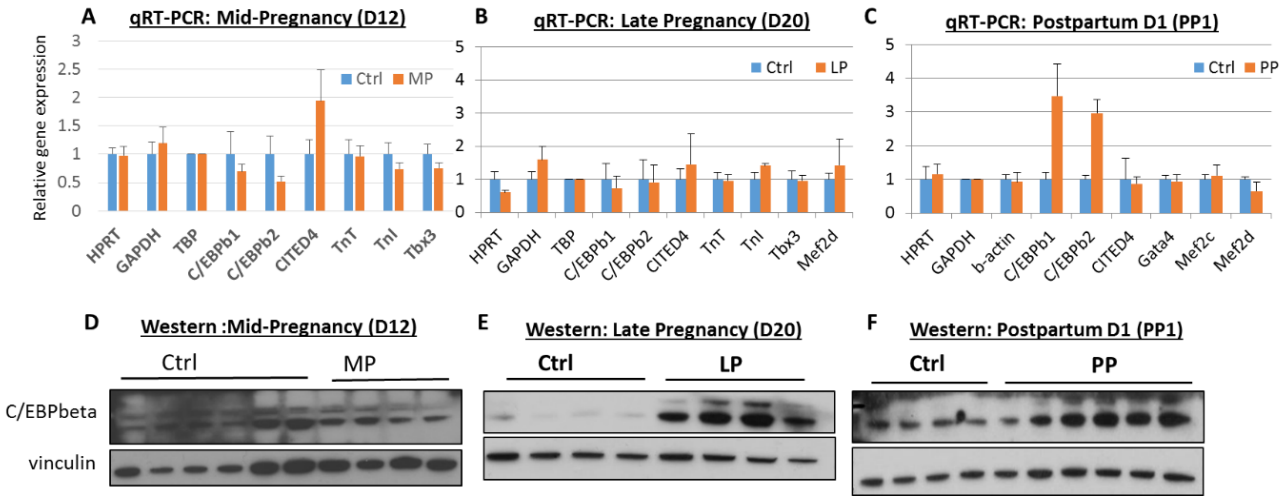

Figure A.1: C/EBPβ is induced in the heart in late pregnancy and postpartum day 1. Quantitative, real-time PCR was performed on rat heart tissue at mid-pregnancy (day 12, A), late pregnancy (day 20, B), and postpartum day 1 (C). Western blot was also performed in rat hearts at same times as the gene expression.

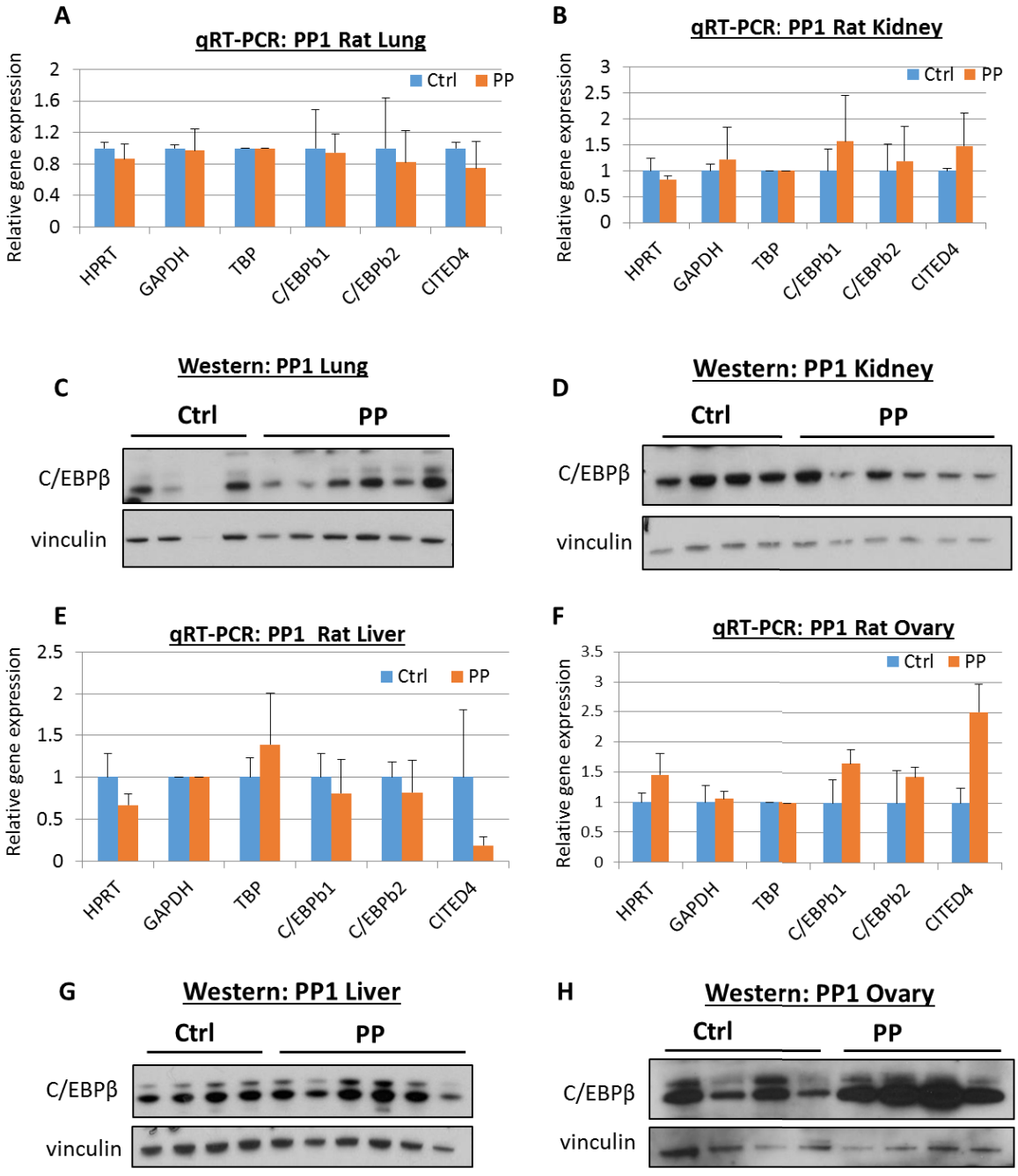

Figure A.2: C/EBPβ expression in other tissues of postpartum day 1 rats. Quantitative, real-time PCR and western blot was performed on rat heart tissue at postpartum day 1 for lung (A and C), kidney (B and D), liver (E and G), and ovary (F and H).

observed (Figure A.1E), as protein is strongly induced while no gene expression changes are seen (Figure A.1B). Furthermore, there is an induction in both gene and protein expression of C/EBPβ at postpartum day 1. However, no change was seen in CITED4 at any time point, a gene that is negatively regulated by C/EBPβ (Figure A.1).

Protein and gene expression of C/EBPβ was determined in lung, kidney, liver, and ovary tissues of postpartum day 1 rats. We do not observe significant changes in gene expression (Figure A.2A, B, E, and F). Protein expression appears decreased in the kidney (Figure A.1D), increased in the ovary (Figure A.2H), while unchanged in the lung and liver (Figure A.2C and G). Interestingly, this may also indicate post-transcriptional modifications of C/EBPβ in these tissues. In addition, the late pregnant expression profile was determined in the lung, liver, kidney and ovaries of rats, and no alterations are seen in C/EBPβ (Figure A.3). A prominent induction of CITED4 occurs in the liver in the absence changes in C/EBPβ (Figure A.3B). Western blot was not performed on these samples.

Placental conditioned media induces C/EBPβ in cardiomyocytes

Since C/EBPβ is induced in late pregnancy, we hypothesized that perhaps placental secreted factors played a role. Thus, we obtained human placental explants from term deliveries and then incubated them in DMEM for 48 hours before treatment on neonatal rat ventricular myocytes (NRVMs) for 24 hours. Quantitative, real-time PCR (qRT-PCR) showed drastic inductions in C/EBPβ gene and protein (Figure A.4). Other genes downstream of C/EBPβ, such as CITED4 and troponin T (TnT), are oppositely altered, while no significant changes were observed for genes involved in angiogenesis or metabolism (Figure A.4). Furthermore, we show that this induction is not a nutrient deprivation response (Figure A.5A) and is also due to a protein in the conditioned media (Figure A.5B) by dilution of conditioned media and treatment

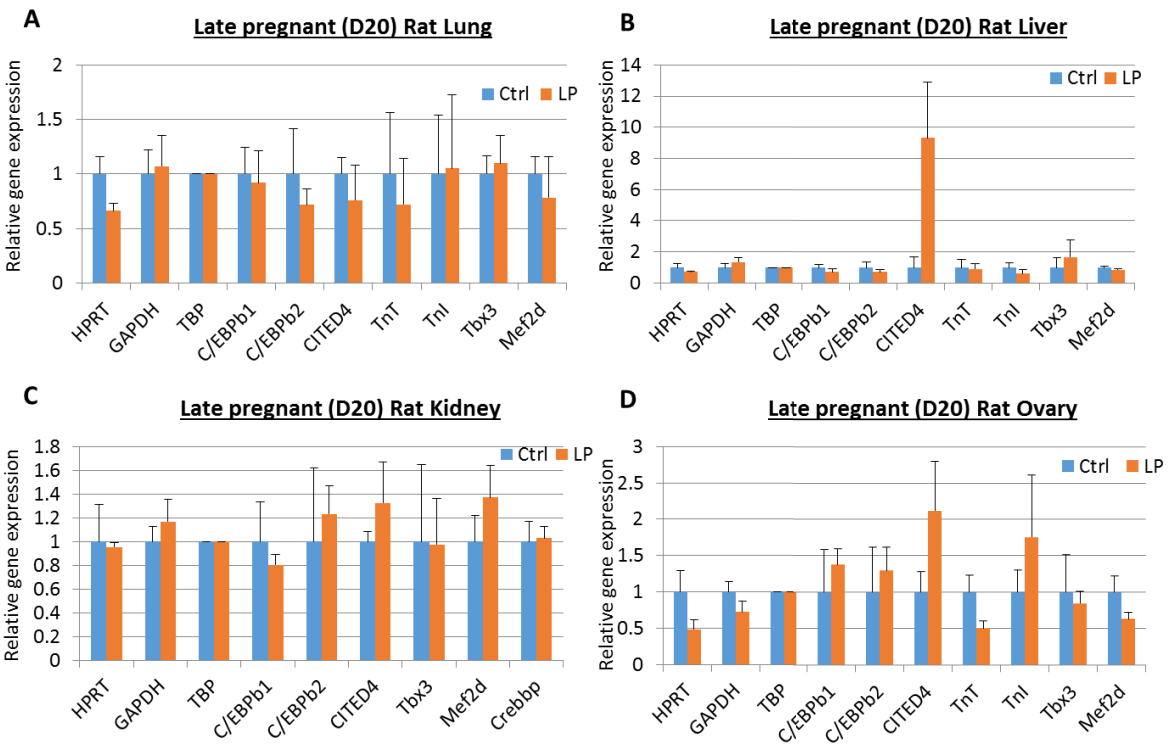

Figure A.3: C/EBPβ expression in late pregnancy. Quantitative, real-time PCR was performed on late pregnant rat tissues, including lung (A), liver (B), kidney (C), and ovary (D).

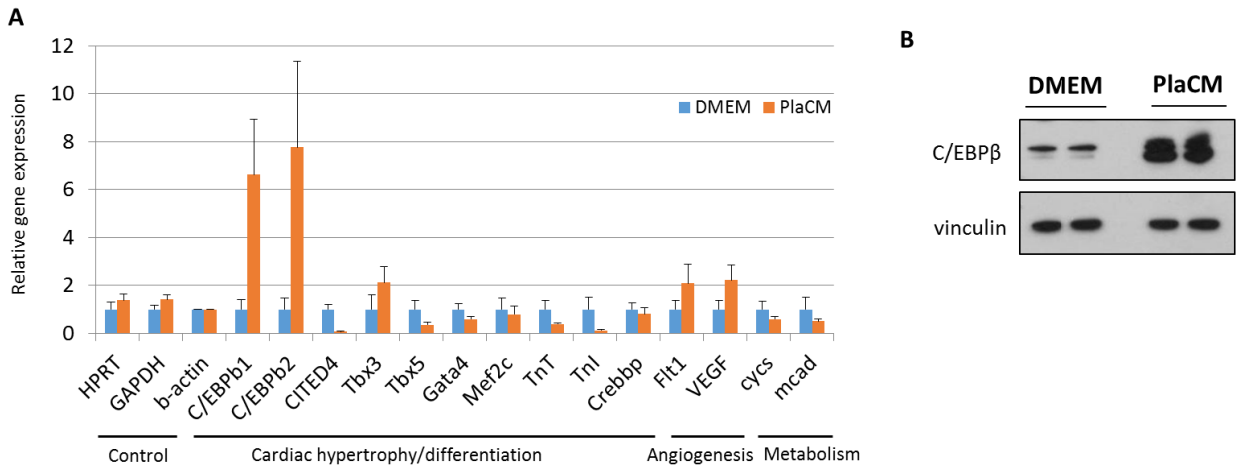

Figure A.4: Induction of C/EBPβ in NRVMs after 24 hours incubation with placental conditioned media. NRVMs were incubated with human placental conditioned media for 24 hours. Then, quantitative, real-time PCR was performed (A) and western blot was carried out (B).

with trypsin and heating. In addition, placental conditioned media can induce C/EBPβ expression in NRVMs by 4 hours of treatment and is sustained by 8 hours (Figure A.6).

As both heart tissue and isolated NRVMs contain more than one population of cells, we explored if C/EBPβ upregulation is a cardiomyocyte-specific effect or if it is mediated through non-cardiomyocytes by isolating these two populations in adult rat hearts by Langendorff perfusion. Though C/EBPβ is induced in both populations, a much higher upregulation is observed in non-cardiomyocytes (Figure A.7). In addition, we obtained placental conditioned media from late pregnant rats and observed an induction of C/EBPβ on NRVMs (Figure A.8A). Furthermore, both mildly preeclamptic and preeclamptic human placental conditioned media

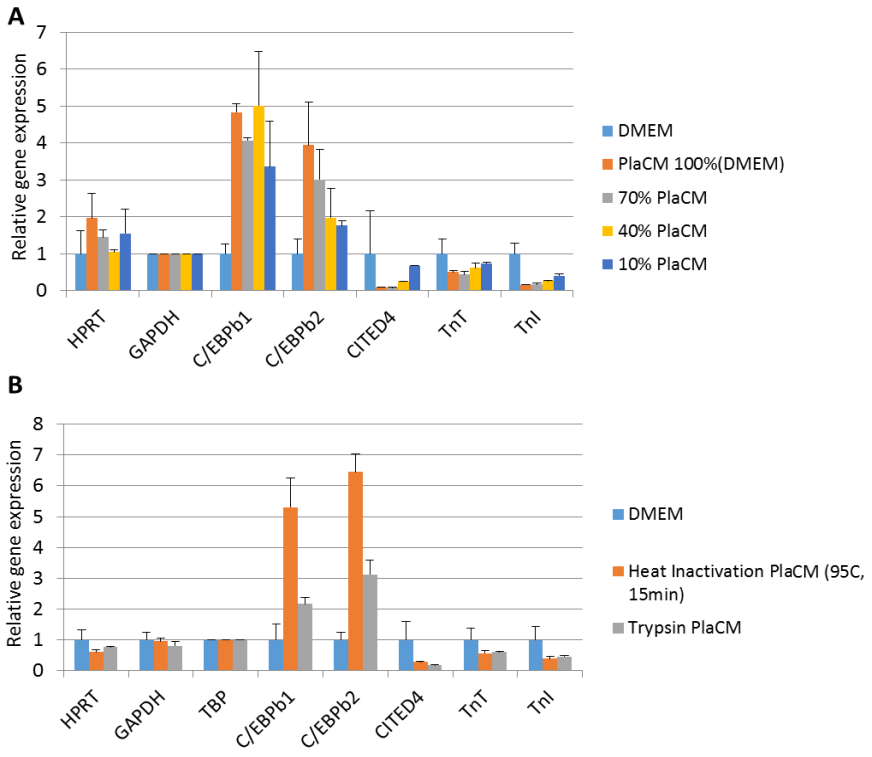

Figure A.5: Induction of C/EBPβ in NRVMs is not a nutrient deprivation response and is mediated by protein effects. (A) NRVMs were incubated with different dilutions of human placental conditioned media for 24 hours. Then, quantitative, real-time PCR was performed. (B) Human placental conditioned media was either heat inactivated (95C, 15min) or treated with trypsin for 1 hour at 37C and then incubated on NRVMs for 24 hours. qRT-PCR was then performed.

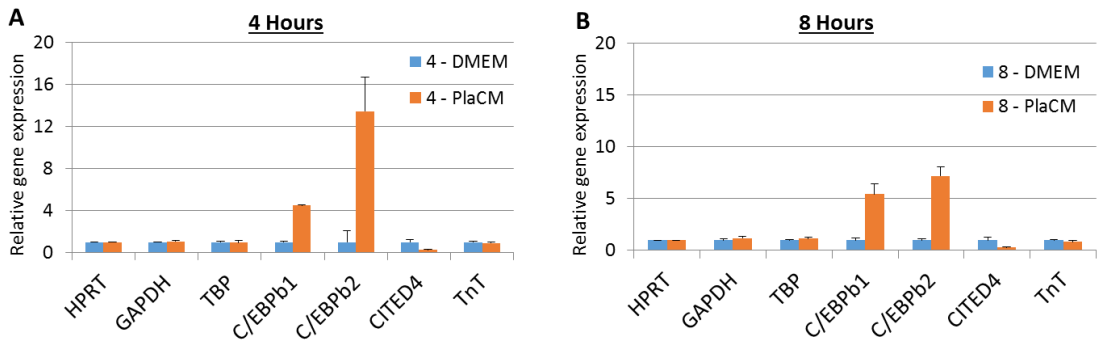

Figure A.6: Induction of C/EBPβ occurs at 4 hours and 8 hours of conditioned media treatment. NRVMs were incubated with human placental conditioned media for 4 hours (A) and 8 hours (B). Then, quantitative, real-time PCR was performed.

induced C/EBPβ in NRVMs (Figure A.8B, C, and D). Treatment of pregnancy sex hormones, including progesterone and estrogen, however, did not alter C/EBPβ expression in NRVMs (Figure A.9A). Soluble Flt (sFlt), an anti-angiogenic, soluble VEGFR1 receptor that is elevated at late pregnancy, also did not induce C/EBPβ (Figure A.9B).

The C/EBPβ response, however, is surprisingly not specific to placental conditioned media, as treatment of conditioned media from fibroblasts, MS1 cells (endothelial cell line), and 10T1/2s differentiated to become pericyte-like cells with TGF-β treatment, also induces C/EBPβ expression in NRVMs (Figure A.10). In addition, we observe that other cell types incubated with placental conditioned media similarly promote C/EBPβ expression (data not shown).

Placental conditioned media induces apoptosis in cardiomyocytes

To explore the consequences of C/EBPβ upregulation, we performed microarray analysis on NRVMs incubated with placental conditioned media for 24 hours. One of the top upregulated pathways found was apoptosis, of which C/EBPβ has been well characterized to play a role in.

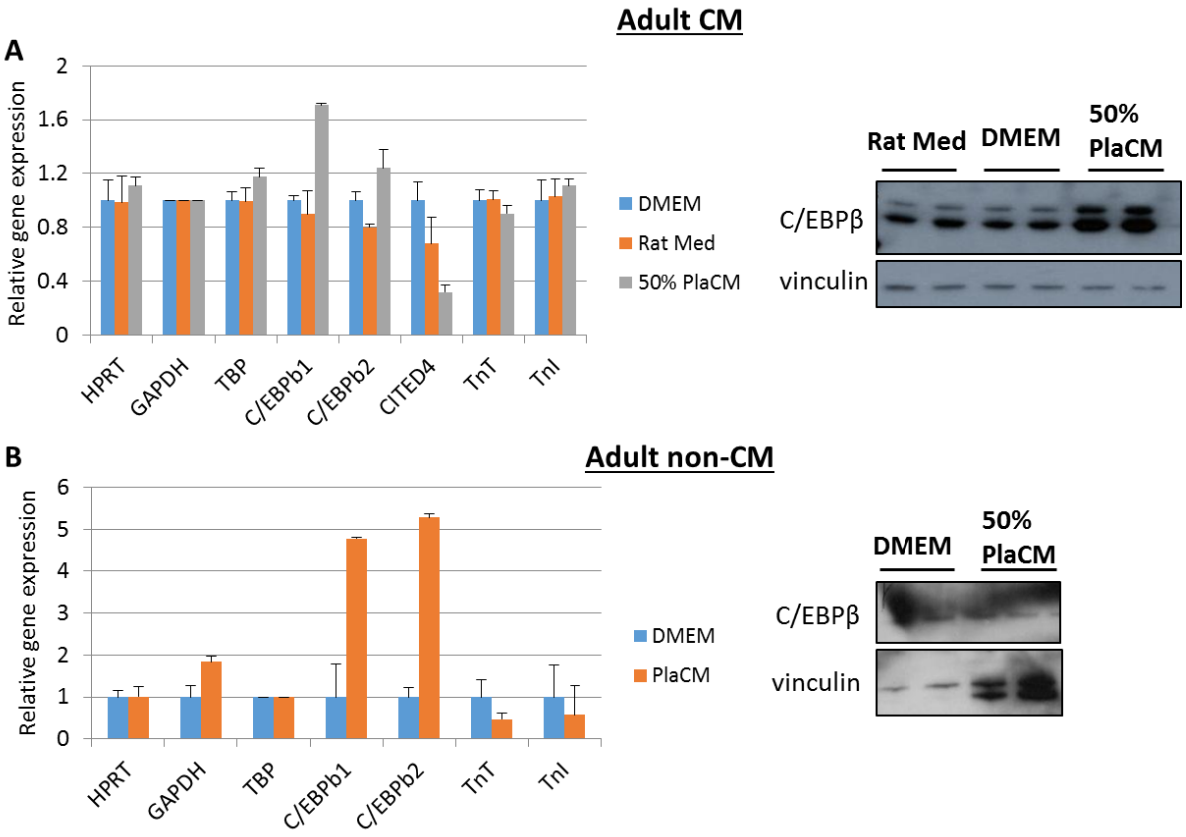

Figure A.7: C/EBPβ is upregulated more strongly in non-cardiomyocytes than cardiomyocytes. Adult rat cardiomyocytes and non-cardiomyocytes were isolated from the heart via Langendorff perfusion. (A) Adult cardiomyocytes were incubated with human placental conditioned media for 24 hours. Then, quantitative, real-time PCR was performed and western blot was carried out. (B) Adult non-cardiomyocytes were incubated with human placental conditioned media for 24 hours. Then, quantitative, real-time PCR was performed and western blot was carried out.

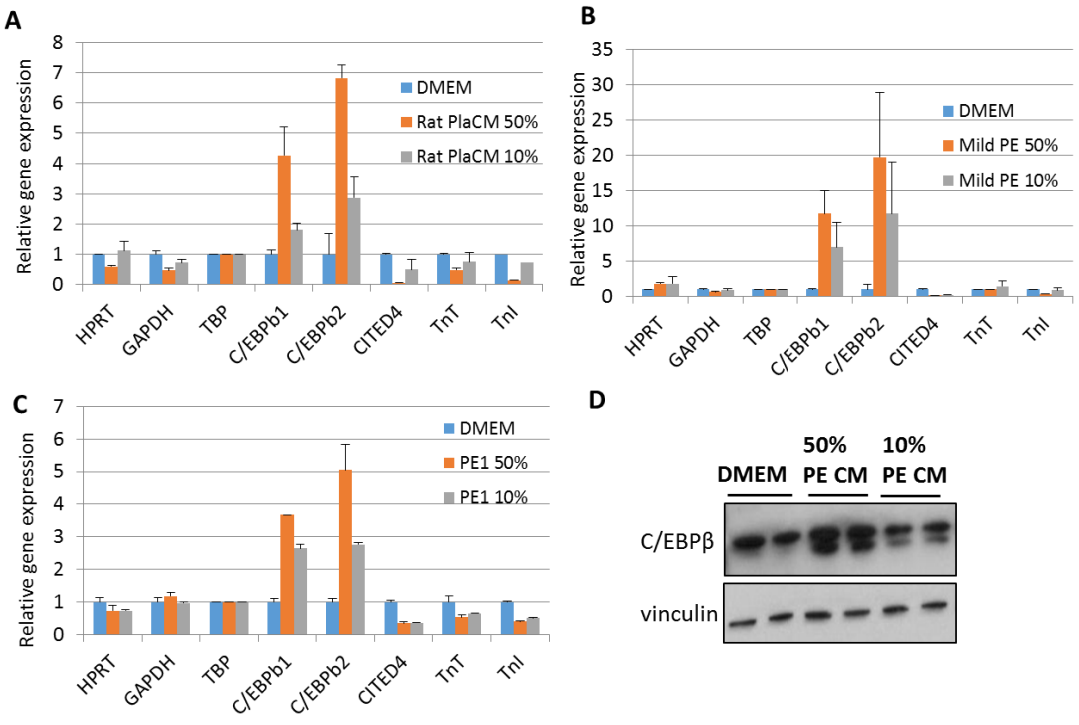

Figure A.8: Rat placental and human preeclamptic placental conditioned media incubation on NRVM induces C/EBPβ expression. NRVMs were incubated with rat placental conditioned media (A) or human preeclampic placental conditioned media (B and C) for 24 hours. Then, quantitative, real-time PCR was performed. Western blot was conducted on treatment of preeclamptic conditioned media on NRVMs (D).

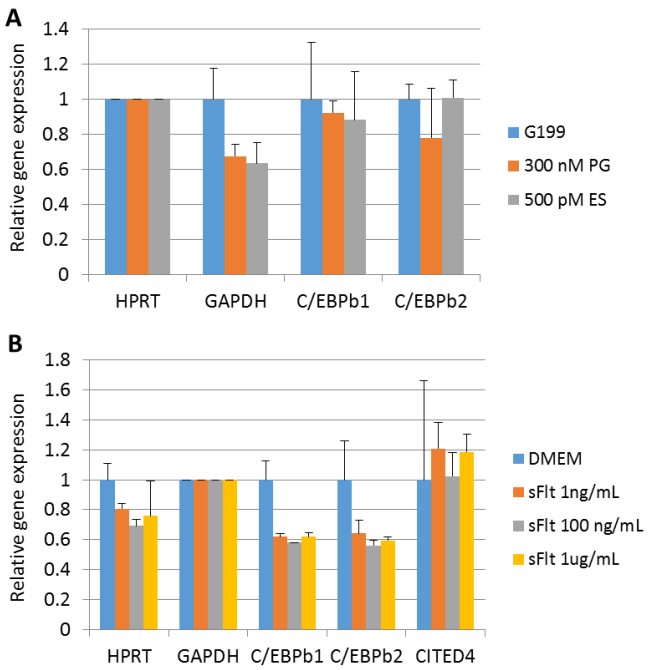

Figure A.9: No effect of sFlt, progesterone, or estrogen on C/EBPβ in NRVMs. NRVMs were incubated with progesterone or estrogen (A) or sFlt (B) for 24 hours. Then, quantitative, real-time PCR was performed.

We determined that placental conditioned media does cause apoptosis in NRVMs (Figure A.11), although not as much as the positive apoptosis control, doxorubicin.

To examine if C/EBPβ is responsible for the increase in apoptosis, we treated NRVMs with siRNA for C/EBPβ before incubating with placental conditioned media. We found that a second dose of siRNA ("boost") was necessary to overcome the dominant induction by placental conditioned media (Figure A.12A). There is surprisingly no change in apoptosis with knock down of C/EBPβ (Figure A.12B), suggesting that C/EBPβ is not necessary for apoptosis induction by placental conditioned media in NRVMs.

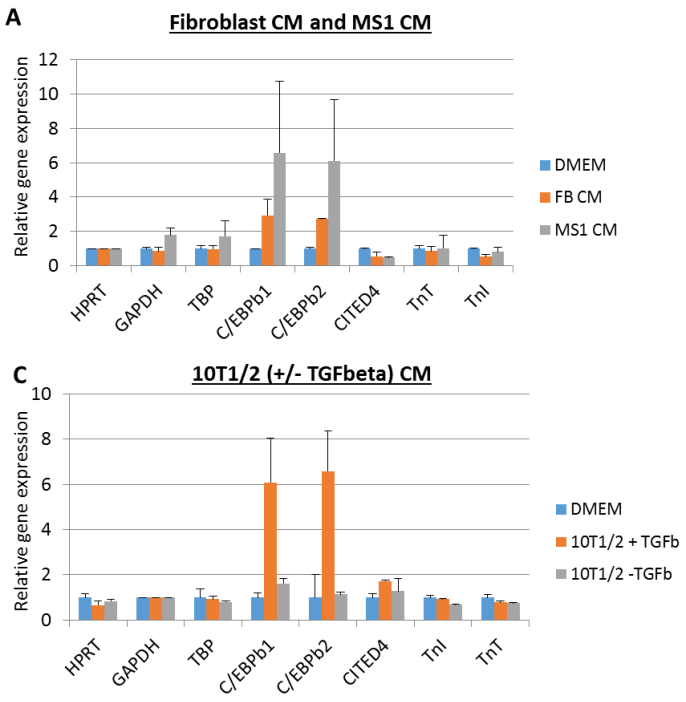

Figure A.10: C/EBPβ induction is not specific to placental conditioned media. NRVMs were incubated fibroblast (A), MS1 (A), and 10T1/2 (with and without treatment of TGFβ, C) conditioned media for 24 hours. Then, quantitative, real-time PCR was performed.

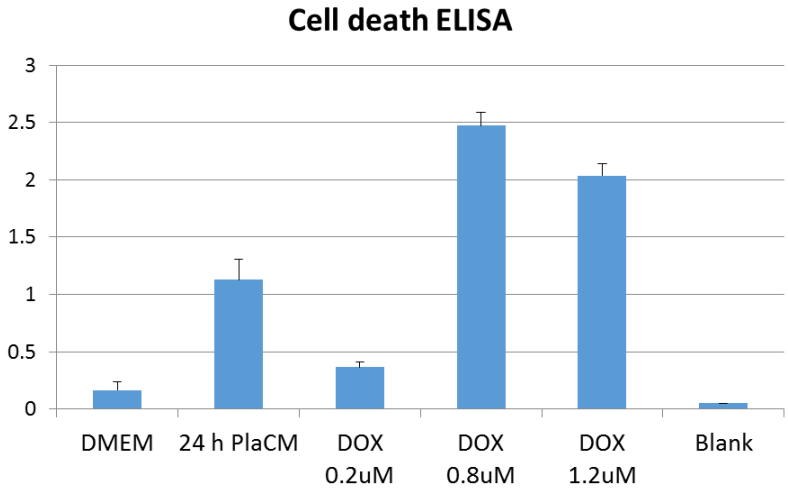

Figure A.11: Placental conditioned media induces cell death in NRVMs. NRVMs were incubated with human placental conditioned media for 24 hours or different concentrations of doxorubicin (DOX) as control. Then, cell death detection ELISA (Roche) was performed to determine apoptosis status of NRVMs.

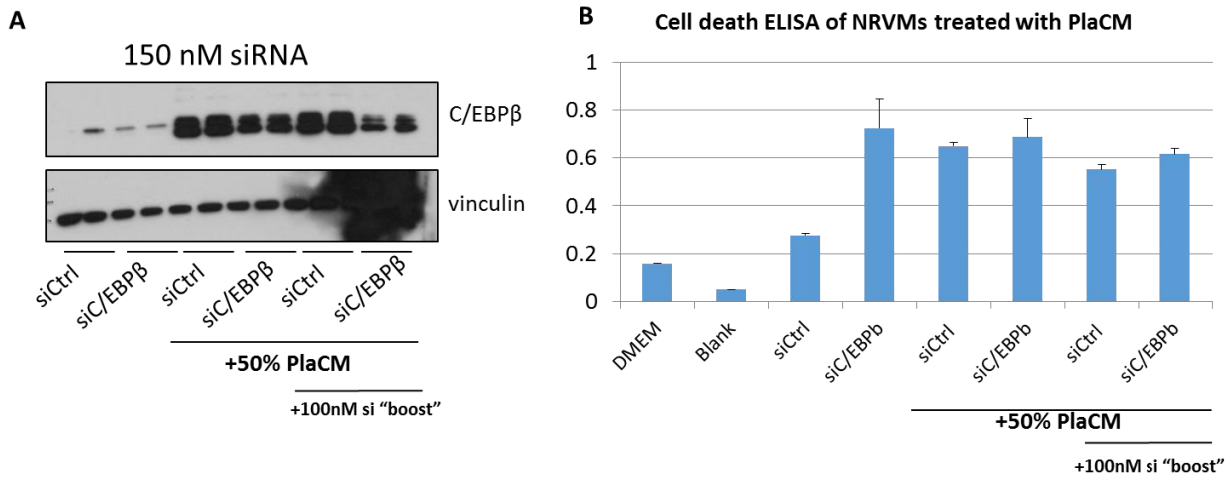

Figure A.12: Placental conditioned media upregulaton of C/EBPβ does not mediate cell death. NRVMs were treated with siRNA for C/EBPβ and then incubated with human placental conditioned media for 24 hours. During this time a second "boost" of siRNA was added to cells to ensure knockdown of protein (A). Then, the cell death ELISA was performed on all samples (B).

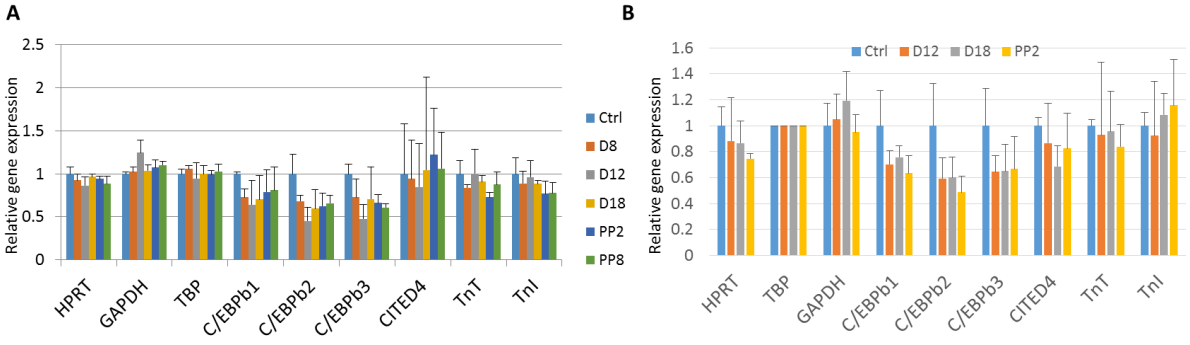

Figure A.13: C/EBPβ is not upregulated in mouse timed pregnancy in the heart. Mice were set up on timed pregnancies at a barrier (A) and non-barrier (B) facility. RNA was isolated from heart tissue and qRT-PCR was performed on the selected genes.

In vivo induction of C/EBPβ in the hearts of mice during pregnancy

In order to continue to explore the effects of C/EBPβ on pregnancy, a shift to mouse models was necessary to conduct genetic manipulations *in vivo*. Thus, we profiled C/EBPβ expression levels in mouse timed pregnancy. There is no change in C/EBPβ expression in mouse hearts at any point in gestation (Figure A.13). We explored timed pregnancies in both a barrier and non-barrier animal facility to eliminate the possibility of environment that is too clean to observe the effect, given the known role of C/EBPβ in inflammation.

Discussion

We observe marked inductions of C/EBPβ in late pregnancy and day 1 postpartum. In late pregnancy, this response may result from post-transcriptional modifications. We also do not see a negative regulation on CITED4 with increased C/EBPβ expression. Furthermore, we found that this phenotype can be mimicked *in vitro* with treatment of placental conditioned media on isolated cardiomyocytes. However, this upregulation is neither specific to placental conditioned media nor to NRVMs, as C/EBPβ induction is observed in other cell types with placental conditioned media treatment and also with other types of conditioned media on NRVMs. Furthermore, we determined that the C/EBPβ response is not necessary for induction of cell death observed with treatment of conditioned media. We did not however, test if C/EBPβ is sufficient to induce cell death in NRVMs. This can be done by overexpressing C/EBPβ in NRVMs and determining the levels of apoptosis compared to control. If so, this would suggest that placental conditioned media stimulates multiple pro-apoptotic pathways, and inhibition of the C/EBPβ pathway is insufficient to prevent apoptosis.

We also carried out timed pregnancy studies in mice, which showed no change in C/EBPβ expression at any time in pregnancy. We did not assess C/EBPβ expression levels in isolated cardiomyocytes from pregnant mice. However, a previous study found an induction of C/EBPβ in mid-pregnancy, though not late pregnancy or postpartum (Chung et al., 2012b). The striking increase in C/EBPβ in rat hearts during pregnancy, in addition to its known roles in exercise-induced hypertrophy, suggests that C/EBPβ could also be important for pregnancy-related adaptations in the heart. The lack of CITED4 repression in our experiments, however, suggests that perhaps hypertrophy is not the downstream phenotype that is provoked by C/EBPβ. It is difficult to perform genetic manipulations in rats, and the disparity between rat and mouse physiology in pregnancy made it difficult for us to further explore the role of C/EBPβ in pregnancy with genetically manipulated models. We hypothesize that C/EBPβ plays a role in rat pregnancy, and perhaps AAV9-mediated delivery of C/EBPβ, which specifically targets the heart, during pregnancy could provide an answer on its role.

Materials and Methods

Animal studies. All animal studies were performed according to procedures approved by the Institutional Animal Care and Use Committee (IACUC) at Beth Israel Deaconess Medical Center (BIDMC). Mice were maintained on a standard rodent chow diet with 12 hours light and dark cycles with water and food ad libitum. C57/bl6 mice were purchased from Jackson Laboratories (Bar Harbor, Maine). Wild-type, three-month-old female C57/bl6 undergoing estrus were mated with wild-type, C57/bl6 breeder males. The presence of a copulatory plug is denoted as day 0 of pregnancy. Pregnant females were singly placed in a new cage. Timed pregnancies were carried

out to day 11-12 (mid-pregnancy) and day 17-18 (late pregnancy) of gestation. Timed pregnant rats (Sprague Dawley) were obtained directly from Charles River.

Reagents and Materials. Unless otherwise stated, all reagents are from Sigma. The cell death ELISA kit was obtained from Roche.

Gene expression studies. Upon harvesting, mouse tissues were immediately frozen in liquid nitrogen. Total RNA was isolated from with the TRIzol (Invitrogen) and chloroform method. RNA concentrations were measured with the ThermoScientific NanoDrop spectrophotometer, 1 μg of RNA was used to synthesize cDNA with the High-Capacity cDNA Reverse Transcription kit (Applied Biosystems, CA). Gene expression was assayed with quantitative, real-time PCR using SYBR Green dye with specific primer set specially designed and the Bio-rad CFX 384 Touch Real-Time PCR Detection System. The primers used for mice and rats are listed in Tables 3.1 and 3.2.

Western blots. To determine protein expression, frozen mouse tissues were homogenized in the Qiagen TissueLyser for 10-15 minutes in RIPA lysis buffer, in the presence of phosphatase and protease inhibitors. Protein concentration was determined by the Bradford assay. Approximately 10 μg of protein were separated by SDS-PAGE, before transferred onto PVDF membrane. The primary antibodies were for immunoblot were: vinculin (Cell Signaling) and C/EBPβ (abcam). Primary antibodies were incubated overnight at 1:1000. Three TBS-T washes were conducted before incubating with secondary antibody at 1:10,000 for 1 hour.

Conditioned media collection and incubation. Human placental explants were obtained and incubated in DMEM for 48 hours. Then, conditioned media was centrifuged at maximum speed for 5 minutes to remove tissue debris before storage in -80C. Placental conditioned media was incubated on NRVMs for 24 hours.

Neonatal cardiomyocyte isolations. Neonatal cardiomyocyte isolations were carried out as previously described (Hajjar et al., 1997). Briefly, hearts of 1-2 day old Sprague Dawley neonates were excised and ventricles were isolated. Sequential incubations with collagenase type II (Worthington) were carried out in a 37^{o}C shaker. Cells were purified from non-cardiomyocytes via a crude, 1 hour pre-plating step. Cells were then incubated in DMEM, 10% HS, 5% FBS, and 1% penicillin-streptomycin (PS).

Adult cardiomyocyte isolations. Adult mouse hearts were excised and perfused via Langendorff perfusion, first with perfusion buffer (137 mM NaCl, 4 mM KCl, 1 mM $MgCl_2$, 10 mM HEPES, 0.33 mM NaH_2PO_4, 10mM glucose, 5 mM taurine, and 10 mM BDM), before switching to an enzyme buffer with collagenase D (Roche), collagenase B (Roche), and protease XIV for 10-15 minutes. Calcium was reloaded with concentrations of 0.06 mM, 0.25 mM, 0.60 mM, and 1.2 mM. Adult cardiomyocytes were plated on laminin-coated tissue culture plates for 2 hours in MEM (Invitrogen), 10% calf serum, BDM, 2 mM glutamine, and 2mM ATP before switching to labeled media.

References

Bamfo, J.E., Kametas, N.A., Nicolaides, K.H., and Chambers, J.B. (2007). Maternal left ventricular diastolic and systolic long-axis function during normal pregnancy. Eur J Echocardiogr *8*, 360-368.

Bostrom, P., Mann, N., Wu, J., Quintero, P.A., Plovie, E.R., Panakova, D., Gupta, R.K., Xiao, C., MacRae, C.A., Rosenzweig, A., et al. (2010). C/EBPbeta controls exercise-induced cardiac growth and protects against pathological cardiac remodeling. Cell *143*, 1072-1083.

Chung, E., Yeung, F., and Leinwand, L.A. (2012). Akt and MAPK signaling mediate pregnancy-induced cardiac adaptation. J Appl Physiol (1985) *112*, 1564-1575.

Gonzalez, A.M., Osorio, J.C., Manlhiot, C., Gruber, D., Homma, S., and Mital, S. (2007). Hypertrophy signaling during peripartum cardiac remodeling. Am J Physiol Heart Circ Physiol *293*, H3008-3013.